Functional characterization of electronic materials and devices using MeV ion beams

Ettore Vittone

Department of Physics,

University of Torino (Italy)

Mark Breese

Department of Physics,

National University of Singapore

Basic structures of semiconductor devices

Metal-semiconductor interface

p-n junction

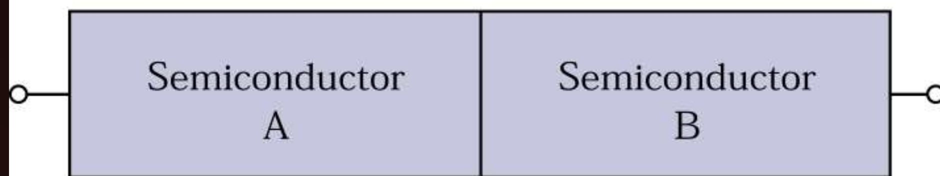

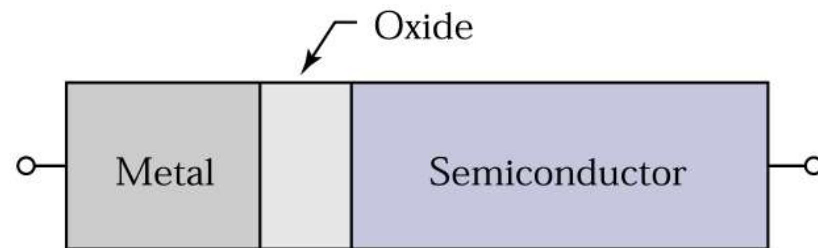

Heterojunction interface

Metal-oxide-semiconductor interface

Semiconductor Devices, 2/E by S. M. Sze

Functional characterization of semiconductor materials and devices

Measurement of the their electronic properties and performances

Main physical observable: current

Current = F(carrier density; carrier transport)

Carrier (electron-hole) generation
Recombination/trapping

Carrier lifetime τ

Free carriers (electron/hole) transport
Two mechanisms:

Drift $\Rightarrow$ electric field $v=\mu\cdot E$
Diffusion $\Rightarrow$ concentration gradient

J.R. Haynes, W. Shockley,

"The mobility and life of injecting holes and electrons in germanium,

Phys. Rev. 81, (1951), 835-843.

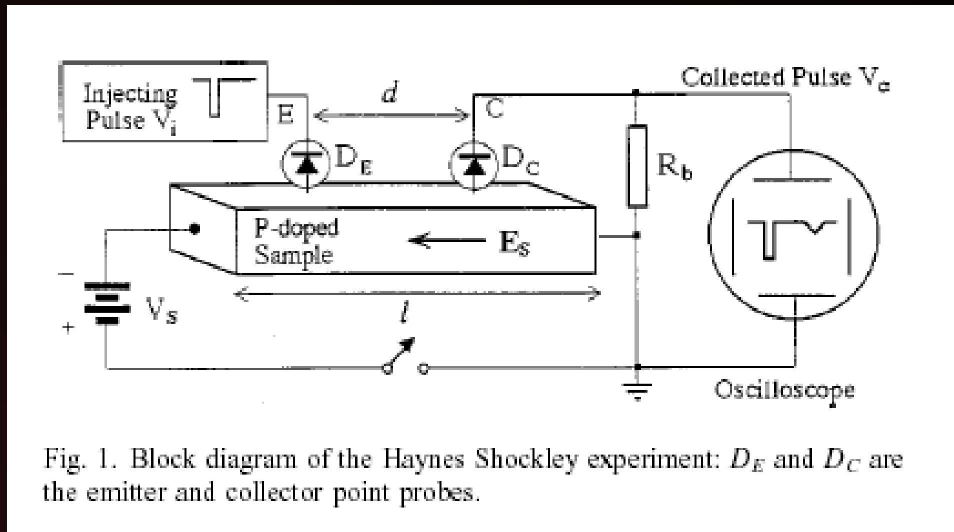

Fig. 1. Block diagram of the Haynes Shockley experiment: D_E and D_C are the emitter and collector point probes.

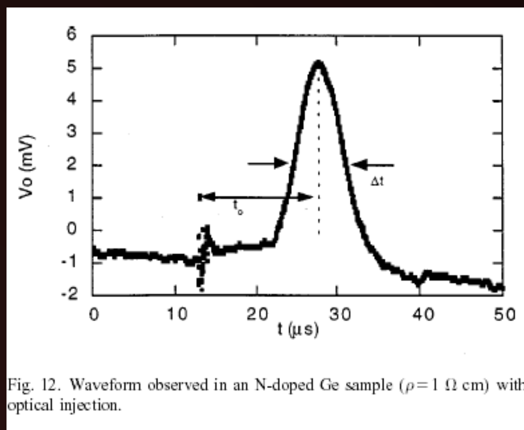

Fig. 12. Waveform observed in an N-doped Ge sample ($\rho = 1\ \Omega$ cm) with optical injection.

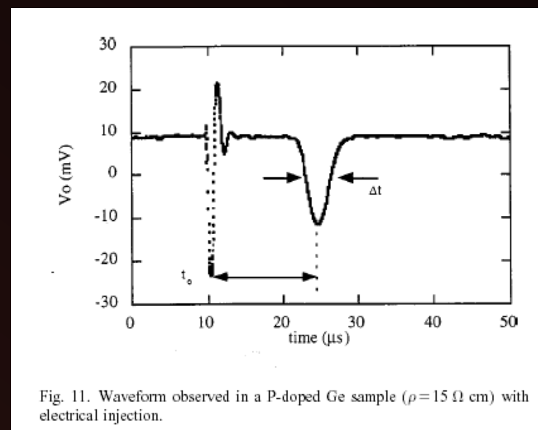

Fig. 11. Waveform observed in a P-doped Ge sample ($\rho = 15\ \Omega$ cm) with electrical injection.

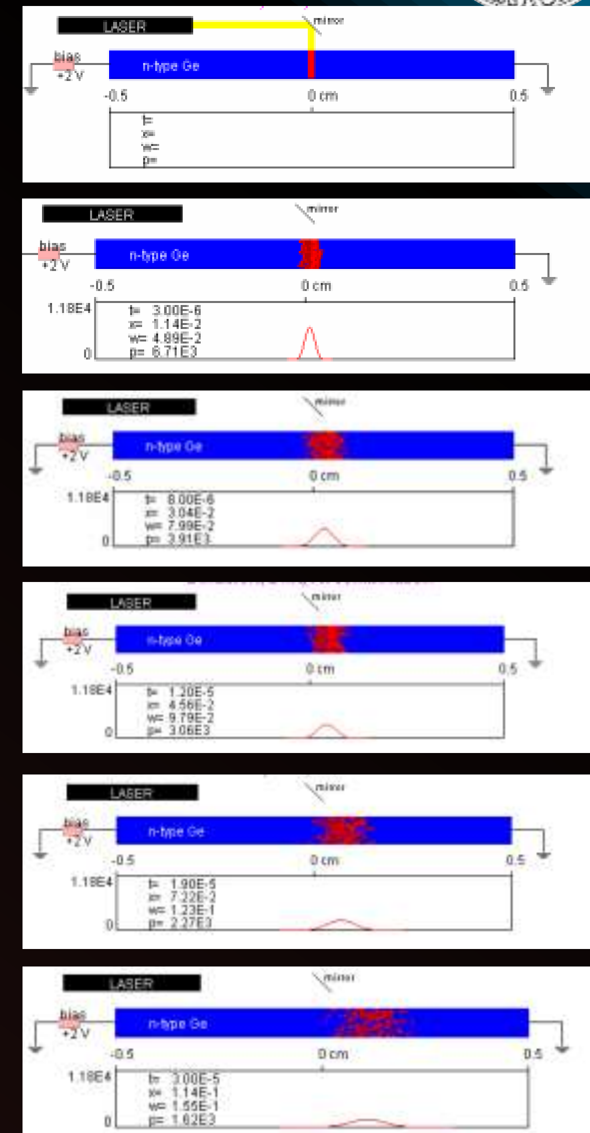

Probe:
Light (Optical) Beam Induced Current (LBIC or OBIC)
Continuous or pulsed laser
Photocurrent mapping
Transparent electrode (solar cells)

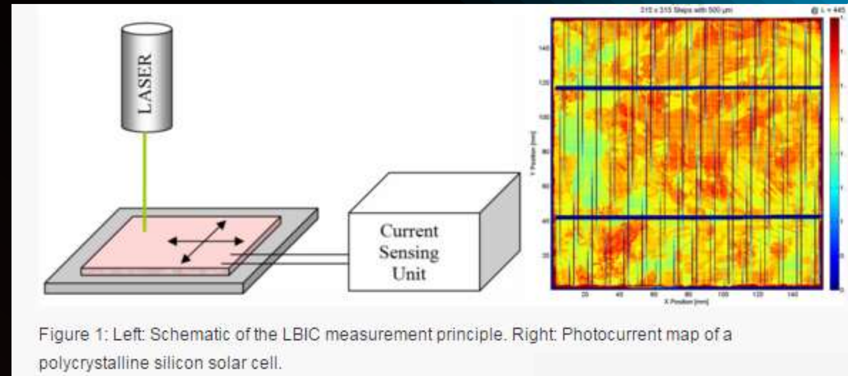

Figure 1: Left: Schematic of the LBIC measurement principle. Right: Photocurrent map of a polycrystalline silicon solar cell.

The SPIRIT of science TECHNISCHE UNIVERSITÄT ILMENAU

Probe: keV photons
X-ray Beam Induced Current (XBIC)
Continuous or pulsed beam
Photocurrent mapping
Metal electrodes

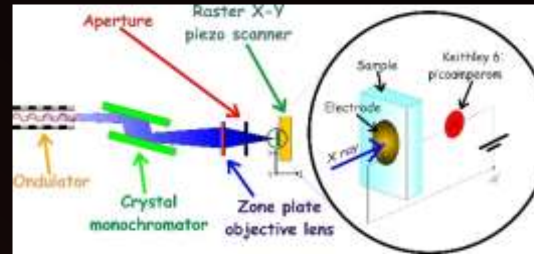

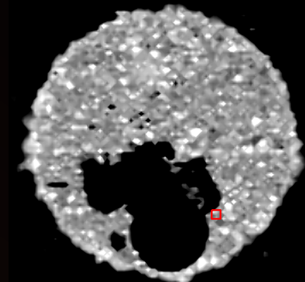

E. Vittone et al. NIMB 210 (2003) 159-163

Probe: keV electrons
Electron Beam Induced Current (EBIC)
Continuous beam
Current mapping
Metal electrodes

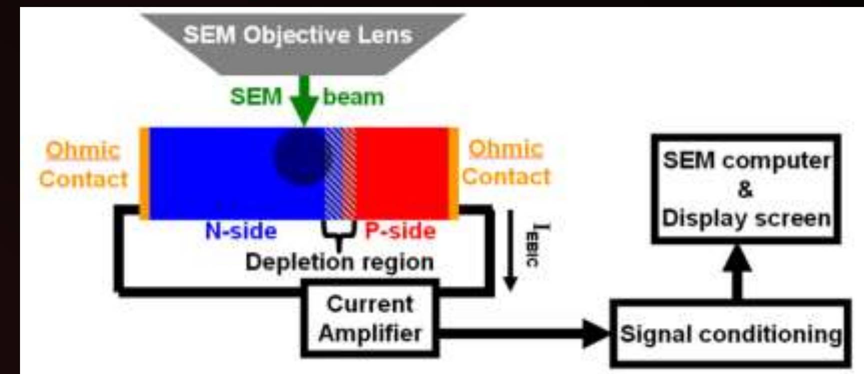

Wikipedia

Ion Beam Induced Charge (IBIC)

Probe: MeV ion beams
Single ion detection
Induced charge mapping
Finished device

M.B.H. Breese, G.W. Grime and F. Watt, Oxford Nuclear Physics rep. OUNP-91-33 (1991).

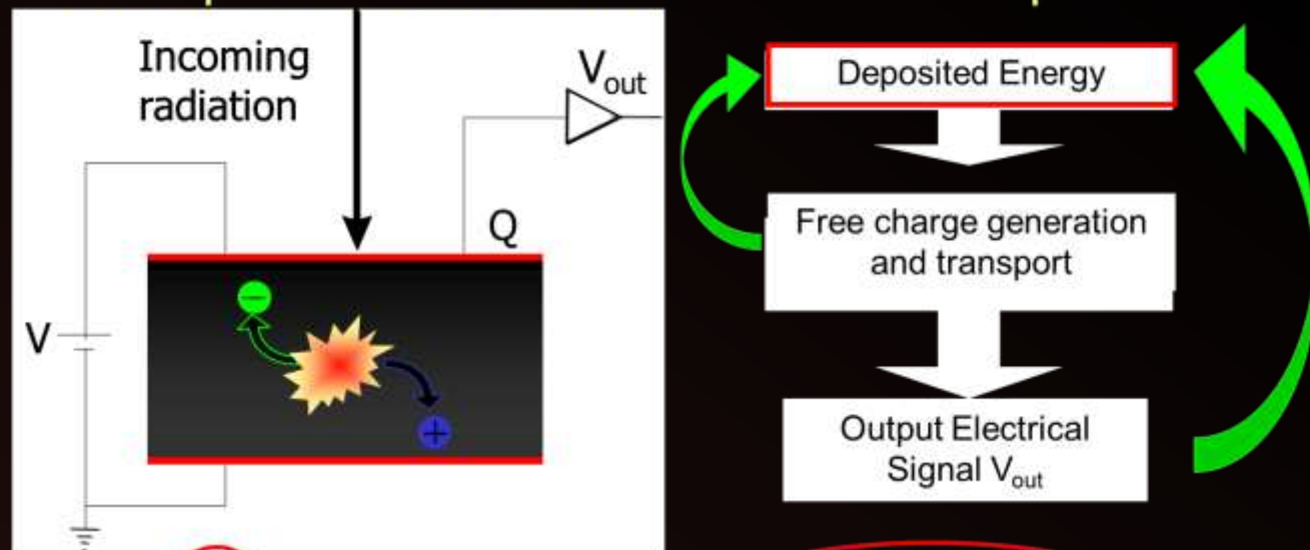

Ion Beam Induced Charge (IBIC)

Probe: MeV ion beams
Single ion detection
Induced charge mapping
Finished device

M.B.H. Breese, G.W. Grime and F. Watt, Oxford Nuclear Physics rep. OUNP-91-33 (1991).

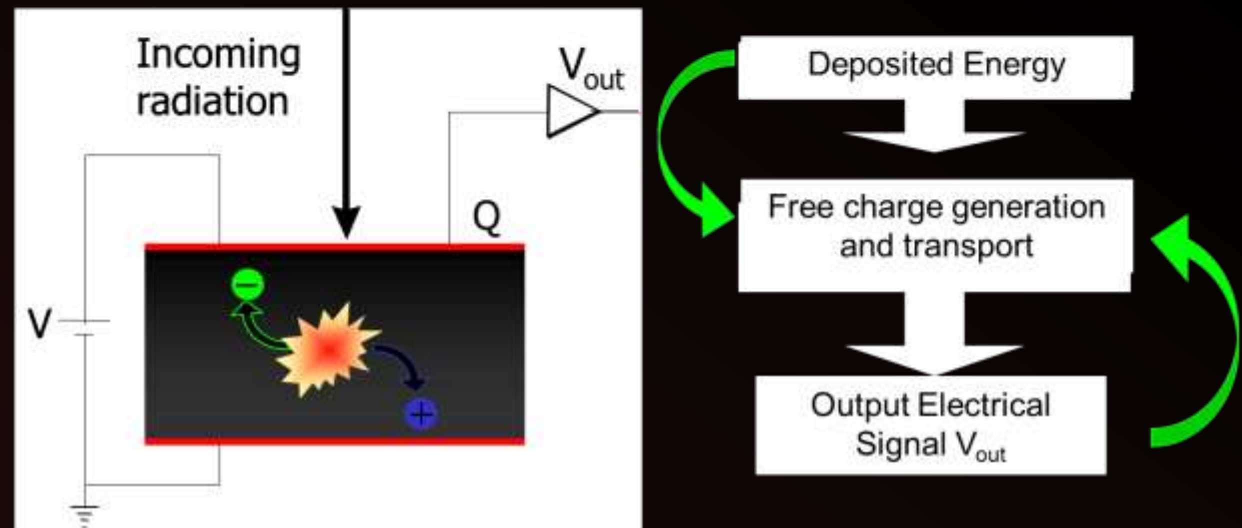

IBIC principles

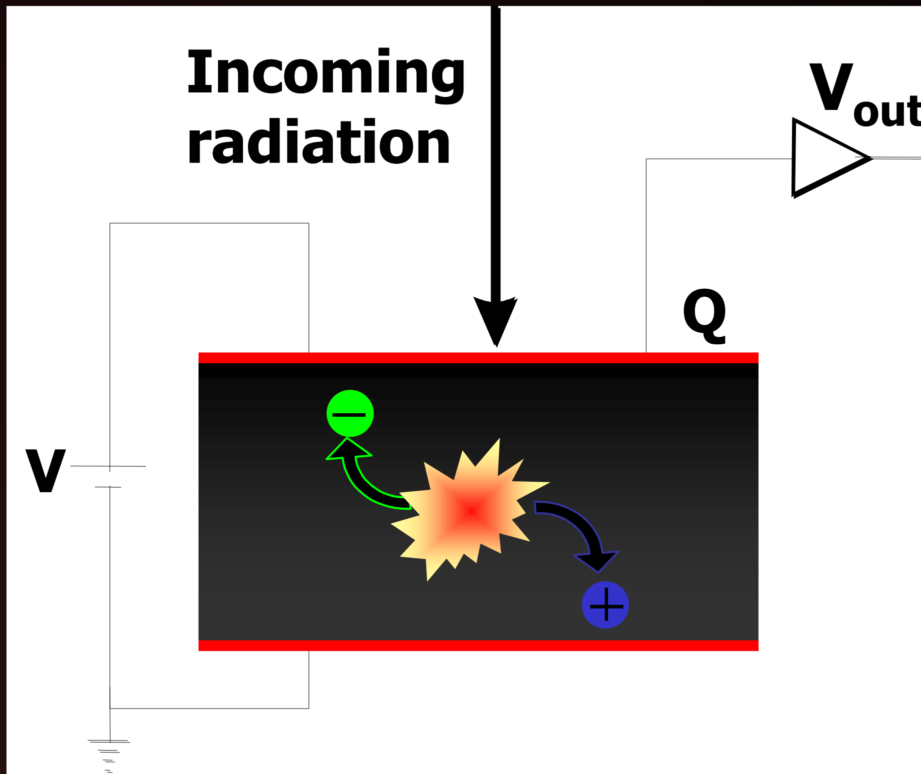

MeV ion Energy deposition

Electron/hole pair generation

Charge carrier transport

Induced Charge at the sensing electrode

Output Signal V_{out}

Elettrons
(Casino 1.0)

Protons
(SRIM 2008)

10 keV
20 keV
30 keV
15 µm
20 µm

2 MeV
3 MeV
4 MeV
110 µm
20 µm

With respect to OBIC, XBIC, EBIC

- larger analytical depth
- lower scattering through the surface layers
- flexibility due to the possibility of using different ions

Higher spatial resolution in buried layers
Depth profiling

IBIC principles

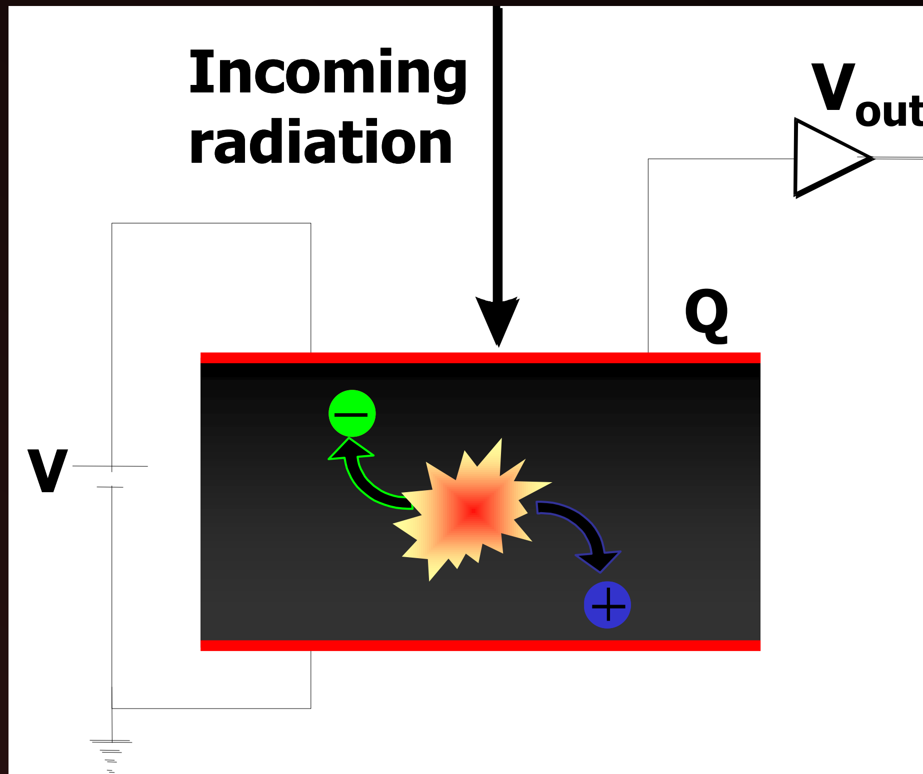

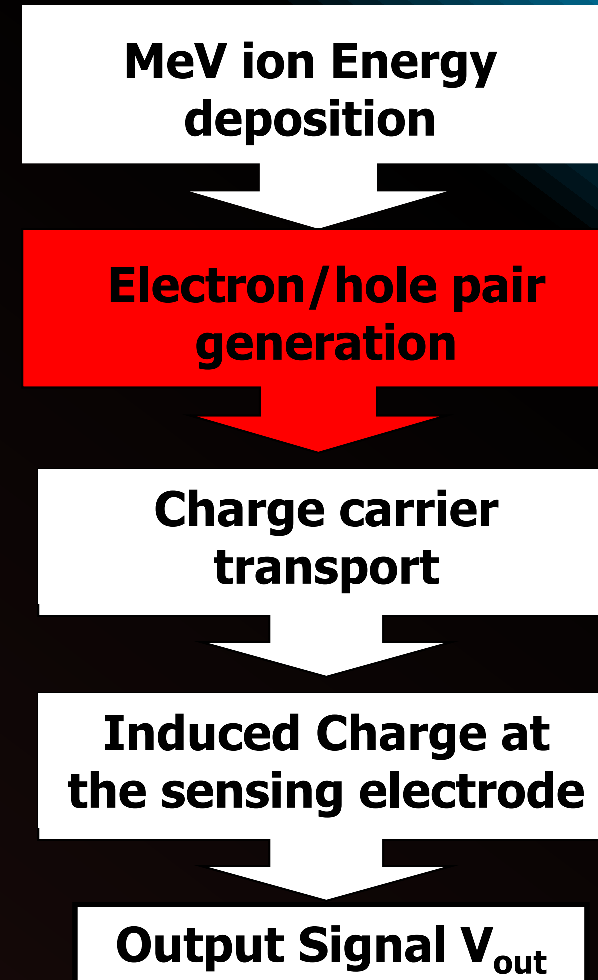

Energy Loss

H+ ion energy (MeV)

IBIC

0.7 0.9 1.1 1.3 1.5 1.7

Stopping power (keV μm^{-1})

200 150 100 50 0

XBICC

3 keV Photon current: $5*10^7$ photons/s

X-ray energy loss rate (keV\g(m)m^{-1} s^{-1})

$3x10^7$ $2x10^7$ $1x10^7$ 0

0 5 10 15 20 25 30

Depth (μm)

Electrode energy loss very small (≅ 1%)

SRIM (Stopping and Range of Ion in Matter)

Electron/Hole pair generation

$$N_{eh} = \frac{E_{ion}}{\varepsilon_{eh}}$$

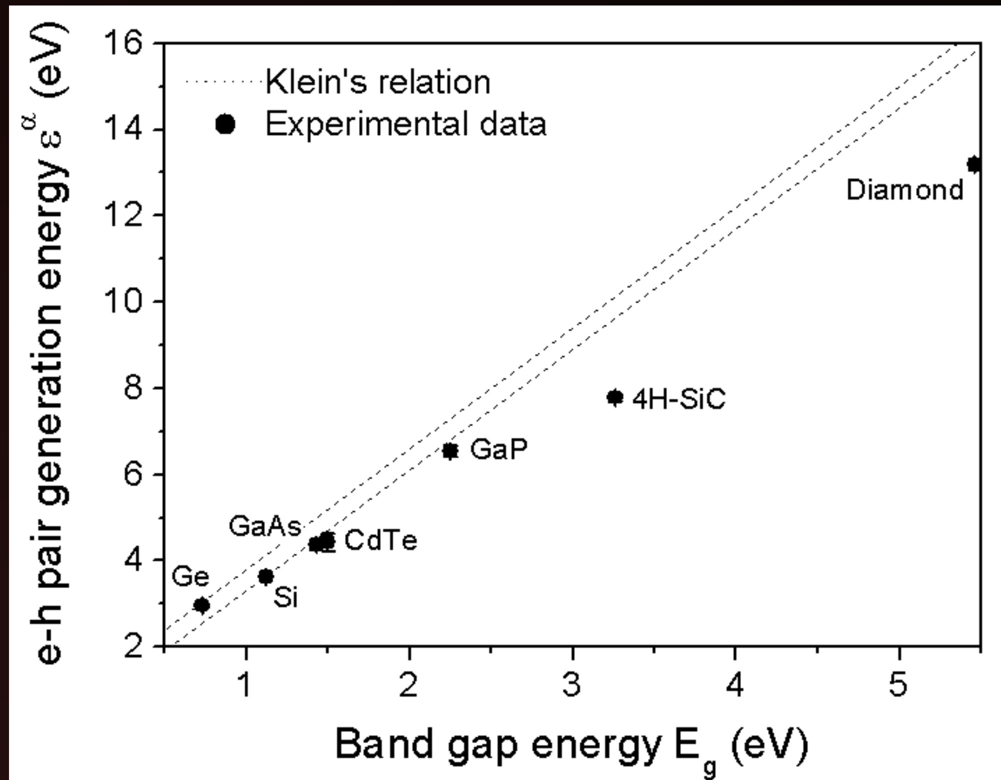

1 MeV in Si generates about 300000 e/h pairs

Single ion detection

A. Lo Giudice et al. Applied Physics Letters 87, 22210 (2005)

IBIC principles

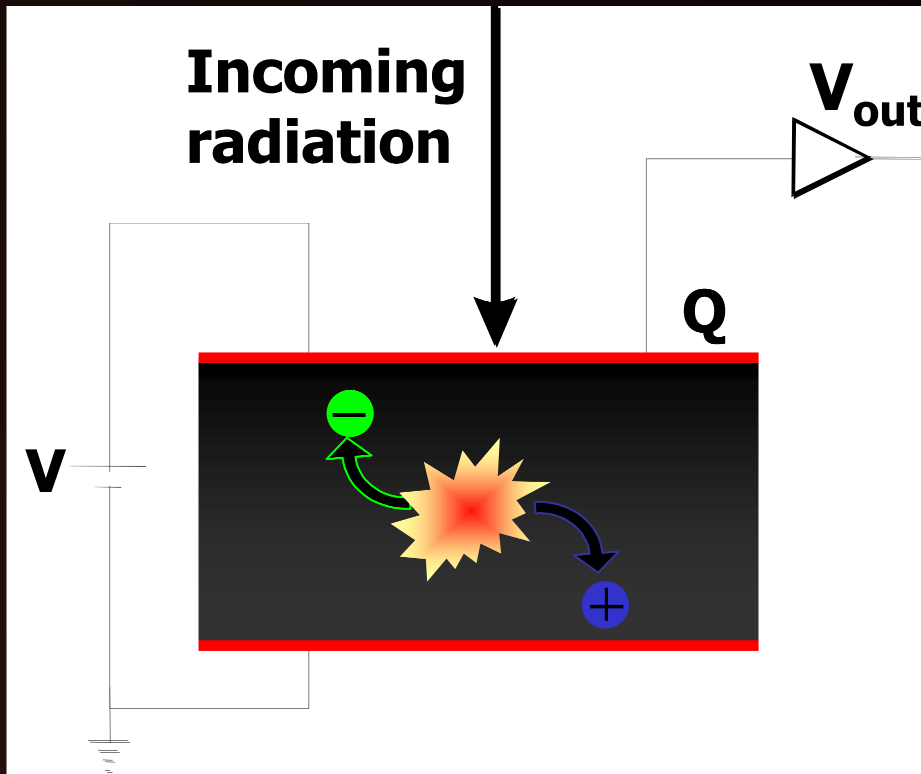

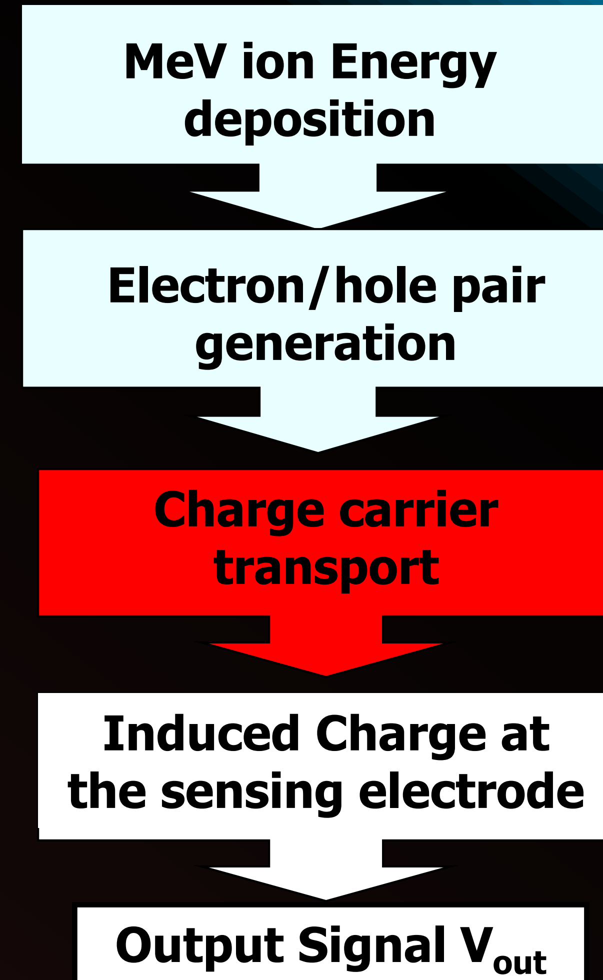

J.R. Haynes, W. Shockley,

“The mobility and life of injecting holes and electrons in germanium,

Phys. Rev. 81, (1951), 835-843.

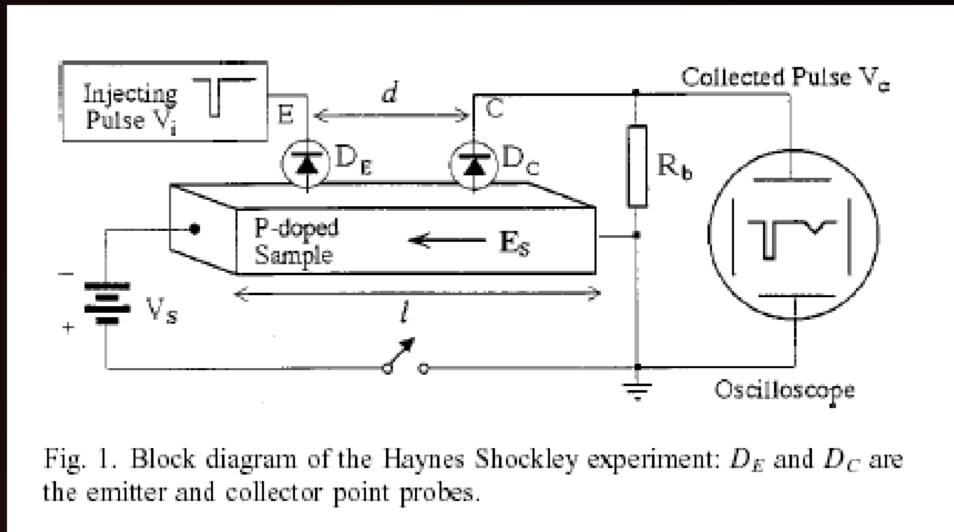

Fig. 1. Block diagram of the Haynes Shockley experiment: D_E and D_C are the emitter and collector point probes.

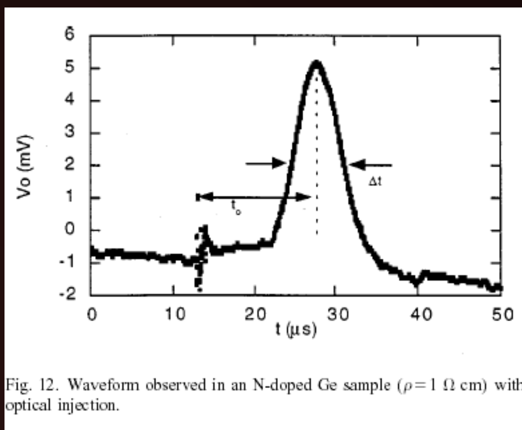

Fig. 12. Waveform observed in an N-doped Ge sample ($\rho = 1\ \Omega$ cm) with optical injection.

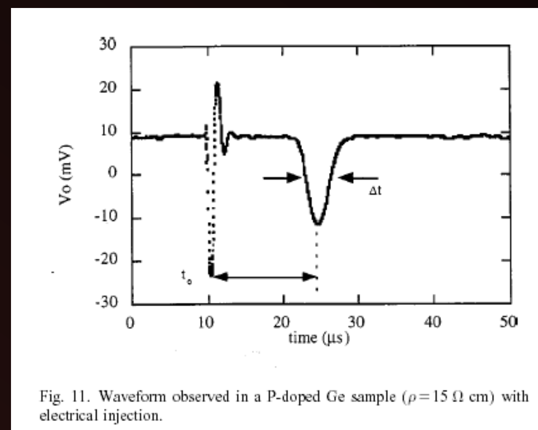

Fig. 11. Waveform observed in a P-doped Ge sample ($\rho = 15\ \Omega$ cm) with electrical injection.

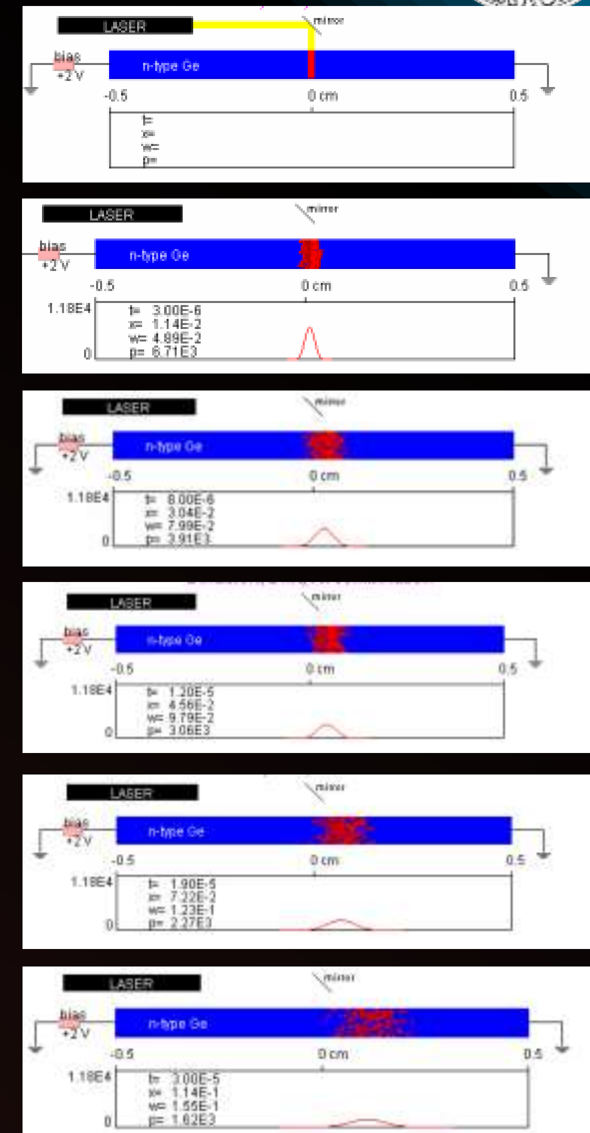

IBIC principles

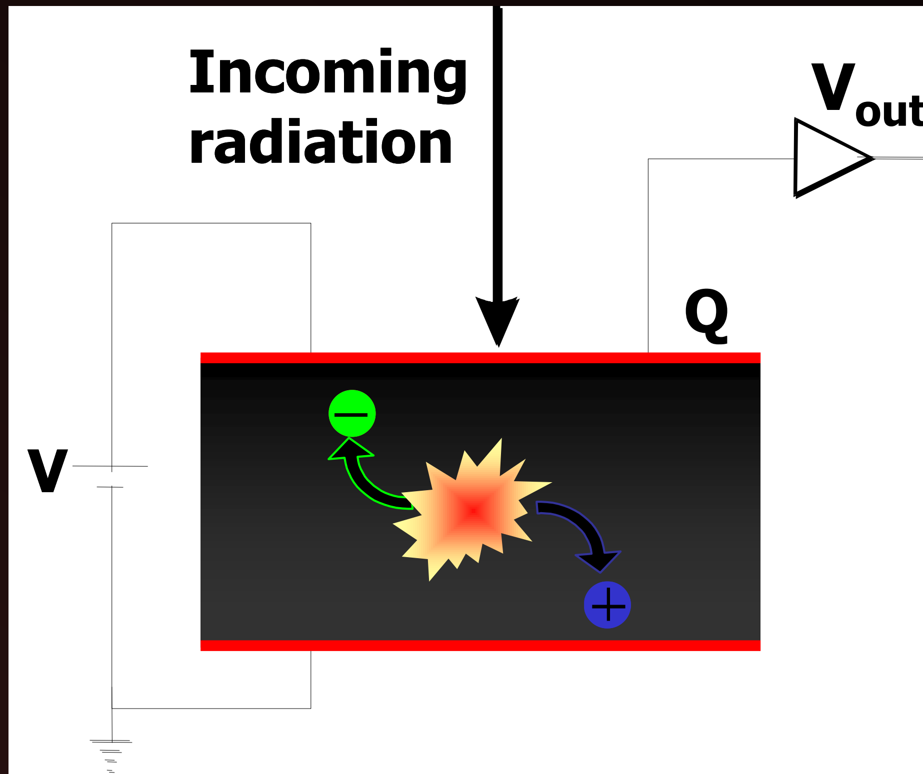

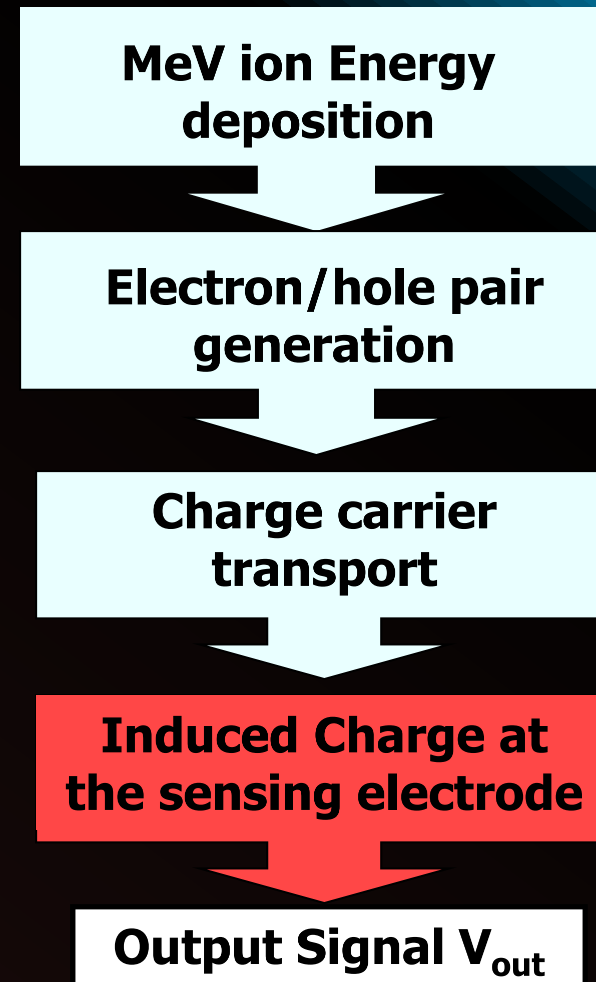

P-doped Ge sample; resistivity about 15 Ω·cm; dielectric constant =1.4pF/cm; Dielectric relaxation time = 21 ps.

IIa diamond; resistivity about 10^{15} Ω·cm; dielectric constant =0.5 pF/cm; Dielectric relaxation time = 500 s.

Charge neutrality not maintained

400 μm thick natural diamond, biased at 40 V @ RT

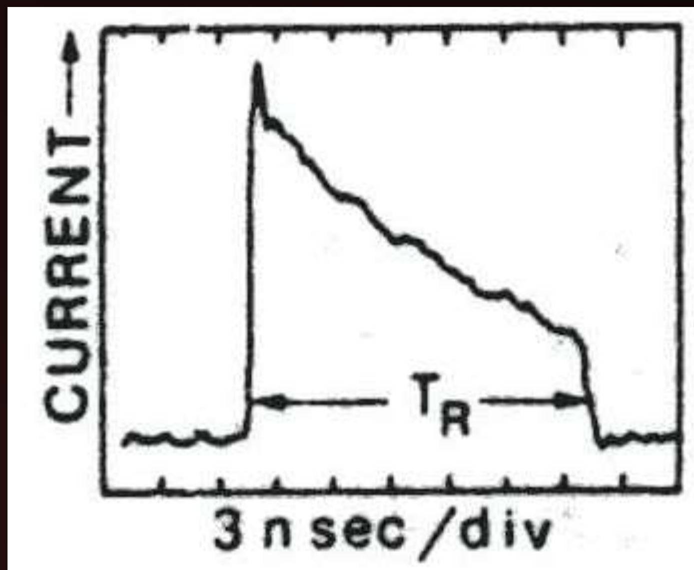

C. Canali et al. Nucl. Instr. Meth. 160 (1979) 73-77

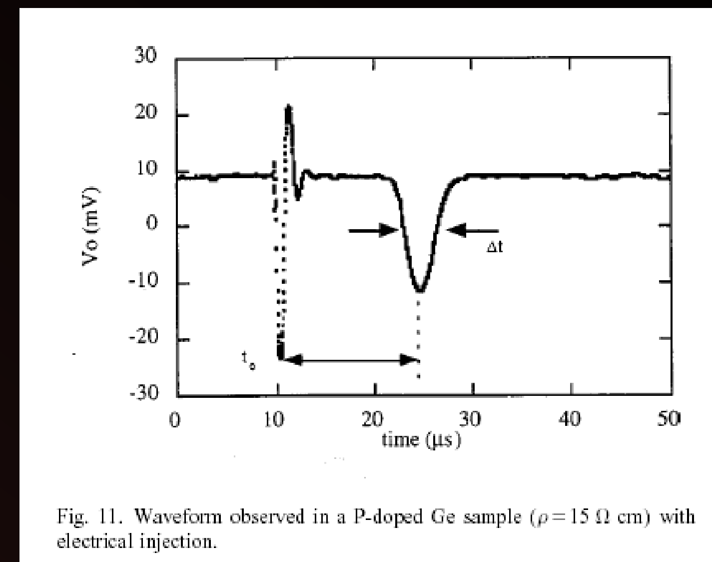

Fig. 11. Waveform observed in a P-doped Ge sample ($\rho = 15$ Ω cm) with electrical injection.

J.R. Haynes, W. Shockley,

Phys. Rev. 81, (1951), 835-843.

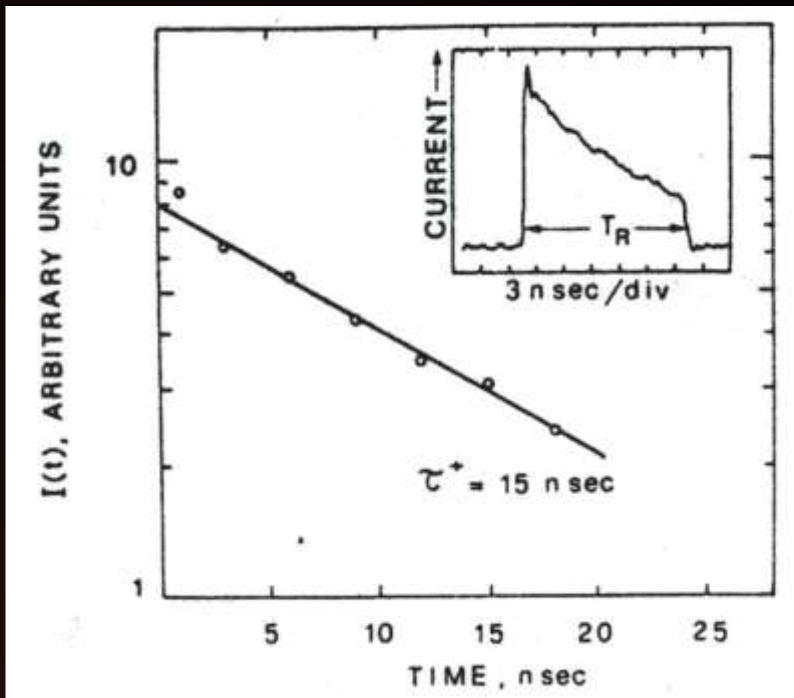

C. Canali et al. Nucl. Instr. Meth. 160 (1979) 73-77

400 μm thick natural diamond,

biased at 40 V @ RT

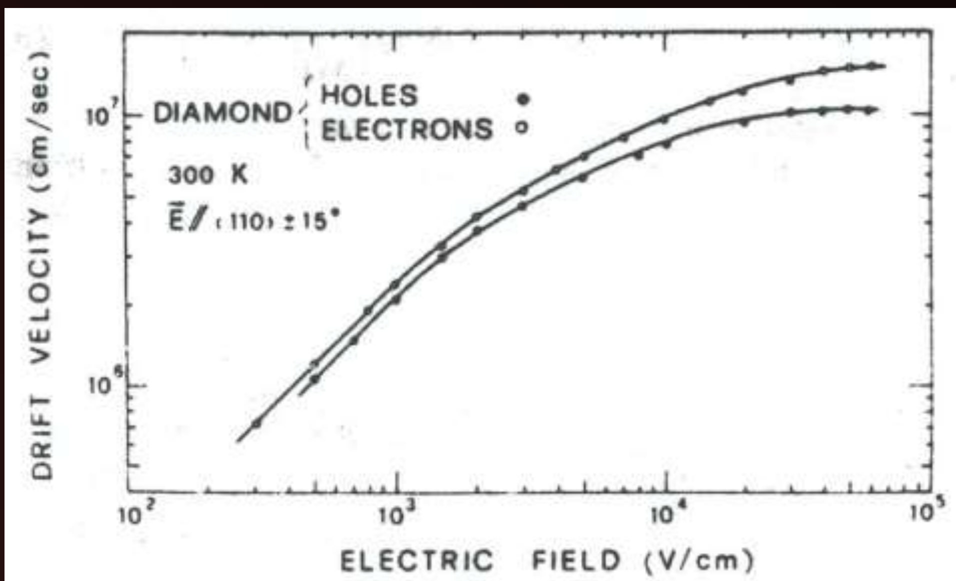

Lifetime = 15 ns

Drift velocity; $v = \mu E = d/T_R$

Mobility; $\mu = d^2/(T_R * V_{Bias})$

Pulse shapes calculation

Shockley-Ramo theorem

Currents to Conductors Induced by a Moving Point Charge
W. Shockley
Bell Telephone Laboratories, Inc., New York, N. Y.
(Received May 14, 1938)

Currents Induced by Electron Motion*
SIMON RAMO†, ASSOCIATE MEMBER, I.R.E.

$$I = -q \cdot \mathbf{v} \cdot \frac{1}{d}$$

Gunn theorem

Gunn's theorem

Solid-State Electronics Pergamon Press 1964. Vol. 7, pp. 739–742. Printed in Great Britain

A GENERAL EXPRESSION FOR ELECTROSTATIC INDUCTION AND ITS APPLICATION TO SEMICONDUCTOR DEVICES *

J. B. GUNN
IBM Watson Research Center, Yorktown Heights, New York
(*Received 2 March 1964; in revised form 26 March 1964*)

Abstract—A new formula is deduced, under rather general conditions, for the charges induced upon a system of conductors by the motion of a small charge nearby. The conditions are found under which this result can be simplified to yield various previously derived formulas applicable to the problem of collector transit time in semiconductor devices.

$$I = -q \cdot \mathbf{v} \cdot \frac{\partial \mathbf{E}}{\partial V}$$

Weighting field

Induced current into the sensing electrode

Gunn's theorem

Solid-State Electronics Pergamon Press 1964. Vol. 7, pp. 739–742. Printed in Great Britain

A GENERAL EXPRESSION FOR ELECTROSTATIC INDUCTION AND ITS APPLICATION TO SEMICONDUCTOR DEVICES

J. B. GUNN

IBM Watson Research Center, Yorktown Heights, New York

(Received 2 March 1964; in revised form 26 March 1964)

Abstract—A new formula is deduced, under rather general conditions, for the charges induced upon a system of conductors by the motion of a small charge nearby. The conditions are found under which this result can be simplified to yield various previously derived formulas applicable to the problem of collector transit time in semiconductor devices.

Equation of motion: $\mathbf{v} = \frac{d\mathbf{r}}{dt}$

$$Q = \int_{t_A}^{t_B} I dt = -q \int_{t_A}^{t_B} \mathbf{v} \cdot E_w dt = -q \int_{\mathbf{r}_A}^{\mathbf{r}_B} E_w d\mathbf{r} =$$

$$= q \cdot \left(\psi_w(\mathbf{r}_B) - \psi_w(\mathbf{r}_A)\right) = q \cdot \left(\left.\frac{\partial\psi}{\partial V}\right|_{\mathbf{r}_B} - \left.\frac{\partial\psi}{\partial V}\right|_{\mathbf{r}_A} \right)$$

The induced charge Q into the sensing electrode is given by the difference in the weighting potentials between any two positions (r_A and r_B) of the moving charge

4H-SiC Schottky diode

Starting Material: 360 μm n-type 4H-SiC by CREE (USA)
Epitaxial layer from Institute of Crystal Growth (IKZ), Berlin, Germany
Devices from Alenia Marconi System

CCE=Charge Collection Efficiency
=
(Charge collected)/(Charge generated)

1.5 or 2.0

MeV H+

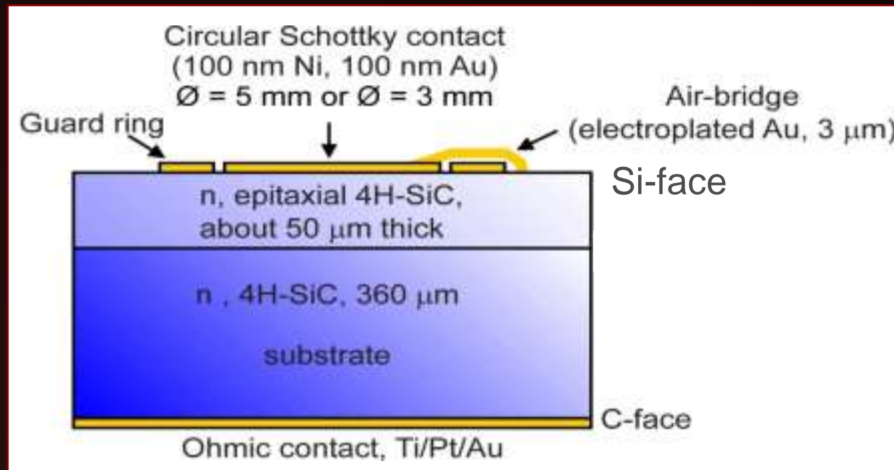

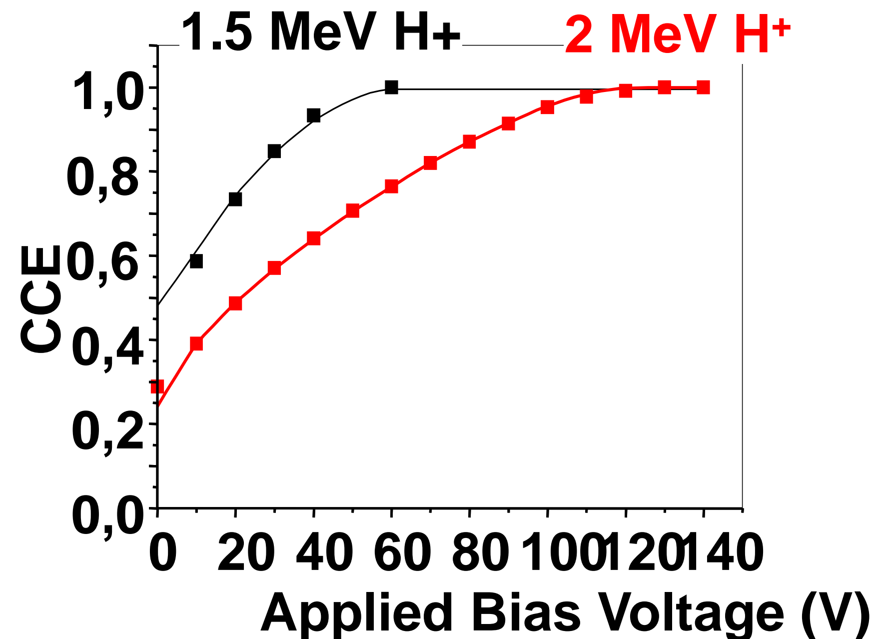

Schottky electrode

50 μm thick N-type epitaxial 4H-SiC layer

Frontal ion Irradiation

Depletion Region

1.5 MeV

2 MeV

Energy Loss (keV/μm^{-1})

Applied Bias Voltage (V)

Depth (μm)

Bragg.opj

FAST DRIFT

COMPLETE COLLECTION

DIFFUSION

Generation of electrons and holes in the

Depletion Region

Electrons

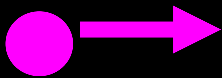

Holes

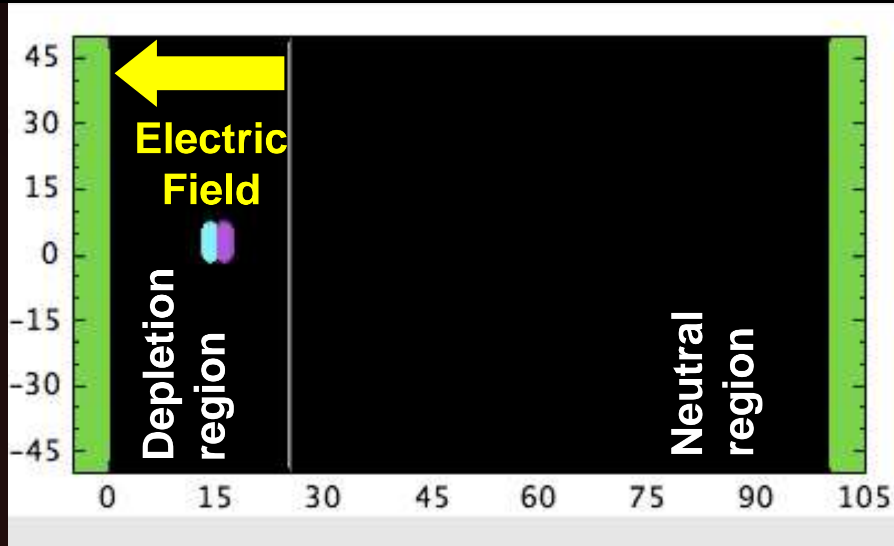

Complete charge collection

Neutral Region

Electrons

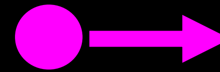

Holes

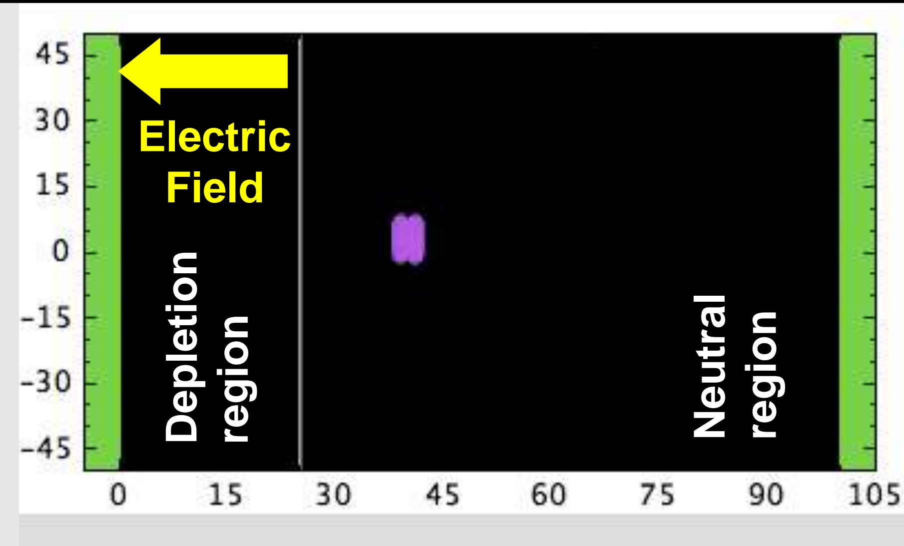

Only holes injected in the depletion region by diffusion induce a charge

Contribution from the neutral region

Contribution from the depletion layer

$$Q = Q_{Depl} + Q_{Neutr} \propto \left[\int_0^W \left(\frac{dE}{dx}\right) \cdot dx\right] + \left[\int_W^d \left(\frac{dE}{dx}\right) \cdot \exp\left[-\frac{x-W}{L_p}\right] \cdot dx\right]$$

Frontal ion Irradiation

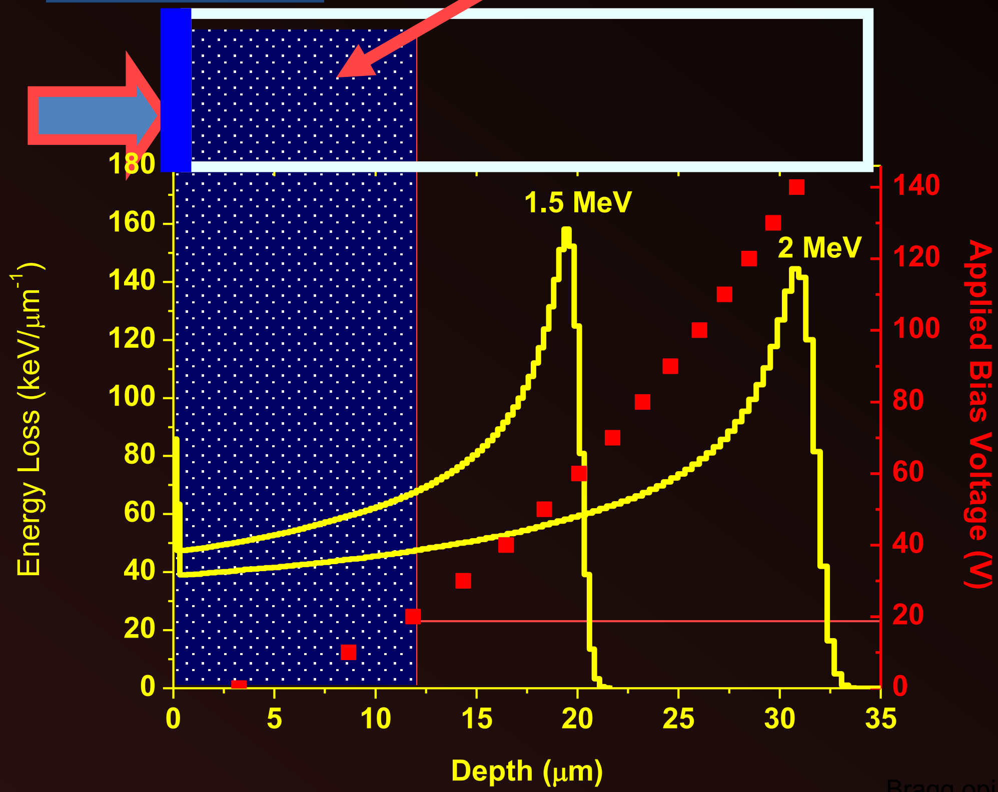

4H-SiC Schottky diode

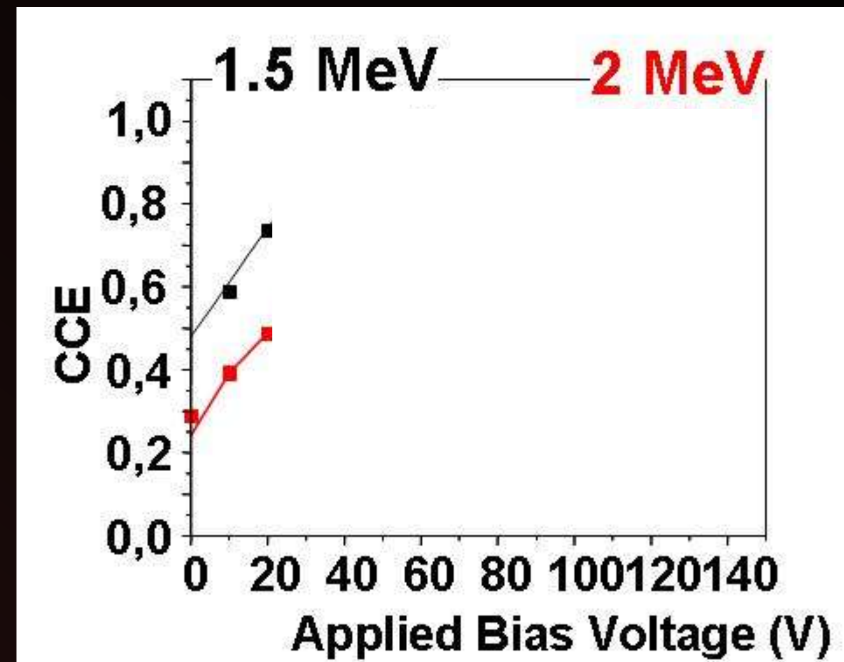

Contribution from the neutral region

Contribution from the depletion layer

$$Q = Q_{Depl} + Q_{Neutr} \propto \left[\int_0^W \left(\frac{dE}{dx}\right)\cdot dx\right] + \left[\int_W^d \left(\frac{dE}{dx}\right)\cdot \exp\left[-\frac{x-W}{L_p}\right]\cdot dx\right]$$

Frontal ion Irradiation

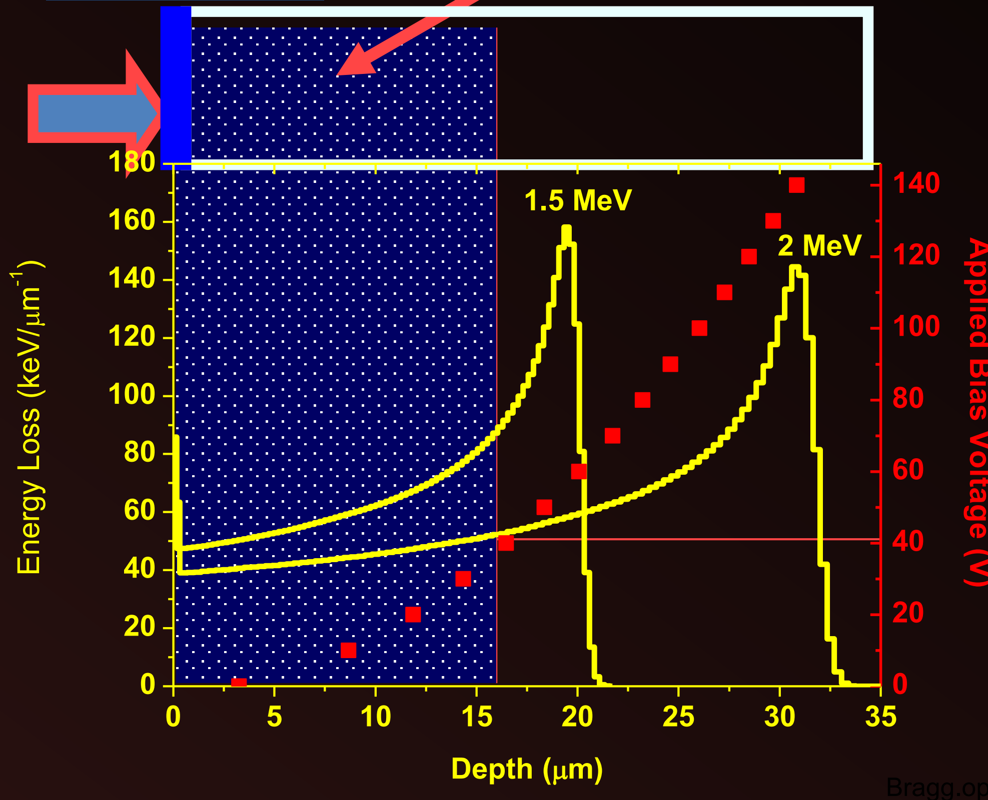

4H-SiC Schottky diode

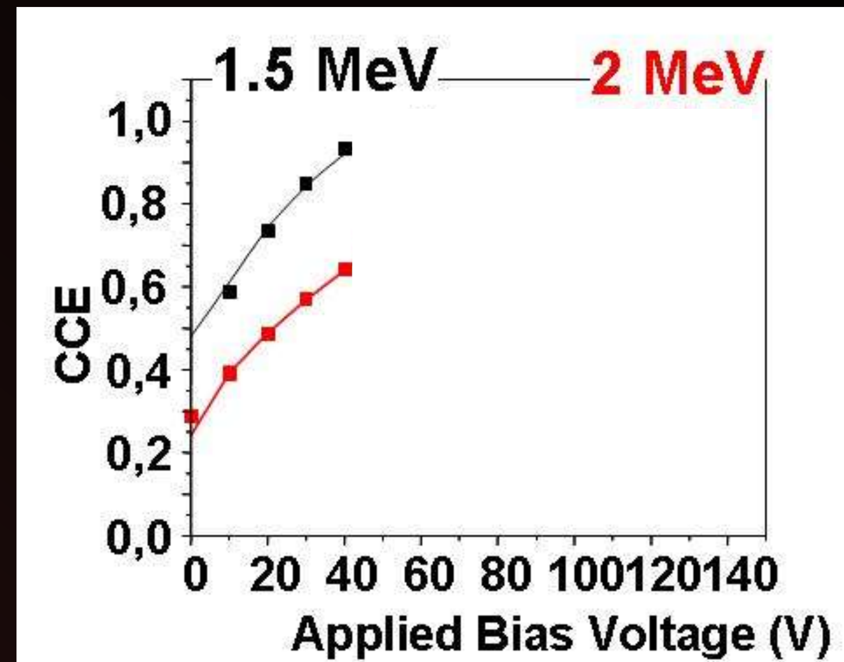

Contribution from the neutral region

Contribution from the depletion layer

$$Q = Q_{Depl} + Q_{Neutr} \propto \left[\int_0^W \left(\frac{dE}{dx}\right)\cdot dx\right] + \left[\int_W^d \left(\frac{dE}{dx}\right)\cdot \exp\left[-\frac{x-W}{L_p}\right]\cdot dx\right]$$

Frontal ion Irradiation

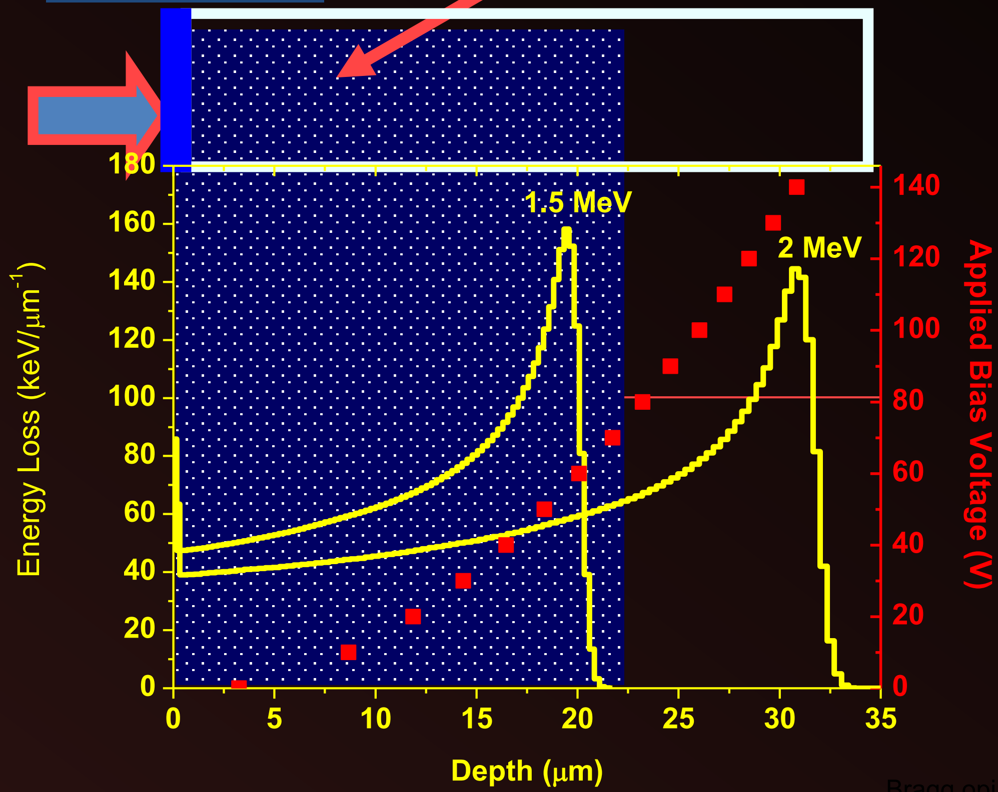

4H-SiC Schottky diode

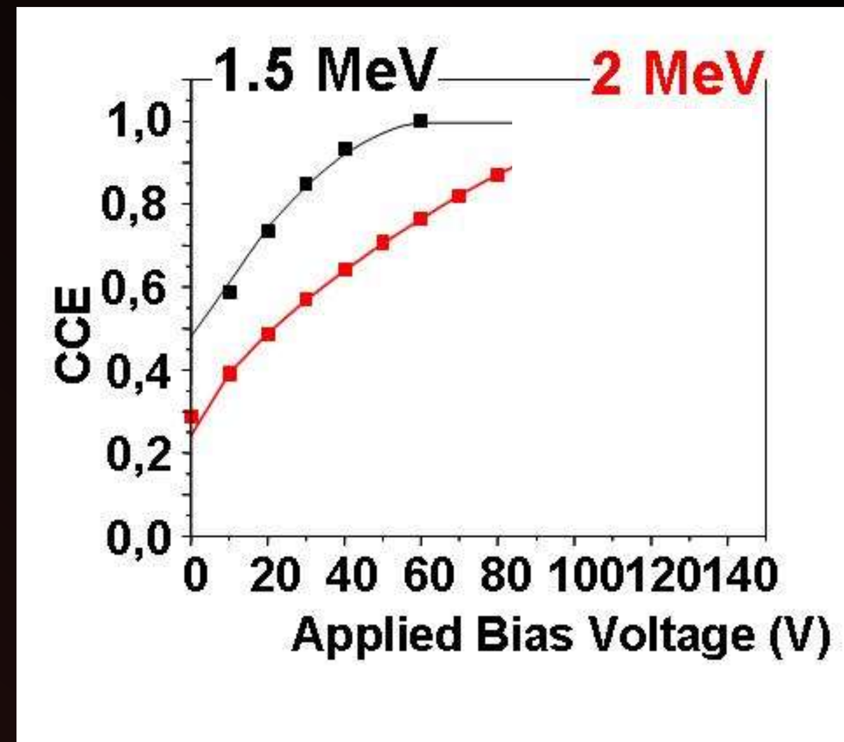

Contribution from the neutral region

Contribution from the depletion layer

$$Q = Q_{Depl} + Q_{Neutr} \propto \left[\int_0^W \left(\frac{dE}{dx}\right) \cdot dx\right] + \left[\int_W^d \left(\frac{dE}{dx}\right) \cdot \exp\left[-\frac{x-W}{L_p}\right] \cdot dx\right]$$

Frontal ion Irradiation

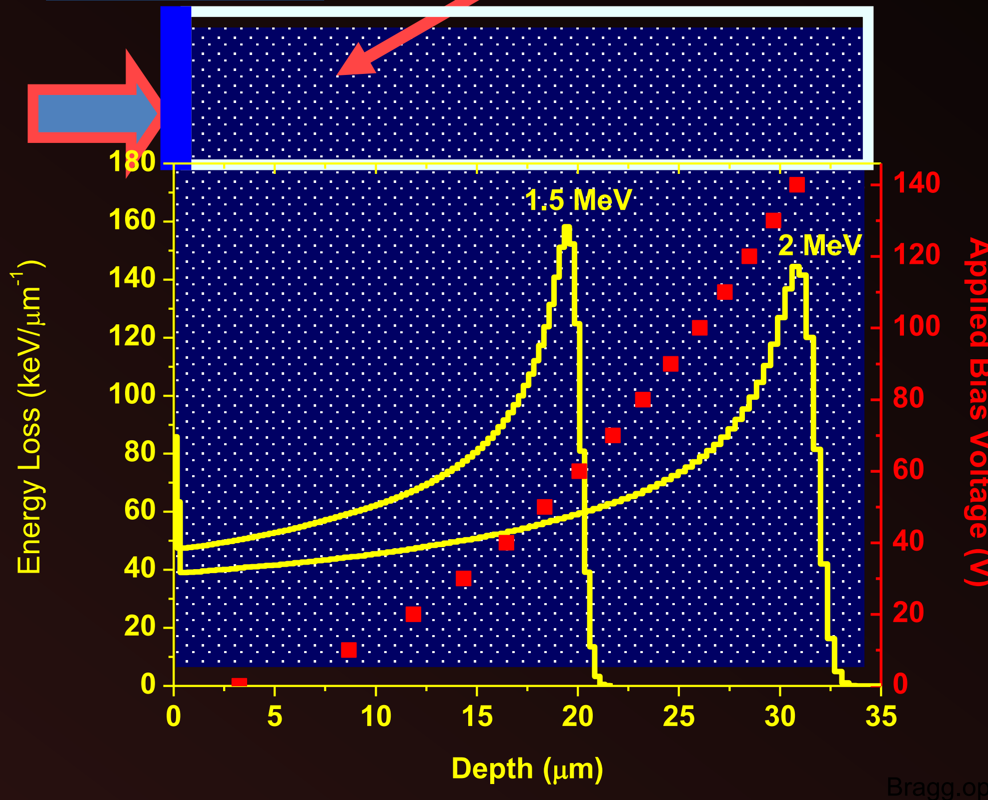

4H-SiC Schottky diode

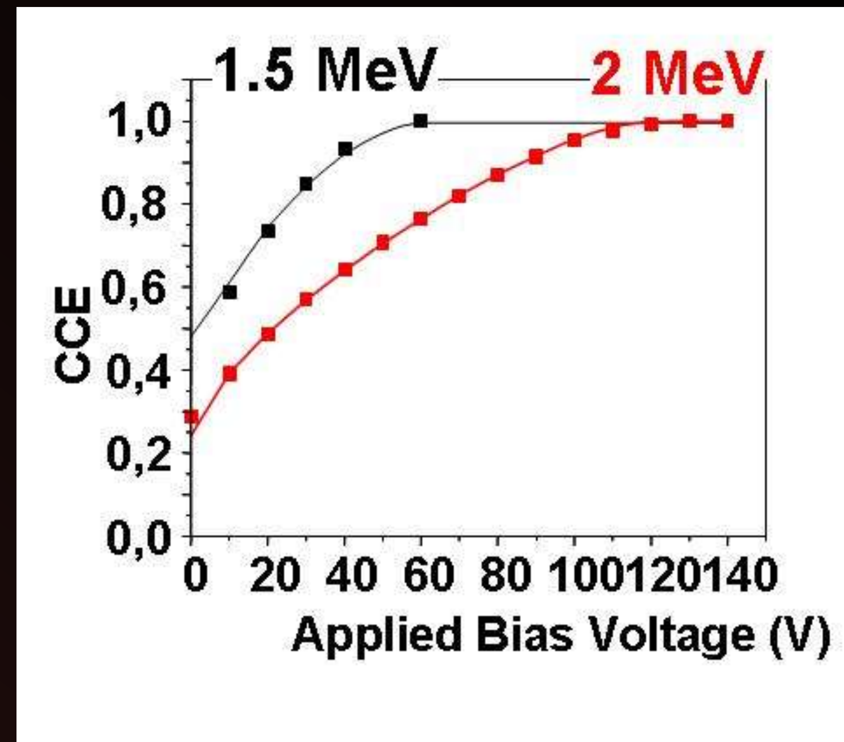

Contribution from the depletion layer

Contribution from the neutral region

$$Q = Q_{Depl} + Q_{Neutr} \propto \left[\int_0^w \left(\frac{dE}{dx} \right) \cdot dx \right] + \left[\int_w^d \left(\frac{dE}{dx} \right) \cdot \exp\left[-\frac{x-W}{L_p} \right] \cdot dx \right]$$

Active region width

minority carrier diffusion length

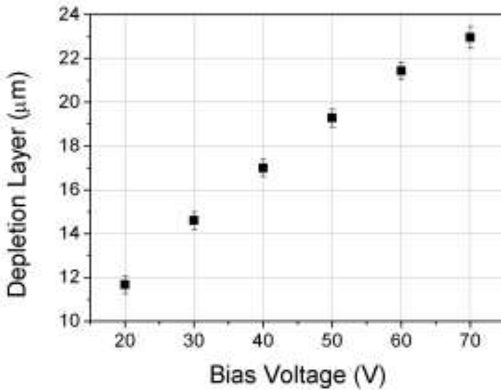

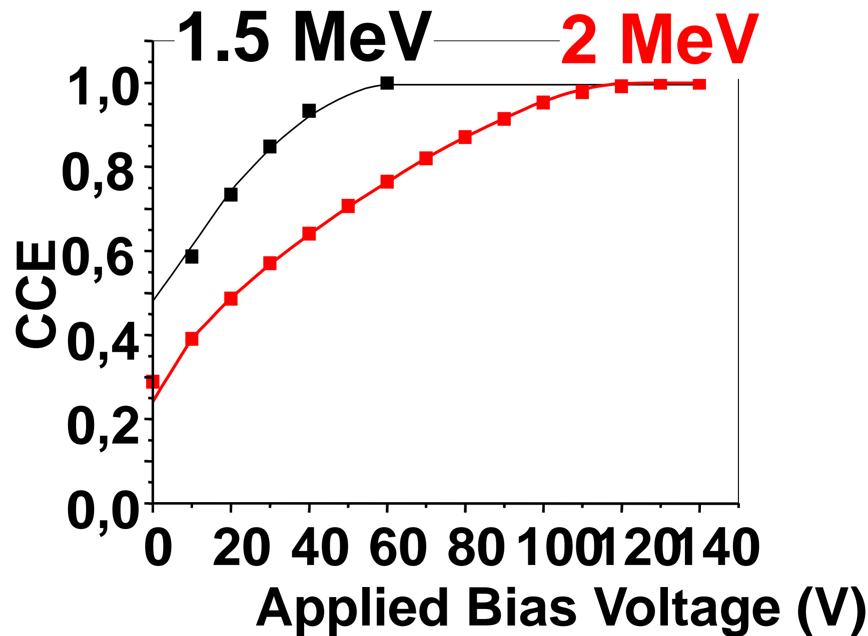

L_p=(9.0±0.3) µm

D_p = 3 cm²/s

τ_p = 270 ns

4H-SiC Schottky diode

ANGLE RESOLVED IBIC (ARIBIC)

2 MeV proton beam

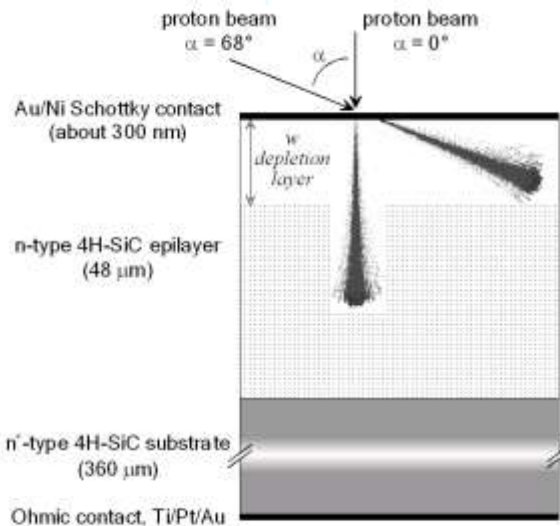

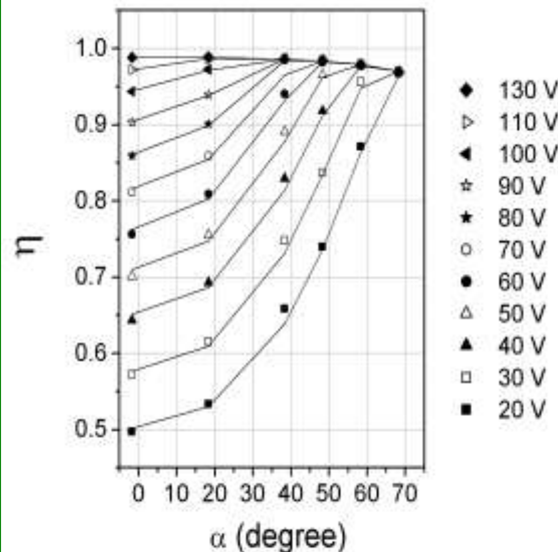

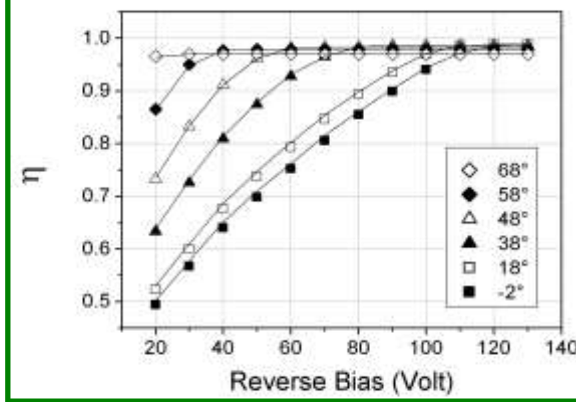

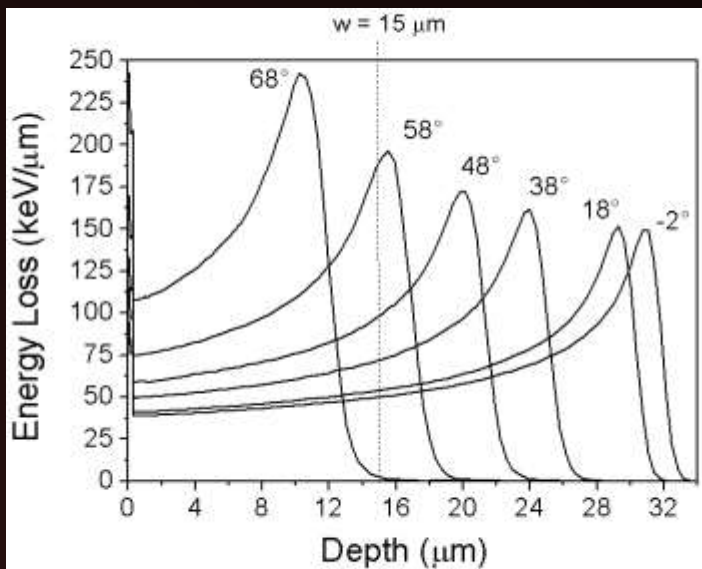

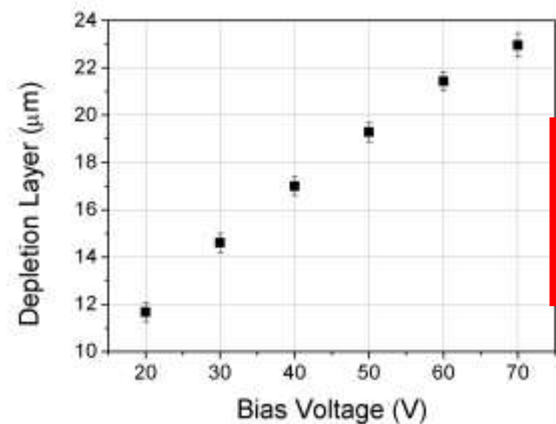

L=(9.9±0.8) μm

Dead layer energy loss of 23±5 keV at α=0°.

A. Lo Giudice et al. Nuclear Instruments and Methods in Physics Research B 249 (2006) 213–216

Temperature dependent IBIC (TIBIC)

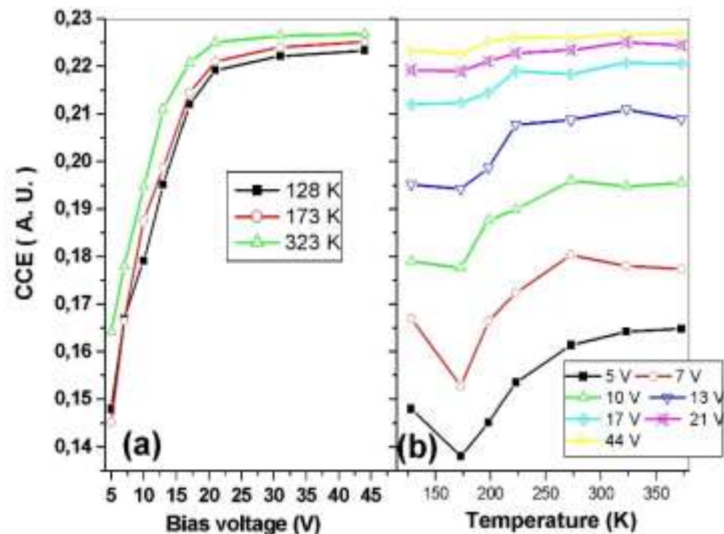

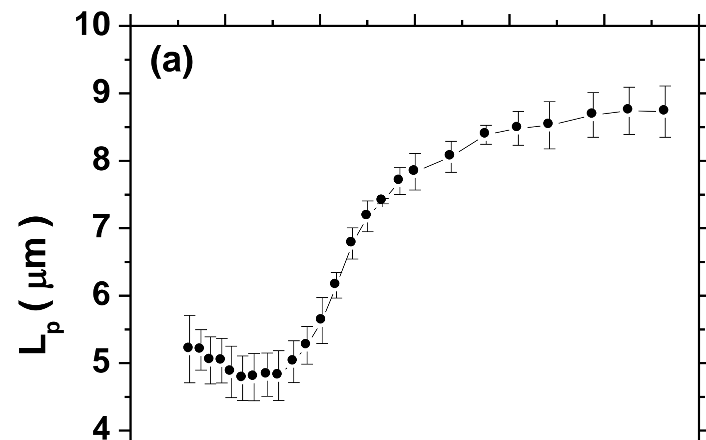

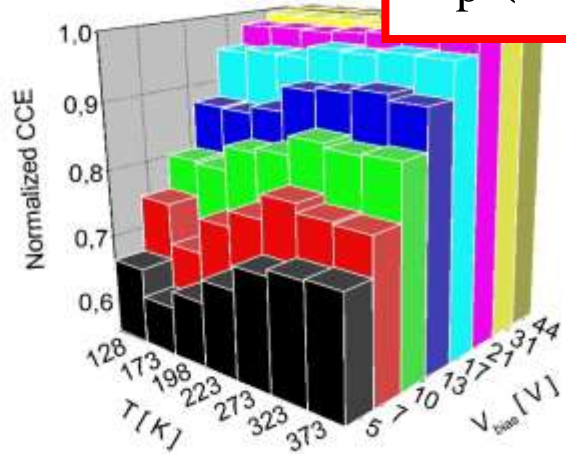

$$L_p(T) = \sqrt{D_p(T) \cdot \tau_p(T)}$$

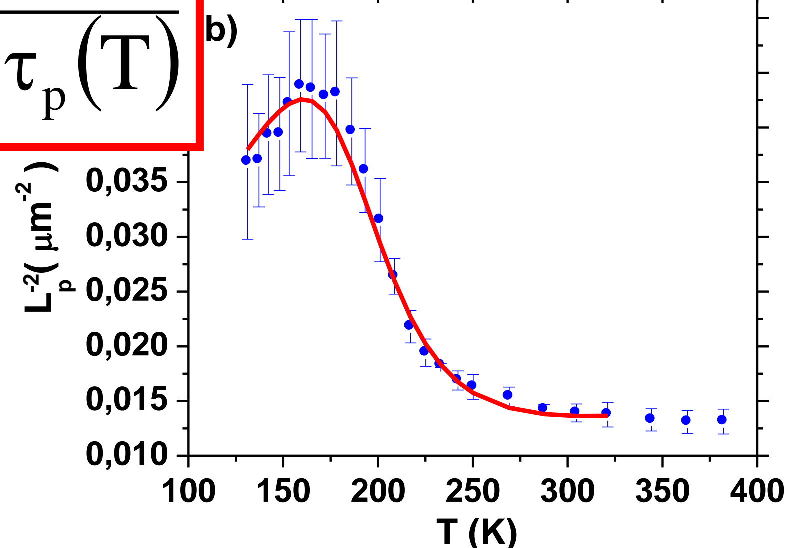

Temperature dependent IBIC (TIBIC)

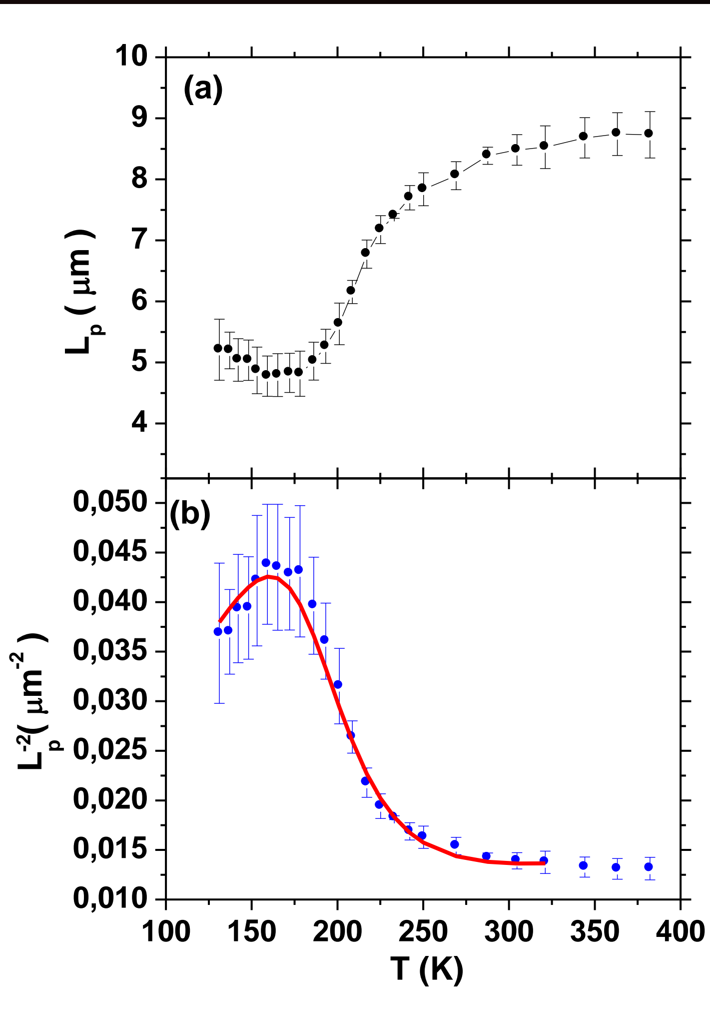

Two trapping levels

SRH recombination model

$$\frac{1}{L_p^2} = \frac{1}{D_p \cdot \tau} = \frac{1}{D_p} \cdot \left(\frac{1}{\tau(T)} + \frac{1}{\tau_B} \right) = A \cdot \frac{1}{T^{-0.5}} \cdot \left[\frac{1}{T^{-0.5} + \frac{B}{N_D} \cdot T \cdot \exp\left(-\frac{E_t}{k_B T} \right)} + \frac{1}{\tau_B} \right]$$

The fitting procedure provides a trapping level of about 0.163 eV which is close to the value found in similar 4H SiC Schottky diodes by DLTS technique (S1 level).

E. Vittone et al., NIM-B 231 (2005) 491.

Time resolved IBIC (TRIBIC) Silicon Power diode Mesa Rectifier

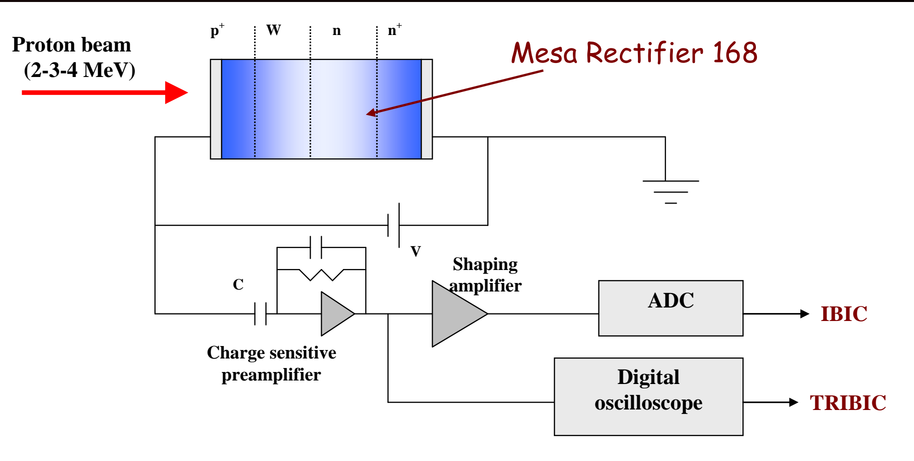

lifetime

$\tau_0 = (5 \pm 1)\ \mu s$

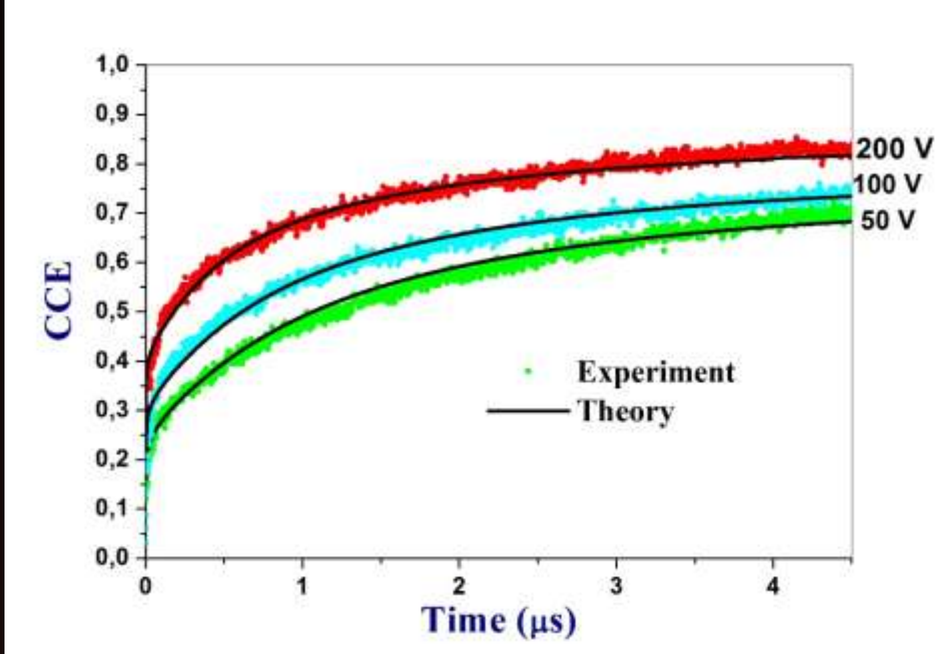

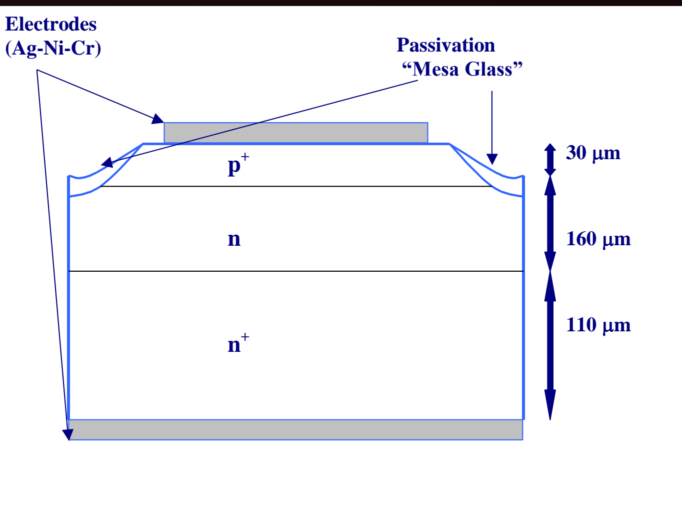

Ballistic deficit

From Spectroscopy to micro-spectroscopy

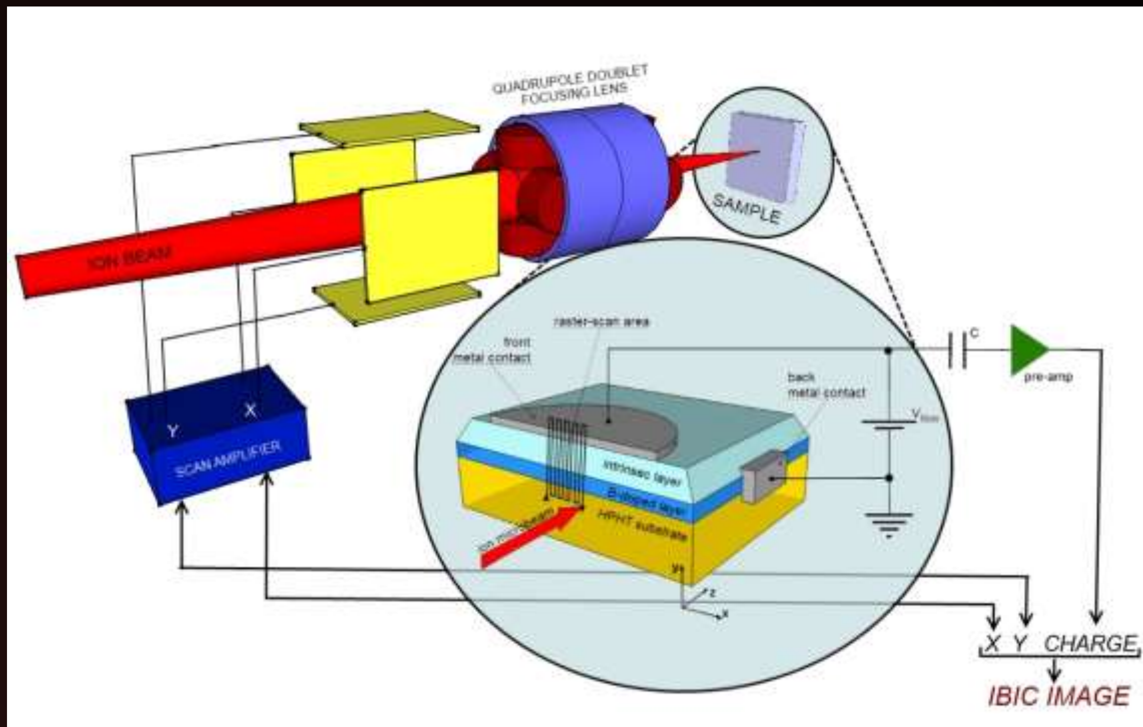

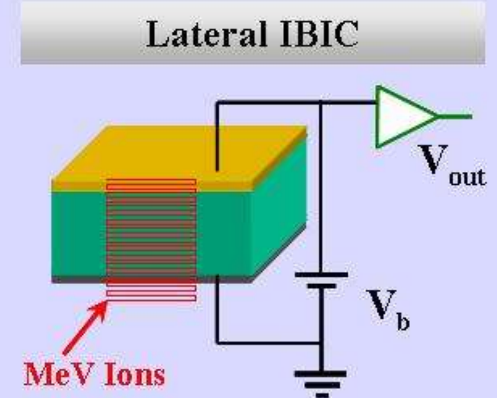

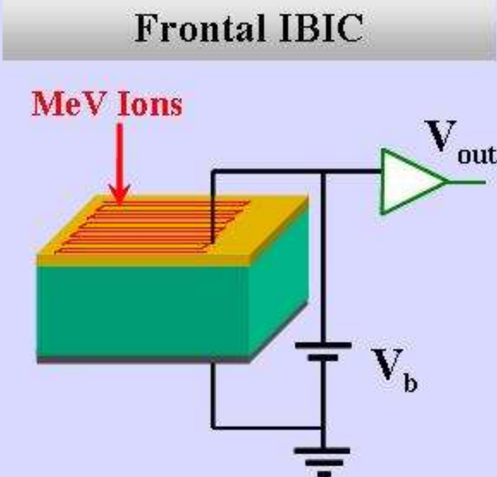

Use of focused ion beams

Trajectories

One advantage of IBIC over other forms of charge collection microscopy is that it provides high spatial resolution analysis in thick layers since the focused MeV ion beam tends to stay 'focused' through many micrometers of material.

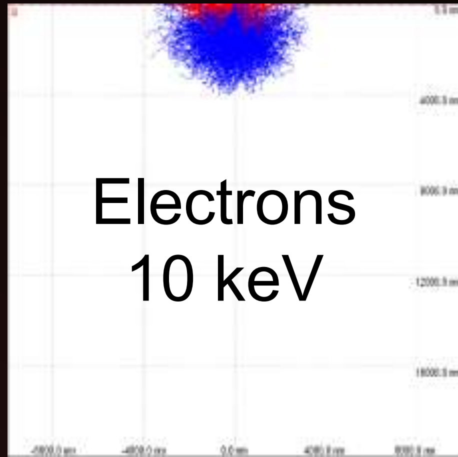

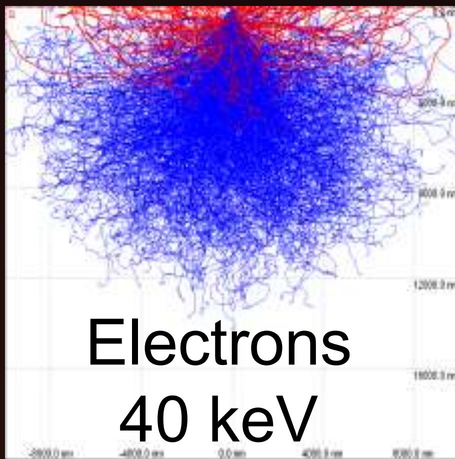

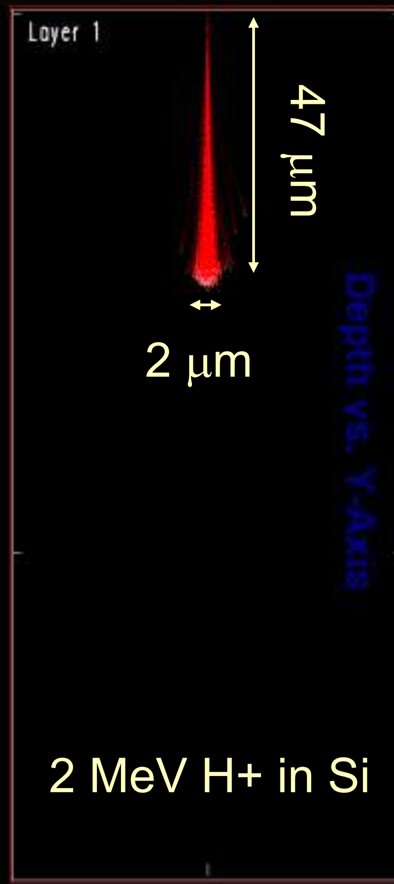

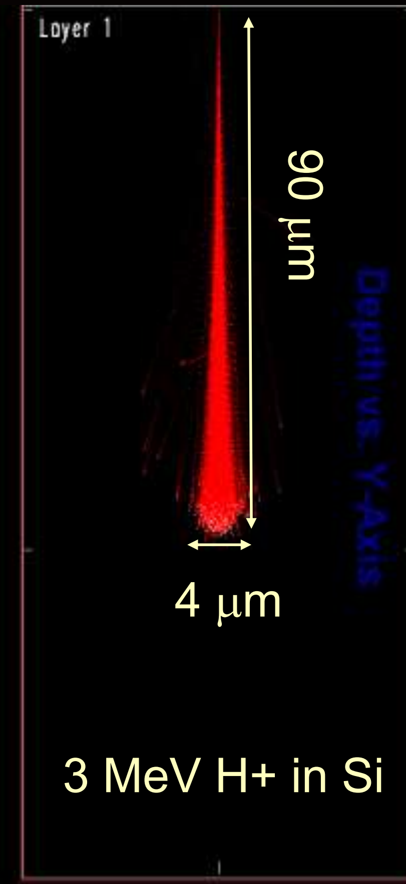

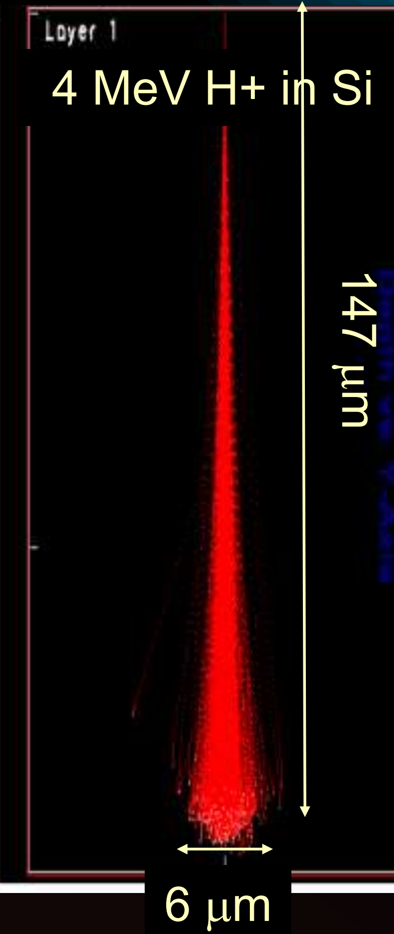

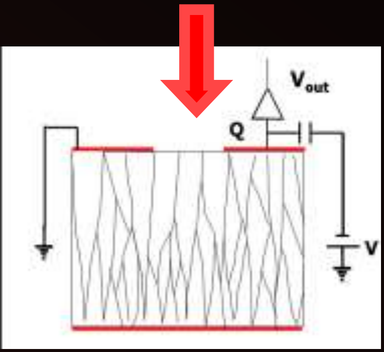

Diamond Detectors

CERN-RD42

collaboration

Frontal IBIC

Polycrystalline

CVD diamond

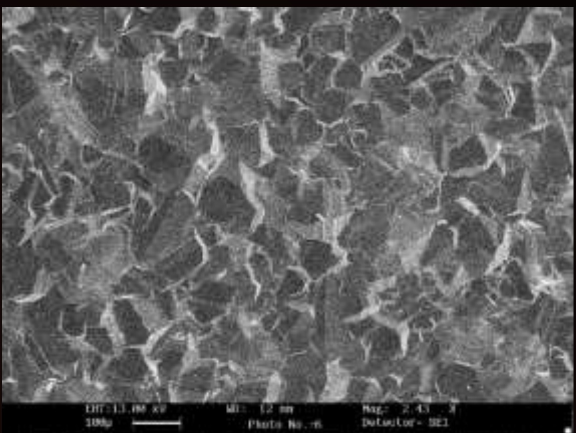

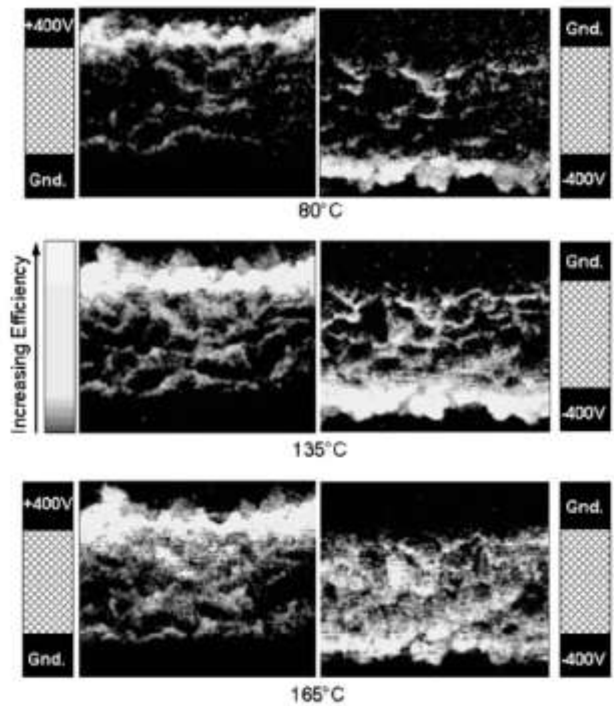

APPLIED PHYSICS LETTERS VOLUME 84, NUMBER 21 31 MAY 2004

Temperature-dependent emptying of grain-boundary charge traps in chemical vapor deposited diamond

S. M. Hearne, D. N. Jamieson,[a] E. Trajkov, and S. Prawer
School of Physics, University of Melbourne, Victoria, 3010, Australia

J. E. Butler

FIG. 1. Ion beam induced charge (IBIC) maps using a scanned 2 MeV He+ microprobe of the charge collection in CVD diamond at various temperatures. The location of the electrodes is shown. Note that the charge collection efficiency is always highest near to the anode.

IBIC imaging with 2 MeV H+

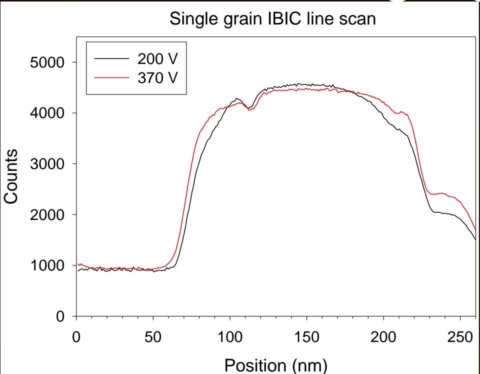

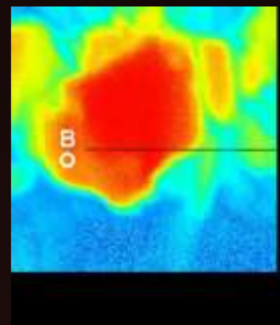

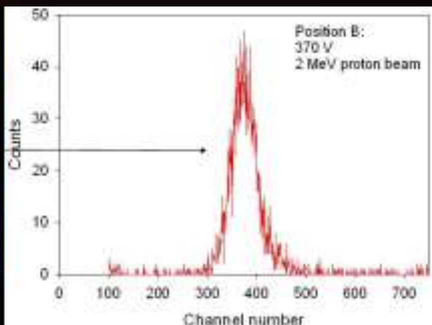

Intra-crystallite charge transport

M.B.H.Breese et al. NIM-B 181 (2001), 219-224; P.Sellin et al. NIM-B 260 (2007), 293-294

GaAs Schottky diode Frontal IBIC

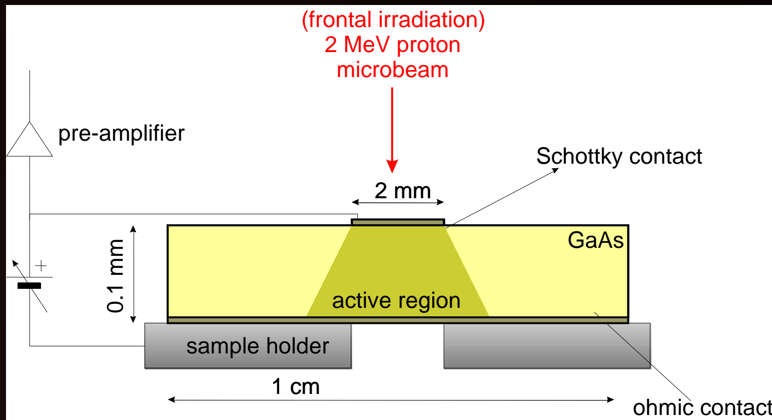

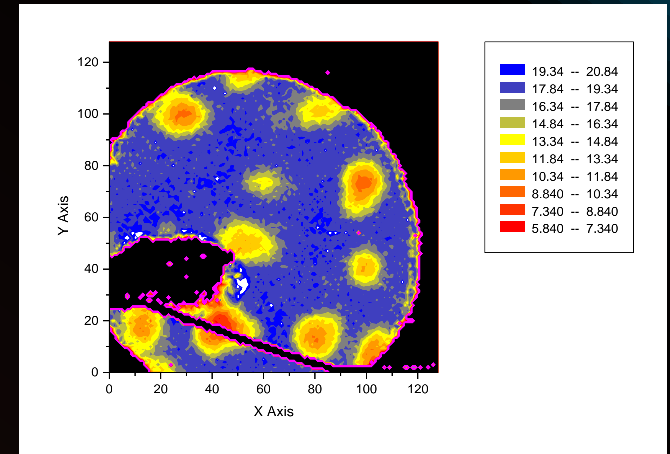

Effects of inhomogeneous cabon doping

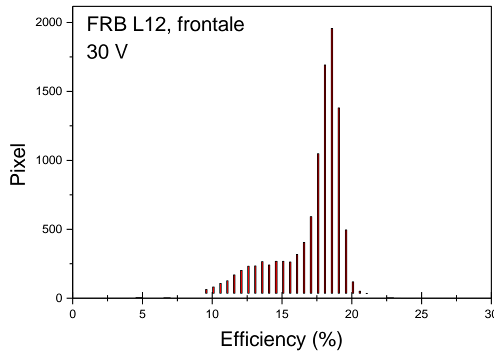

Poor spectral resolution

E. Vittone et al., NIMB 158 (1999) 470-47

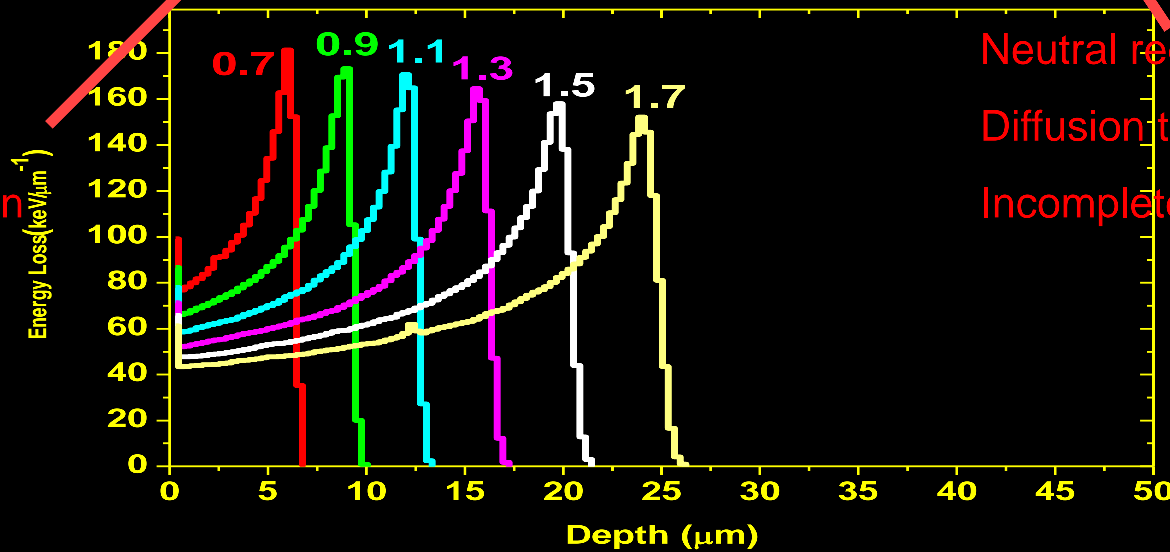

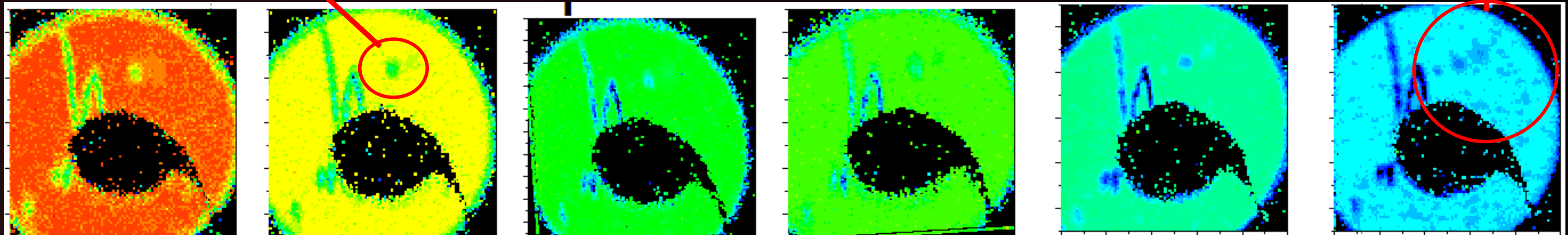

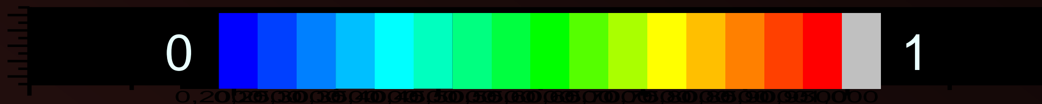

M. Jaksic et al.NIMB188(1-4) (2002) 130-134

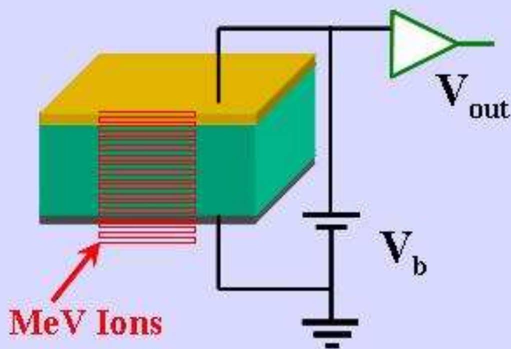

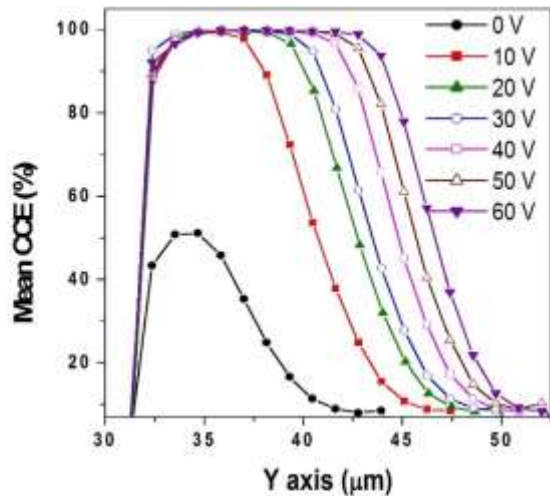

V_{bias} = 0 V | V_{bias} = 5 V | V_{bias} = 10 V | V_{bias} = 15 V | V_{bias} = 20 V

V_{bias} = 25 V | V_{bias} = 30 V | V_{bias} = 40 V | V_{bias} = 50 V | V_{bias} = 60 V

CCE: 100% – 50% – 0%

Lateral IBIC

Si p-n diode

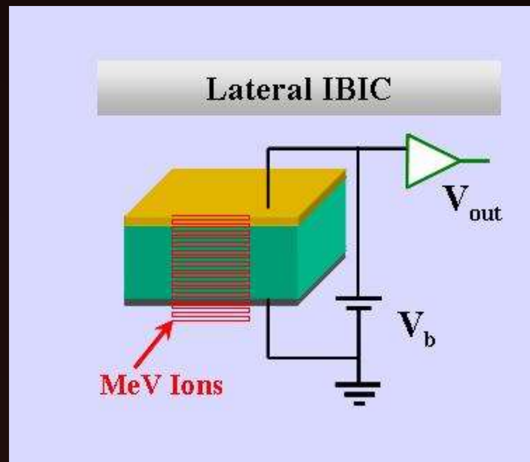

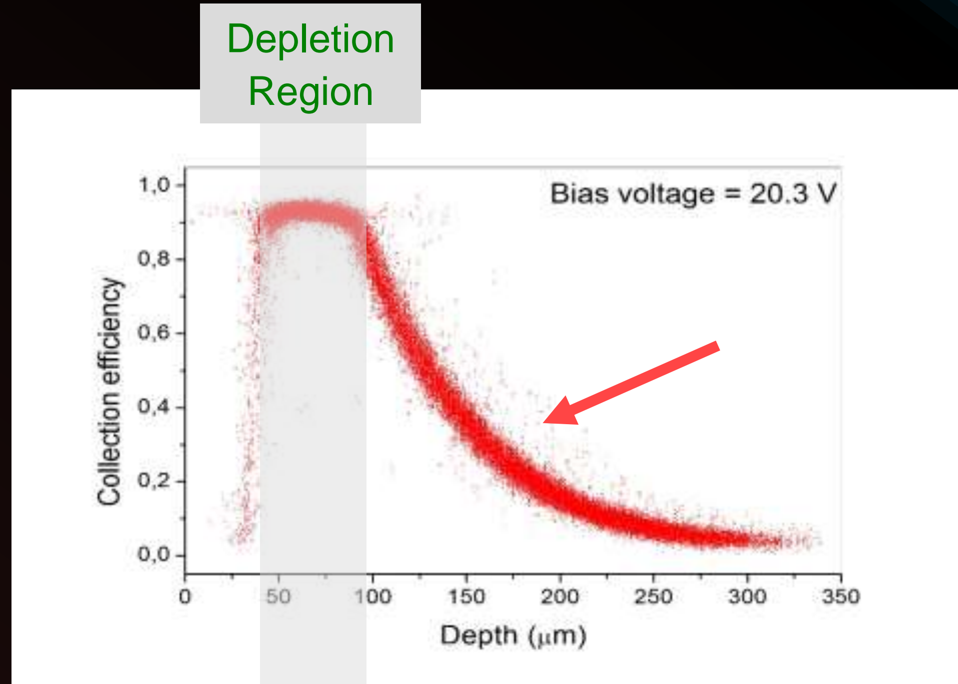

$$\eta(x) = \exp\left[-\frac{x}{L_p}\right]$$

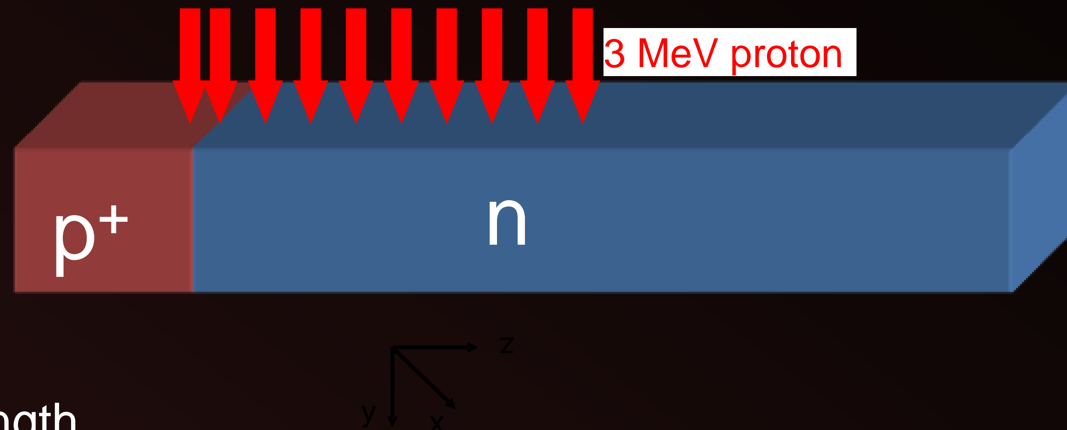

$$L_p = \sqrt{D_p \cdot \tau_p}$$

minority carrier diffusion length

C. Manfredotti et al., NIMB 158 (1999) 476-480

Pristine diode

Au doped diode

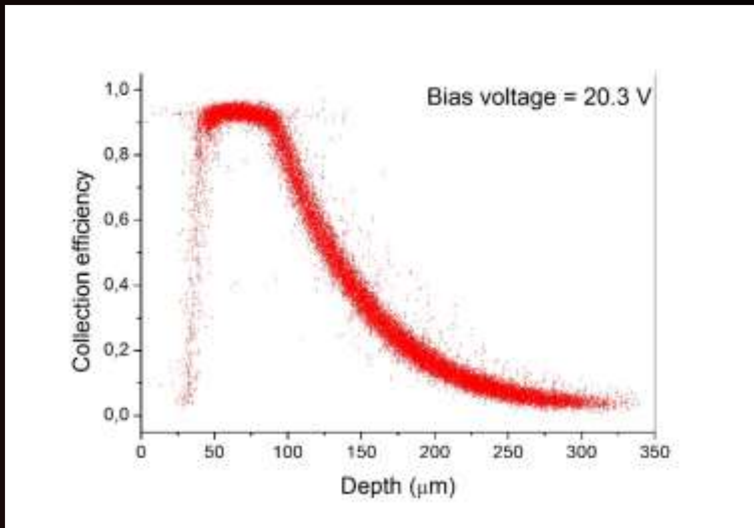

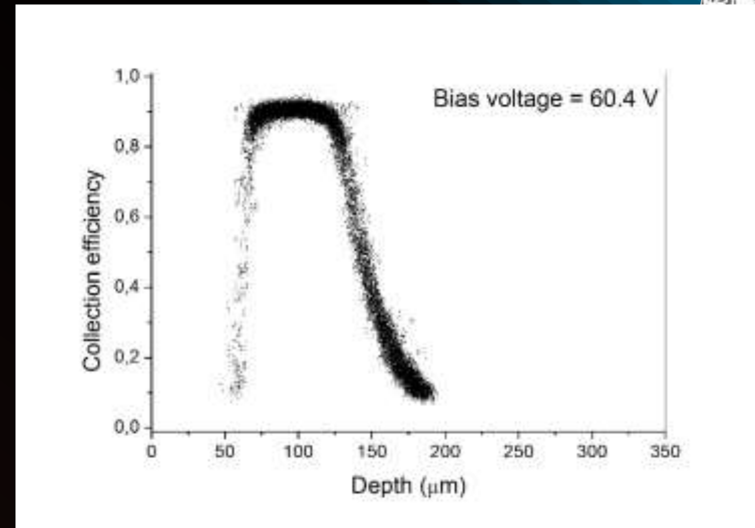

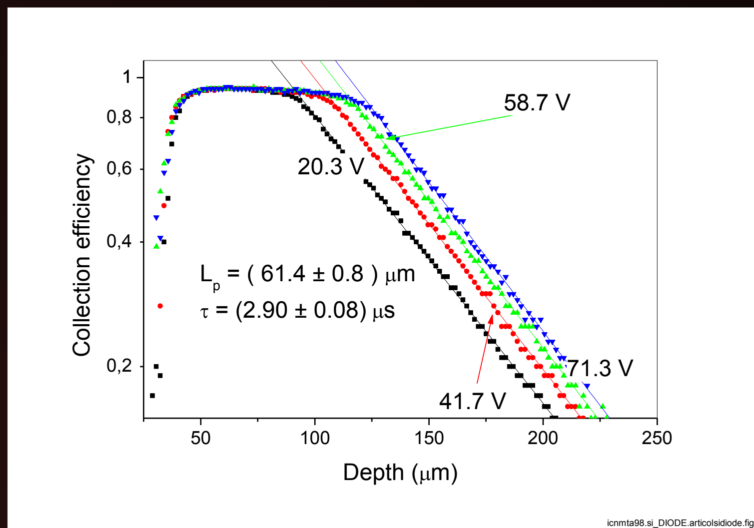

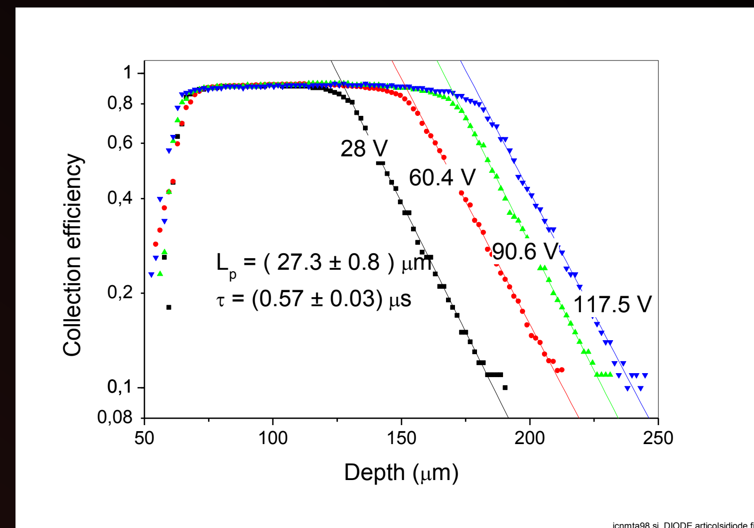

Experiments to validate the theoretical model

SEM image

4H-SiC Schottky diode

Inter-digitated frontal electrodes

- Finger width: 50 μm
- Finger length: 700 μm
- Finger-finger gap = 20 μm;
- Finger-guard ring = 70 μm.

500 μm

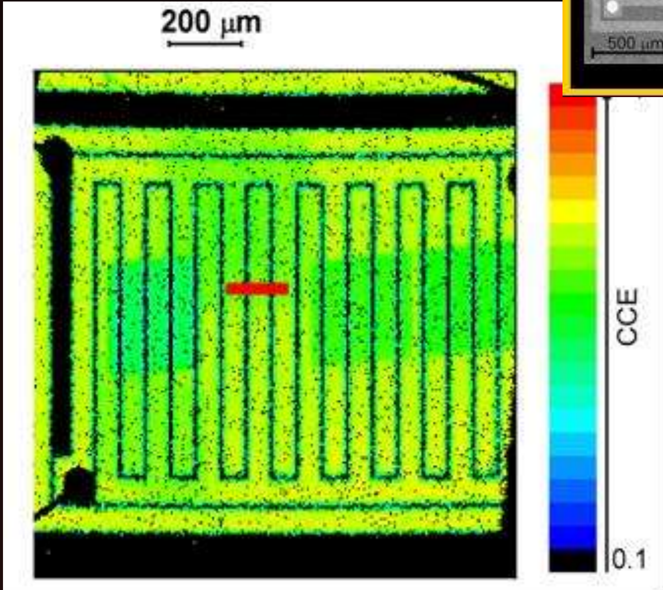

IBIC map
1.5 MeV H^+

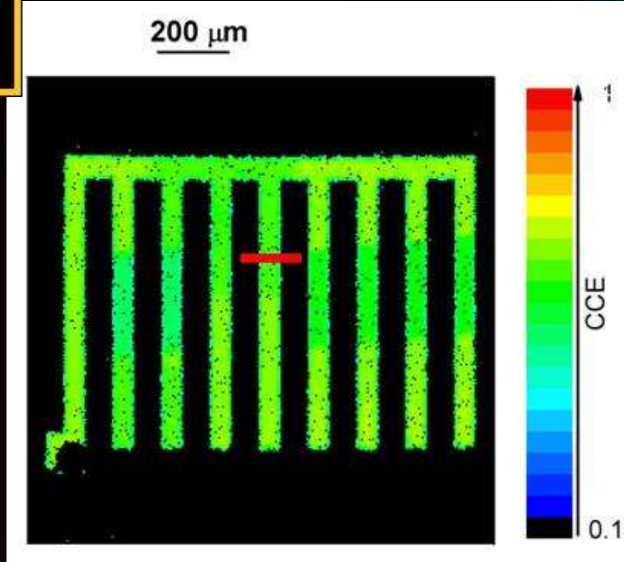

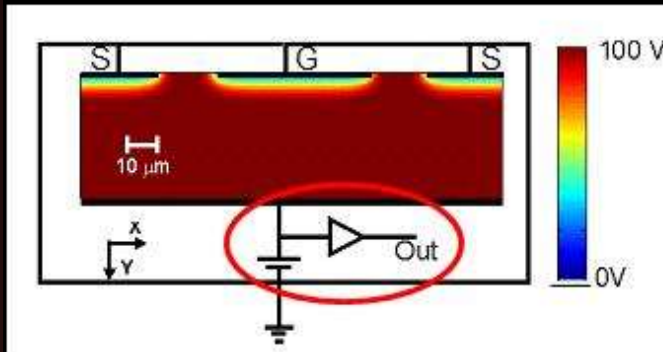

Electrostatic
Potential map
V_{bias}=100V

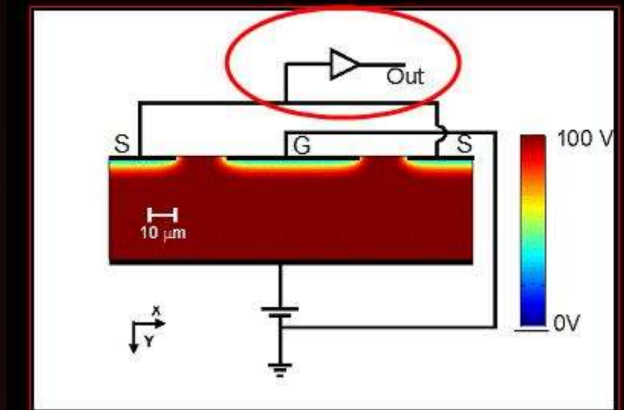

E.Vittone et al. NIMB 266 (2008) 1312–1318.

0.9 MeV protons

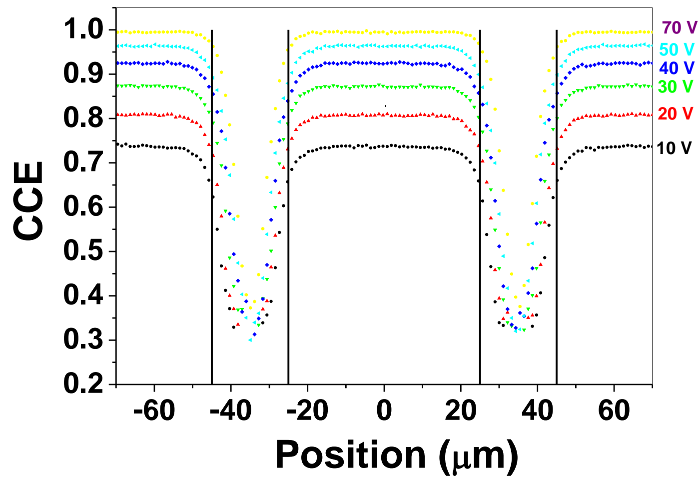

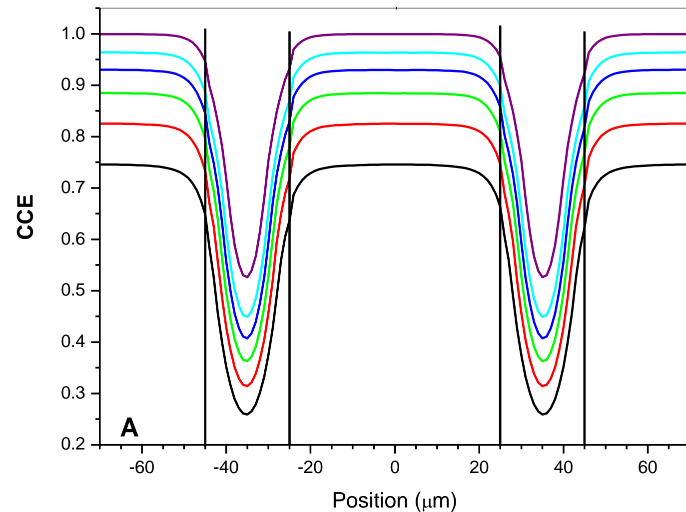

1.5 MeV protons

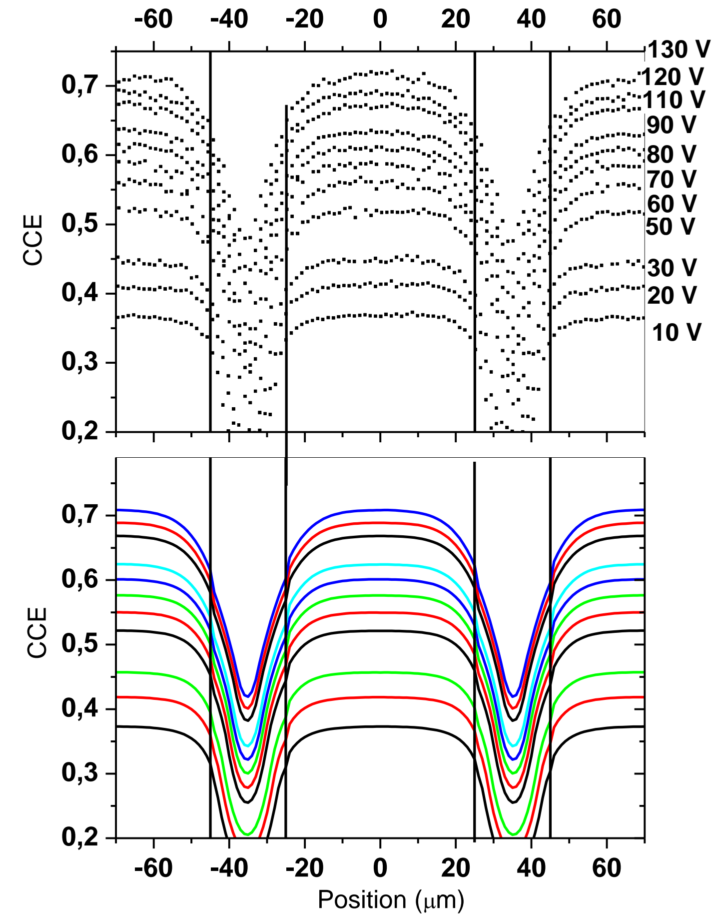

CCE profile details

hole diffusion length = 8.7 μm.
hole lifetime = τp = 250 ns

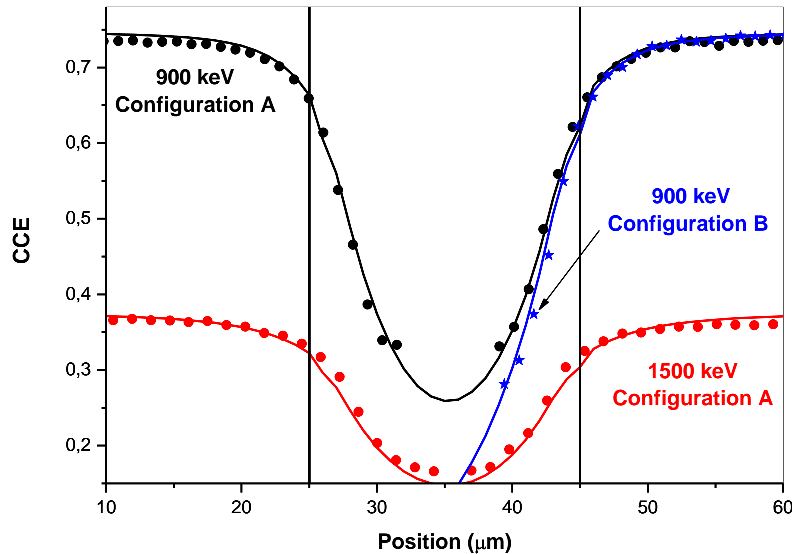

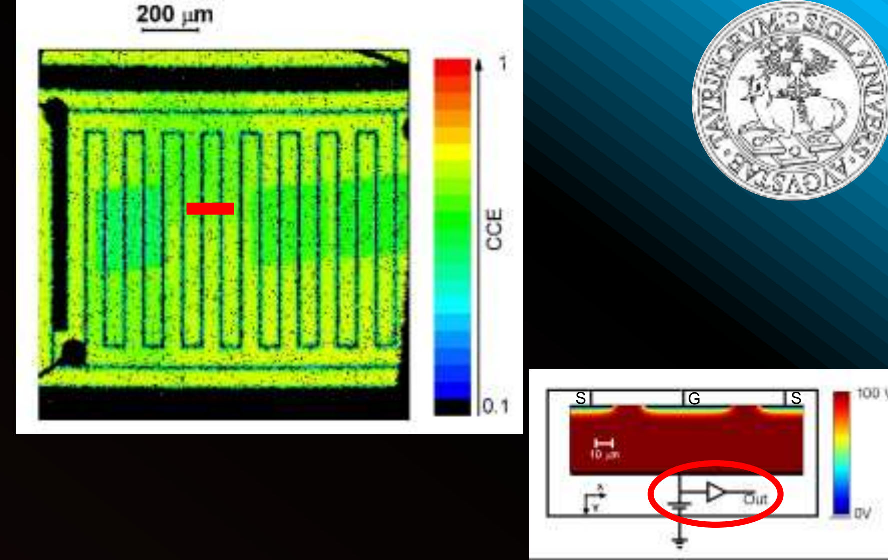

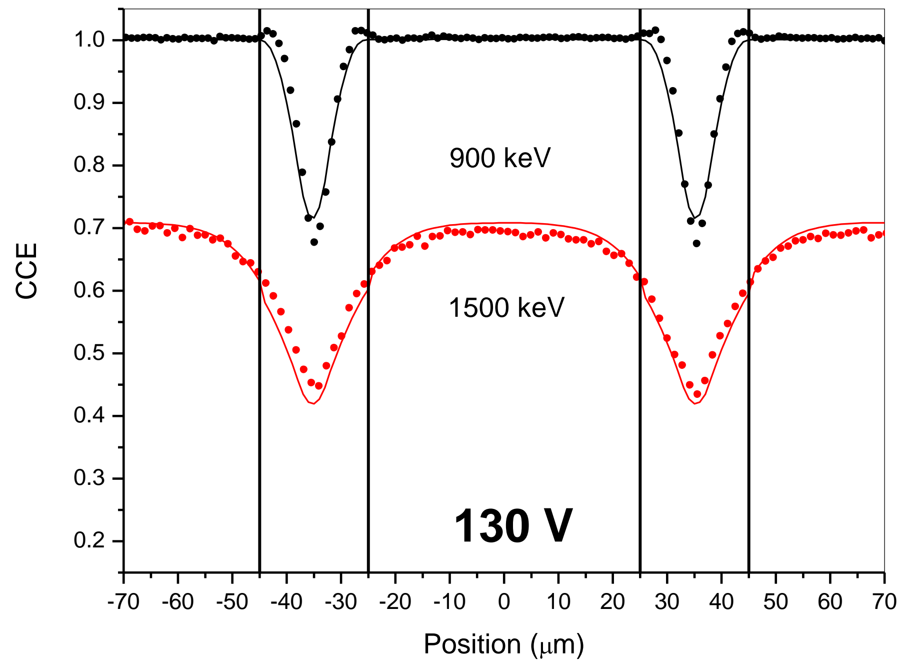

Electrode edges:
vertical black line.

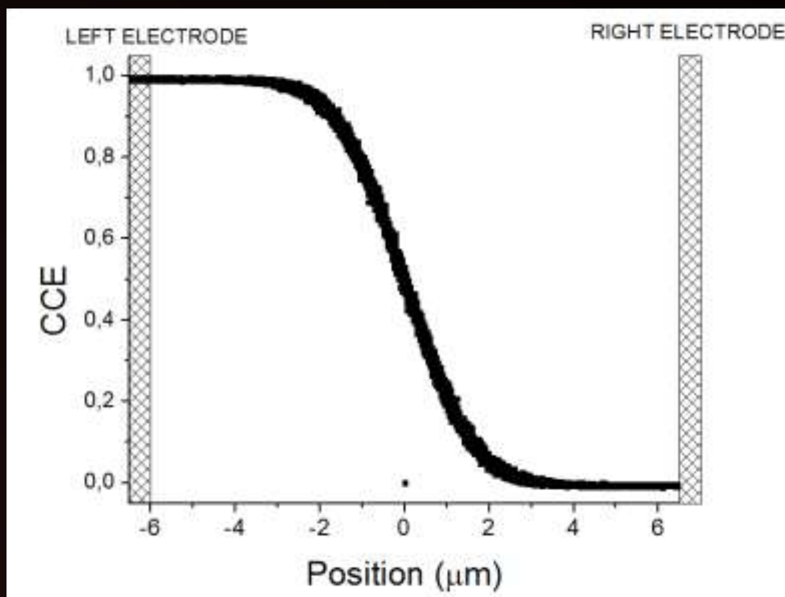

CCE AS FUNCTION OF ION STRIKE POSITION

2 MeV He+

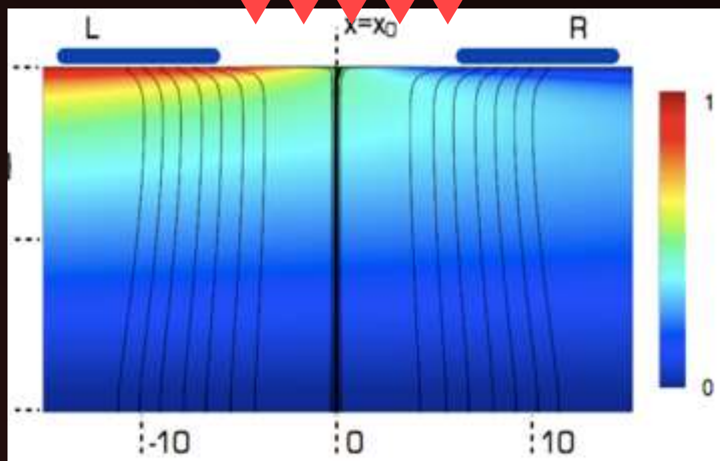

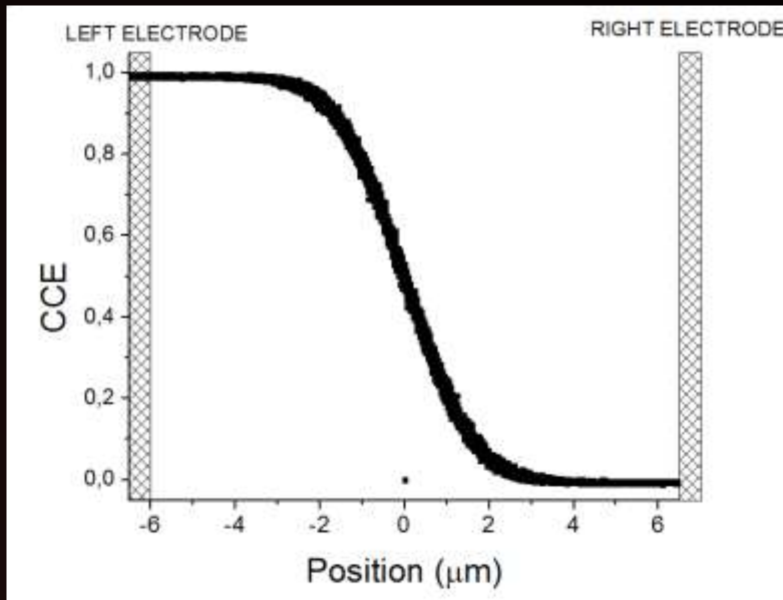

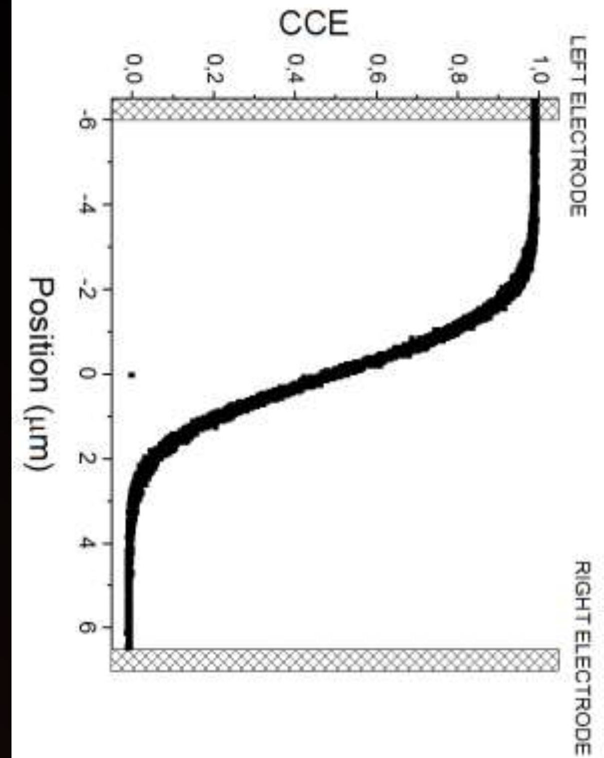

2 MeV He+

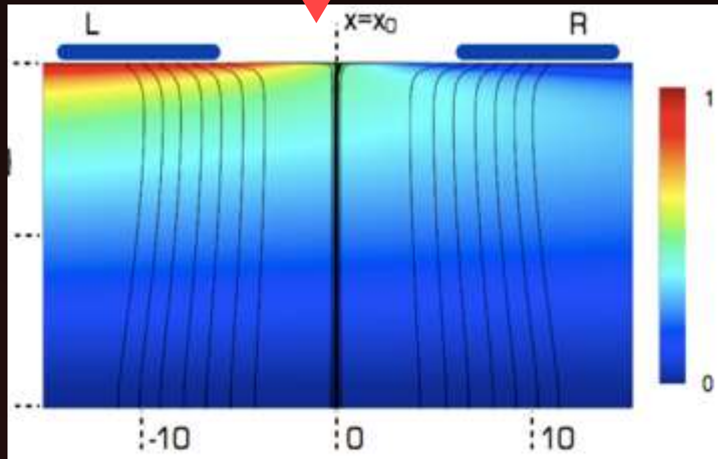

ION STRIKE POSITION AS FUNCTION OF CCE

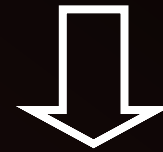

POSITION SENSITIVE DETECTOR

Position sensitivity - proof of concept: three-electrodes test device

L.M. Jong et al., Nuclear Instr. Meth. B 269 (2011) 2336

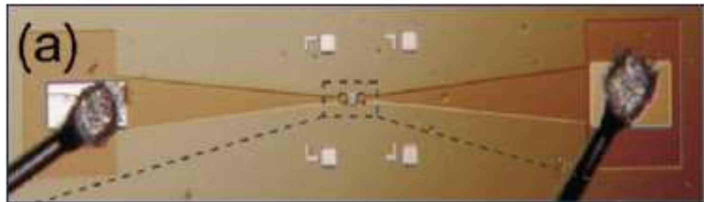

Top view

2 MeV He beam @ NEC 5U Pelletron, Melbourne
1 μm spot size

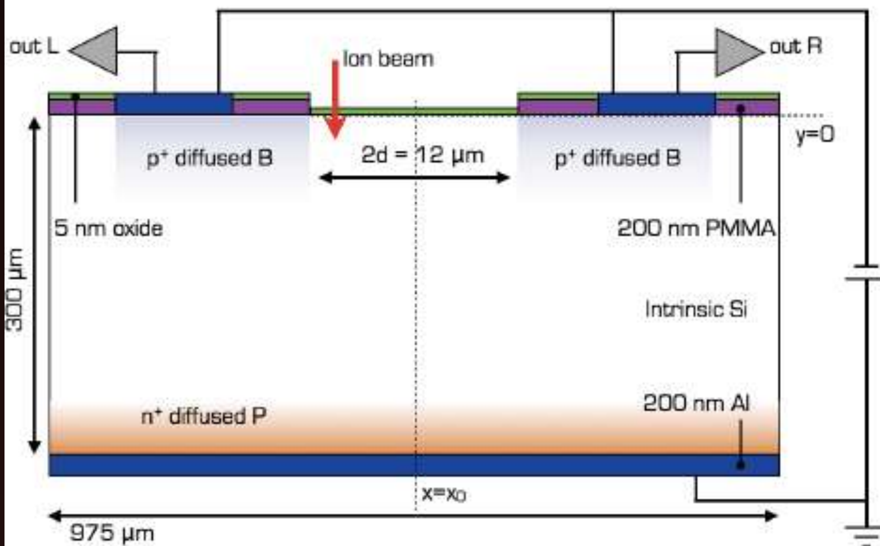

Cross sectional scheme

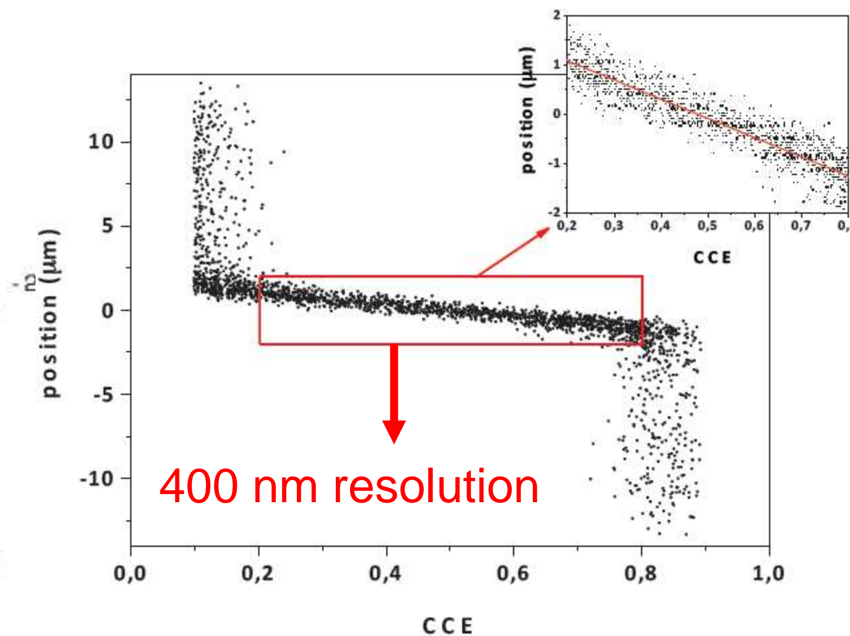

J. Forneris et al.
Modeling of ion beam induced charge sharing experiments for the design of high resolution position sensitive detectors, NIMB 2013

A SUB-MICROMETER POSITION SENSITIVE DETECTOR

IBIC
(Ion Beam Induced Charge)

Analytical technique suitable for the measurement of transport properties in semiconductor materials and devices

- **Control of in-depth generation profile**
- **Suitable for finished devices (bulk analysis).**
- **Micrometer resolution**
- **CCE profiles: Active layer extension; Diffusion length**
- **Robust theory; FEM and MC approaches**
- **Analysis of multi-electrode devices**
- **In-situ analysis of radiation damage.**
  - **IONS TO DAMAGE**
  - **IONS TO PROBE**

Radiation damage is the general alteration of the operational properties of a semiconductor devices induced by ionizing radiation

Three main types of effects:

- Transient ionization. This effect produces electron-hole pairs; particle detection with semiconductors is based on this effect (IBIC).
-Long term ionization. In insulators, the material does not return to its initial state, if the electrons and holes produced are fixed, and charged regions are induced.
- Displacements. These are dislocations of atoms from their normal sites in the lattice, producing less ordered structures, with long term effects on semiconductor properties.

V.A.J. van Lint, The physics of radiation damage in particle detectors, Nucl. Instrum. Meth. A253 (1987) 453.

-Long term ionization. In insulators, the material does not return to its initial state, if the electrons and holes produced are fixed, and charged regions are induced.

Ionizing particle

Gate oxide

Gate terminal

Drain terminal

Source terminal

Metal

P Type

N Type

P Type

Gate

Gate Oxide

N-type Si

Trapped Positive charge

- **Parametric shifts** in transistors parameters due to the build-up of trapped positive charge and interface states caused by several low-LET particles striking a chip
- Total Ionizing Dose affects **dielectric layers** (e.g., gate oxide, isolation oxides)

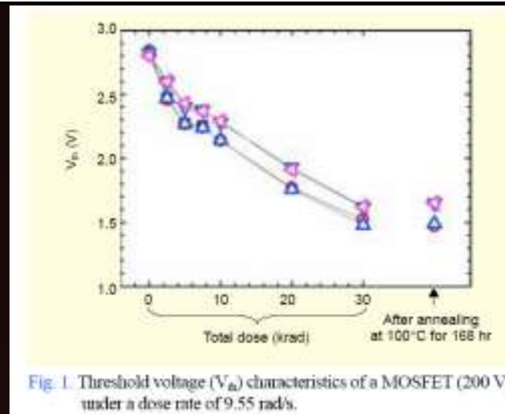

Fig. 1. Threshold voltage (V_{th}) characteristics of a MOSFET (200 V) under a dose rate of 9.55 rad/s.

Young Hwan Lho, Ki Yup Kim

Radiation Effects on the Power MOSFET for space applications

http://etrij.etri.re.kr/Cyber/Download/PublishedPaper/2704/S27-04-14.pdf

- **Displacements**. These are dislocations of atoms from their normal sites in the lattice, producing less ordered structures, with long term effects on semiconductor properties

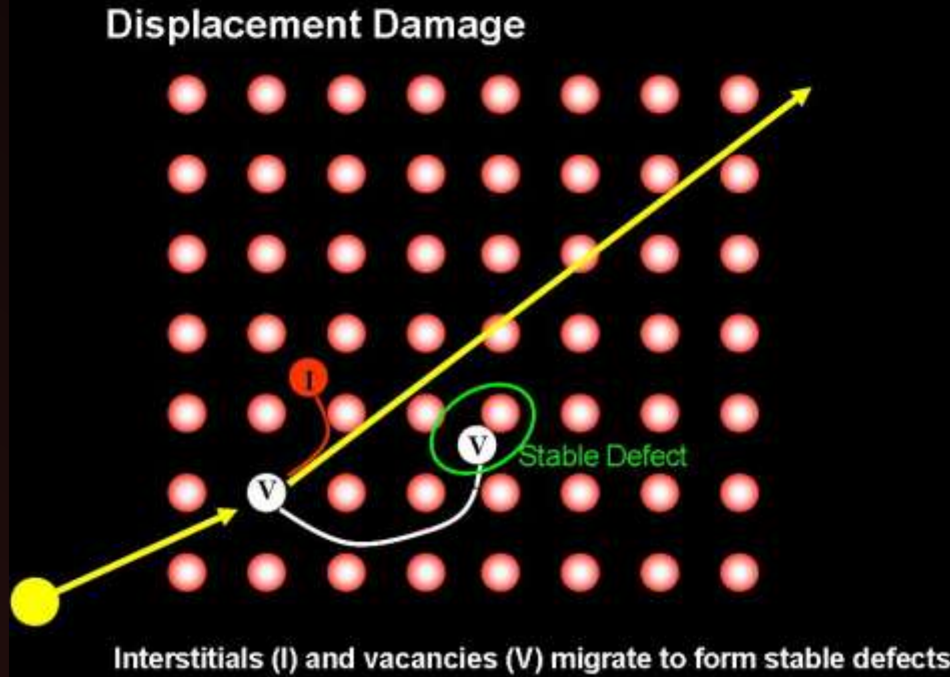

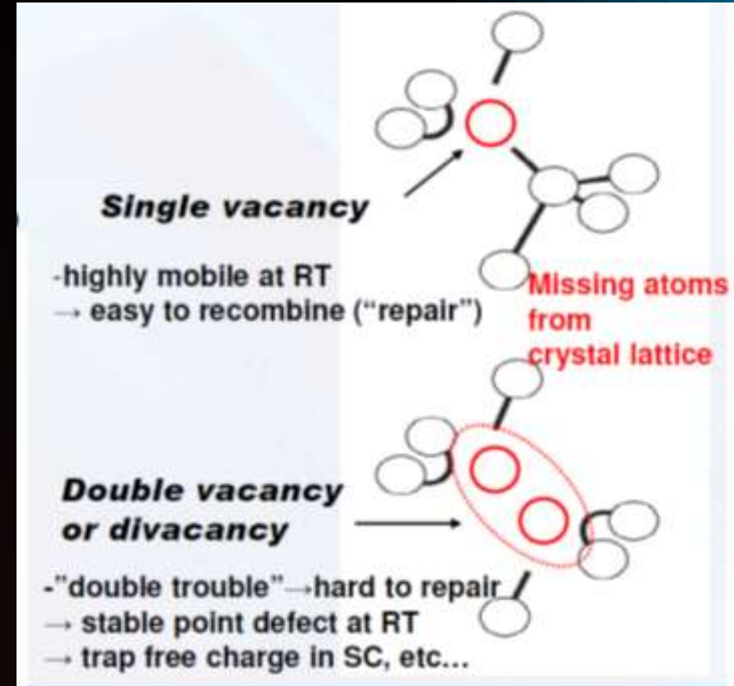

PHYSICAL REVIEW VOLUME 138, NUMBER 2A 19 APRIL 1965

Defects in Irradiated Silicon: Electron Paramagnetic Resonance of the Divacancy

G. D. WATKINS AND J. W. CORBETT

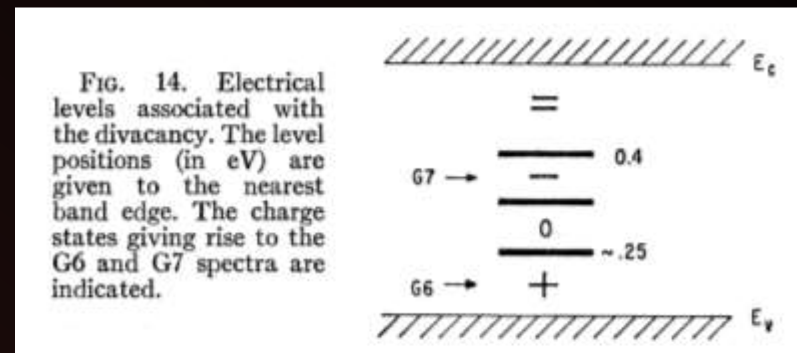

http://holbert.faculty.asu.edu/eee560/RadiationEffectsDamage.pdf

Low level of damage
Shockley-Read-Hall Model

Excess carrier lifetime

$$\tau = \frac{1}{N_{trap} \cdot \sigma \cdot v_{th}}$$

Trap density

Capture cross section

Thermal velocity

MeV ions to induce radiation damage
MeV ions to measure radiation hardness
PHYSICAL OBSERVABLE: CARRIER LIFETIME

$$\tau = \frac{1}{N_{trap} \cdot \sigma \cdot v_{th}}$$

Trap density in pristine material

$$N_{trap} = N^{0}_{trap} + k \cdot \Phi$$

Trap density induced by radiation

$$\frac{1}{\tau(\Phi)} = \frac{1}{\tau_0} + K \cdot \Phi$$

Lifetime reduction

Efficiency degradation

IAEA Coordinate Research Programme (CRP) F11016 (2011-2015)

"Utilization of ion accelerators for studying and modeling of radiation induced defects in semiconductors and insulators"

COOPERATION AND MUTUAL UNDERSTANDING LEAD TO GROWTH AND GLOBAL ENRICHMENT

NUS Singapore

Univ. Delhi India

CAN Spain

Nuclear Agency Malaysa

Ruđer Bošković Croatia

ANSTO Australia

JAEA-Kyoto Univ. JAPAN

Univ. Helsinki - Finland

SANDIA USA

Univ. Surrey UK

Univ. Turin Italy

IAEA

Expected Research Outputs:

- Definition of an experimental protocol to determine the key parameters for the characterization of the effects of radiation damage on semiconductor materials and devices.
- Refined theoretical models for defect generation and for modelling their effect on electronic properties.

The experimental protocol

Experimental protocol

Z. Pastuovic et al., IEEE TNS 56 (2009) 2457; APL (98) 092101 (2011)

Hamamatsu S5821 p-i-n diode

Experimental protocol

- ✓ Commercial p-i-n diodes

Experimental protocol

Z. Pastuovic et al., IEEE TNS 56 (2009) 2457; APL (98) 092101 (2011)

Hamamatsu
S5821 p-i-n diode

C-V characteristics
Depletion width-voltage

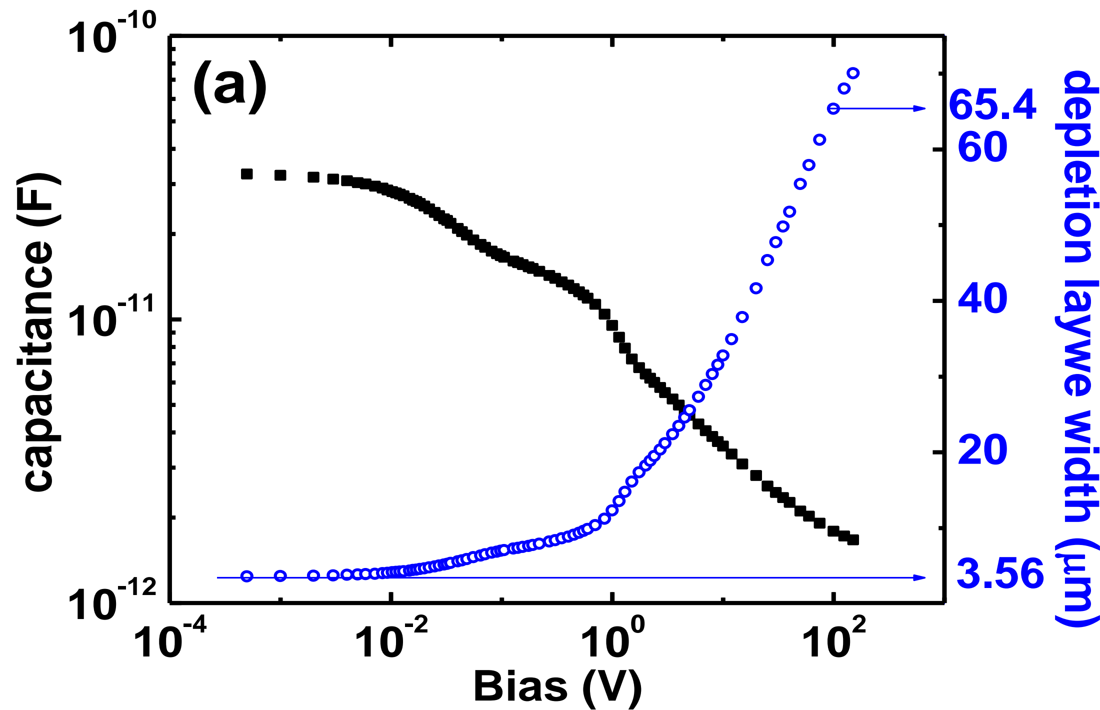

Experimental protocol

- ✓Commercial p-i-n diodes
- ✓Electrical characterization

Laboratory for Ion Beam Interaction
Ruder Boskovic Institute
Zagreb (HR)

QUADRUPOLE DOUBLET FOCUSING LENS
SAMPLE
ION BEAM
Y
X
SCAN AMPLIFIER
X Y CHARGE

He scannimg ion microbeam
Energy 1.4 MeV
Spot size < 3 μm

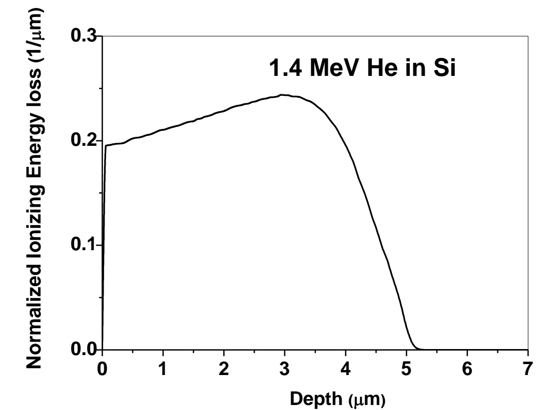

PROBING THE PRISTINE SAMPLE

IBIC map on a pristine diode probed with a scanning 1.4 MeV He microbeam;

Hamamatsu S5821 p-i-n diode

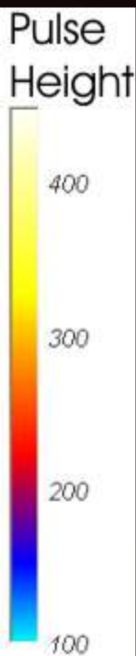

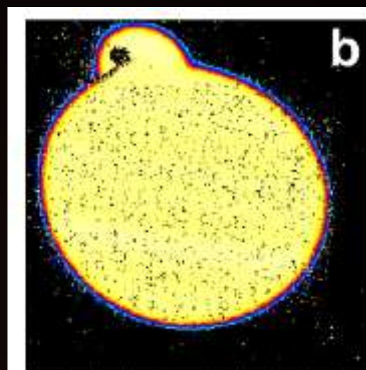

Uniform CCE map

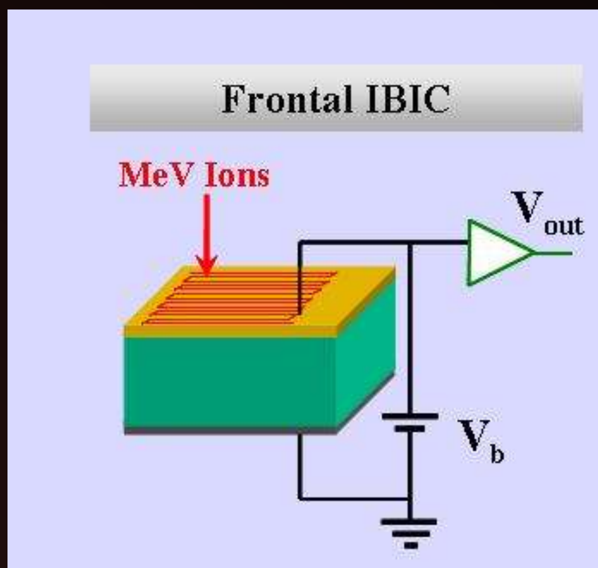

Experimental protocol

- ✓Commercial p-i-n diodes
- ✓Electrical characterization
- ✓IBIC map on pristine sample

Z. Pastuovic et al., IEEE Trans on Nucl. Sc. 56 (2009) 2457; APL (98) 092101 (2011)

Laboratory for Ion Beam Interaction
Ruder Boskovic Institute
Zagreb (HR)

Ion microbeams
He 1.4 MeV
Li 2.15 MeV
O 4.0 MeV
Cl 11.0 MeV
Spot size < 3 μm

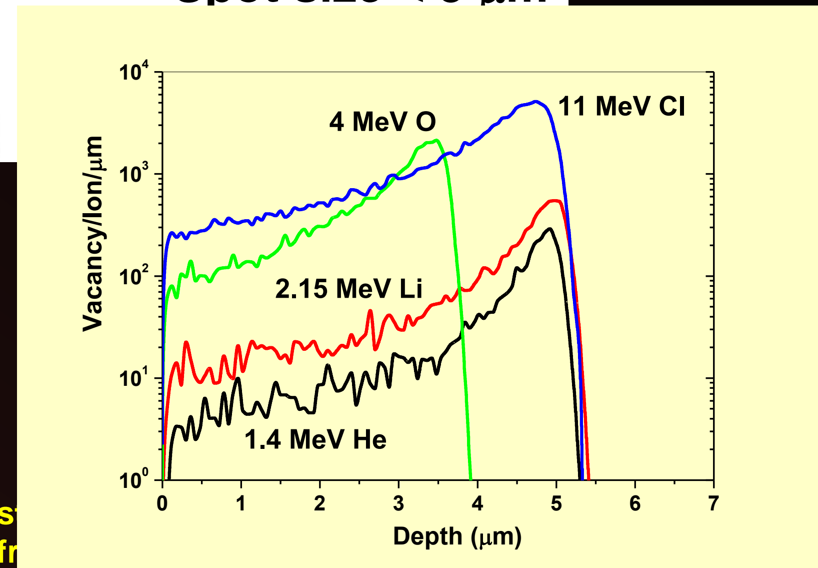

DAMAGING SELECTED AREAS 100X100 μm^2

IBIC map on a pristine diode probed with a scanning 1.4 MeV He microbeam;

ZOOM in view of the selected area for focused ion beam irradiation at different fluences Φ

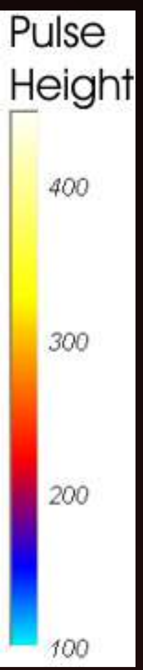

Hamamatsu S5821 p-i-n diode

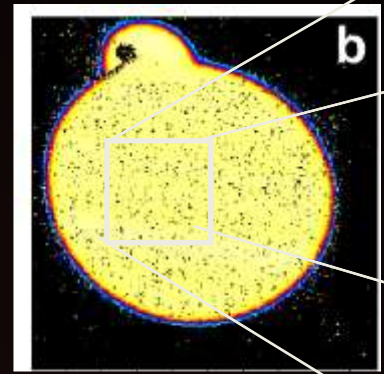

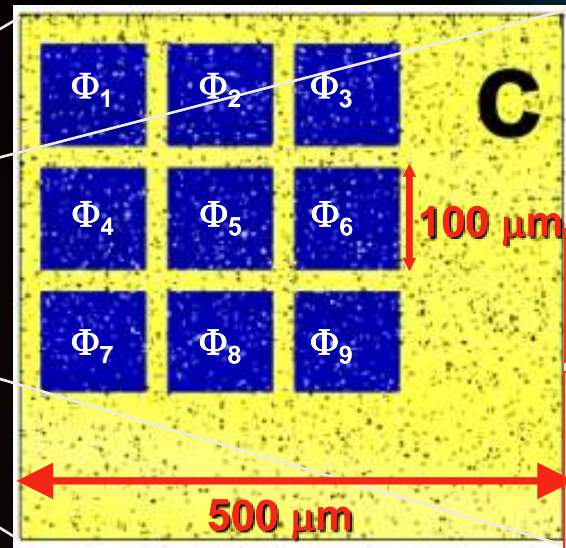

Experimental protocol

- ✓Commercial p-i-n diodes
- ✓Electrical characterization
- ✓IBIC map on pristine sample
- ✓Irradiation of 9 regions at different fluences

Z. Pastuovic et al., IEEE Trans on Nucl. Sc. 56 (2009) 2457; APL (98) 092101 (2011)

Laboratory for Ion Beam Interaction
Ruder Boskovic Institute
Zagreb (HR)

QUADRUPOLE DOUBLET FOCUSING LENS

ION BEAM

SAMPLE

SCAN AMPLIFIER

Y X

X Y CHARGE

He ion microbeam
Energy 1.4 MeV
Spot size < 3 μm

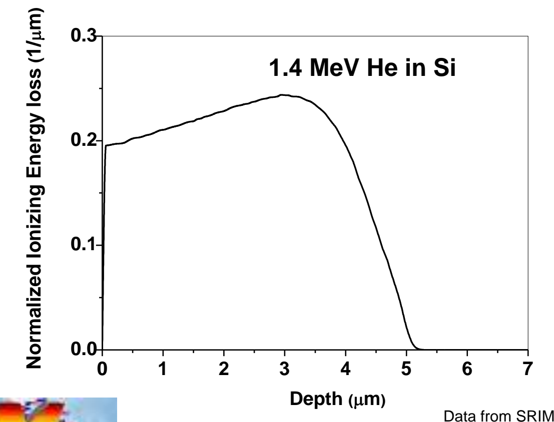

PROBING DAMAGED AREAS

IBIC map on a pristine diode probed with a scanning 1.4 MeV He microbeam;

ZOOM in view of the selected area for focused ion beam irradiation at different fluences Φ

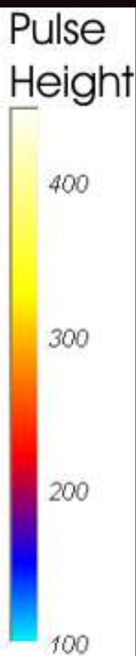

Hamamatsu S5821 p-i-n diode

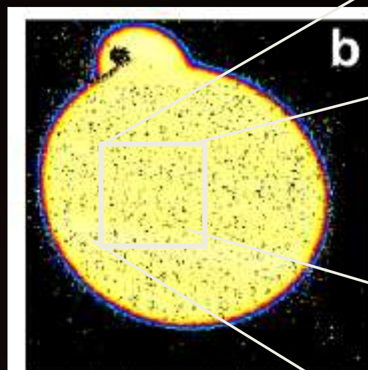

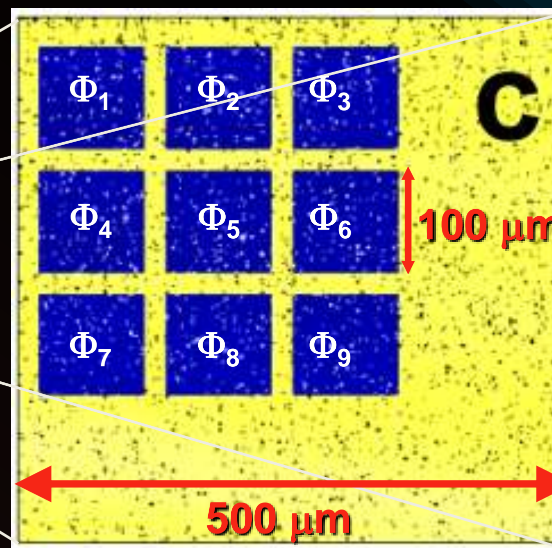

Experimental protocol

- ✓Commercial p-i-n diodes
- ✓Electrical characterization
- ✓IBIC map on pristine sample
- ✓Irradiatoin of 9 regions at different fluences
- ✓IBIC map of irradiated regions

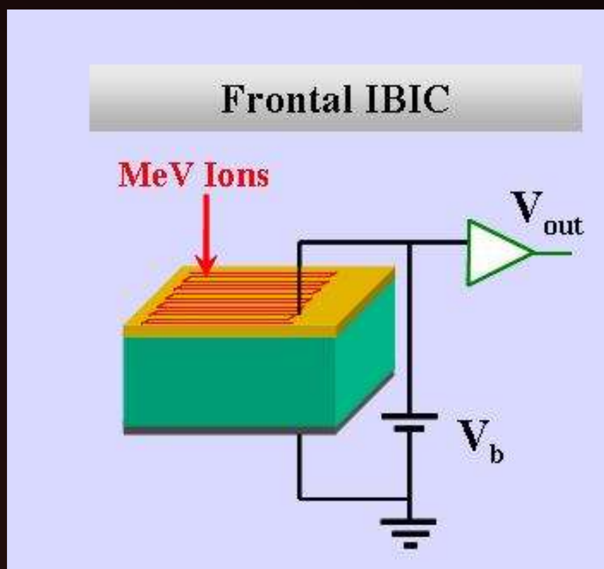

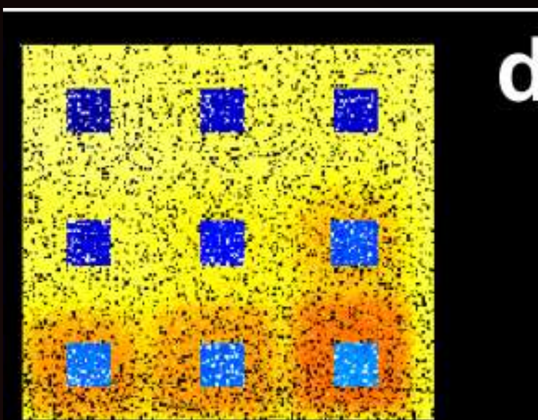

a measured 2D distribution of the IBIC signal amplitude after irradiation

Z. Pastuovic et al., IEEE Trans on Nucl. Sc. 56 (2009) 2457; APL (98) 092101 (2011)

IBIC map on a pristine diode probed with a scanning 1.4 MeV He microbeam;

ZOOM in view of the selected area for focused ion beam irradiation at different fluences Φ

Hamamatsu S5821 p-i-n diode

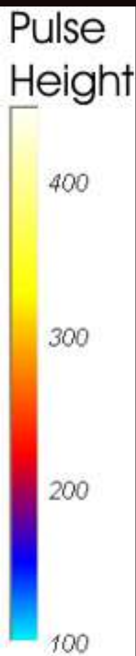

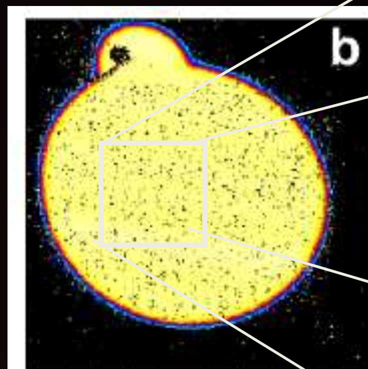

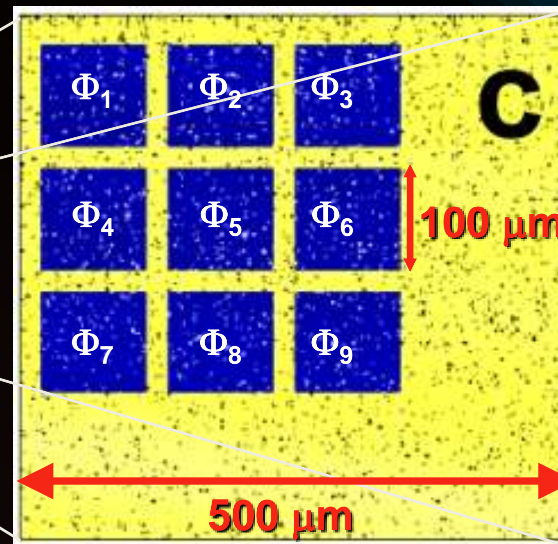

Experimental protocol

- ✓Commercial p-i-n diodes
- ✓Electrical characterization
- ✓IBIC map on pristine sample
- ✓Irradiatin of 9 regions at different fluences
- ✓IBIC map of irradiated regions
- ✓Average pulse height as function of the damage

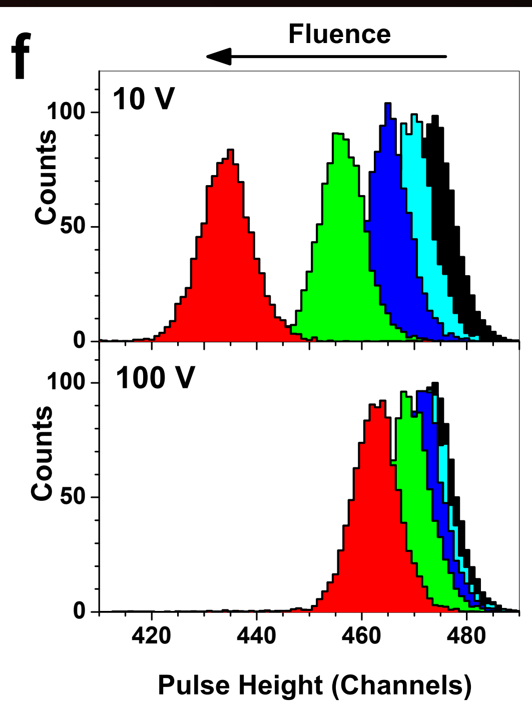

IBIC spectra (bias voltage = 10 V and 100 V) from the central regions of four of the areas shown in Fig. c

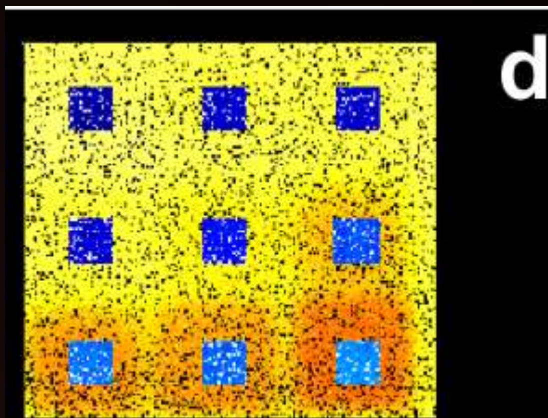

a measured 2D distribution of the IBIC signal amplitude after irradiation

Z. Pastuovic et al., IEEE Trans on Nucl. Sc. 56 (2009) 2457; APL (98) 092101 (2011)

JOURNAL OF APPLIED PHYSICS **106**, 104914 (2009)

Breakdown of silicon particle detectors under proton irradiation

S. Väyrynen,[1,a)] J. Räisänen,[1] I. Kassamakov,[2] and E. Tuominen[3]
[1]Department of Physics, University of Helsinki, P.O. Box 64, FI-00014 Helsinki, Finland
[2]Department of Micro- and Nanosciences, Helsinki University of Technology, P.O. Box 3000, FI-02015 TKK, Finland
[3]Helsinki Institute of Physics, University of Helsinki, P.O. Box 64, FI-00014 Helsinki, Finland

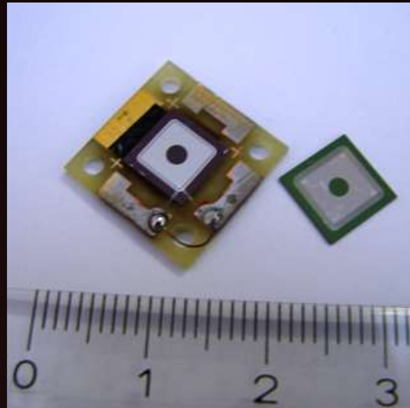

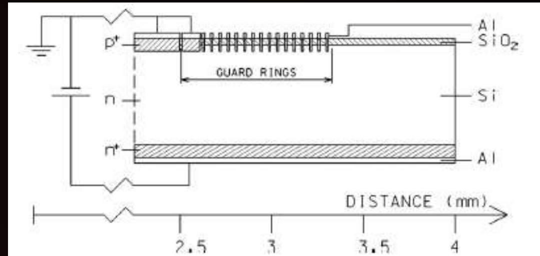

FIG. 1. Cross-sectional view of the Cz and Fz-1 detectors. The front electrode (5×5 mm²) and the surrounding main guard ring are grounded. Positive bias voltage is added to the back side of the detector. The aluminum metallization on the front surface extends over the silicon oxide (SiO_2) layer. The structure of the Fz-2 detector is similar, with the exception of the smaller size and the missing thin guard rings. The shown distance is measured from the detector center.

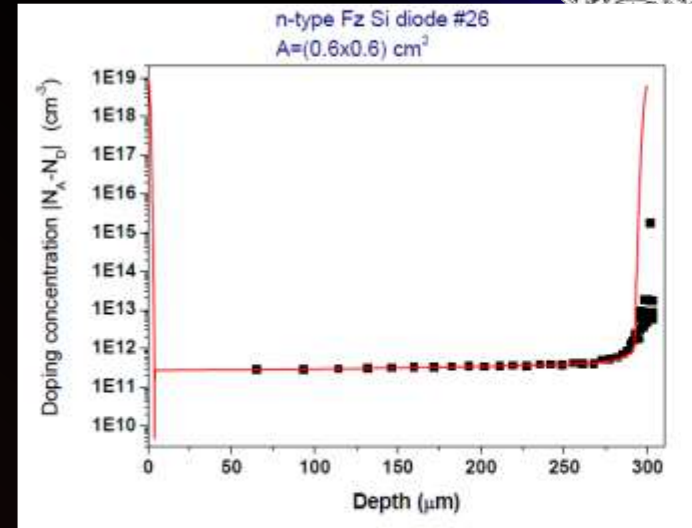

n-type and p-type Fz silicon diodes From University of Helsinki

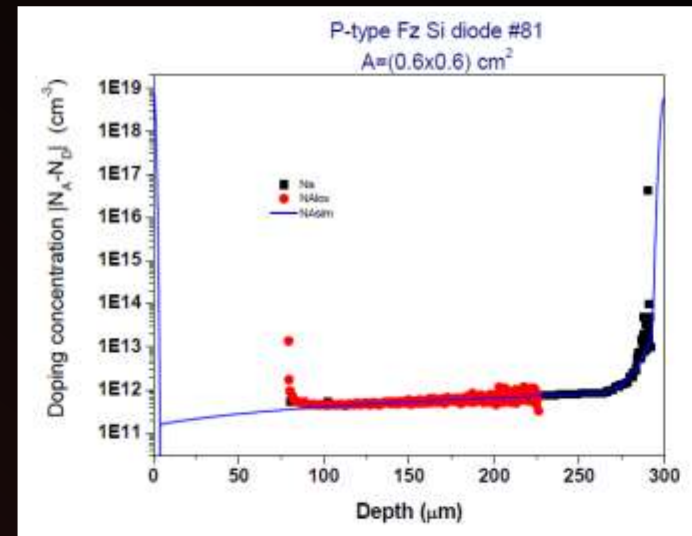

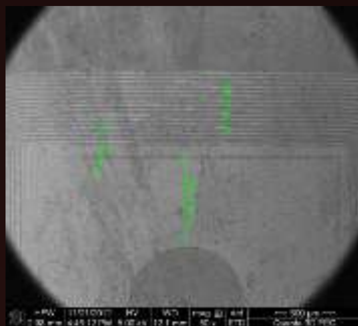

16 floating guard rings

The frontal electrode and the guard rings are coated with Al (0.5 µm). The Al electrode has a hole in the center, 1 mm diameter.

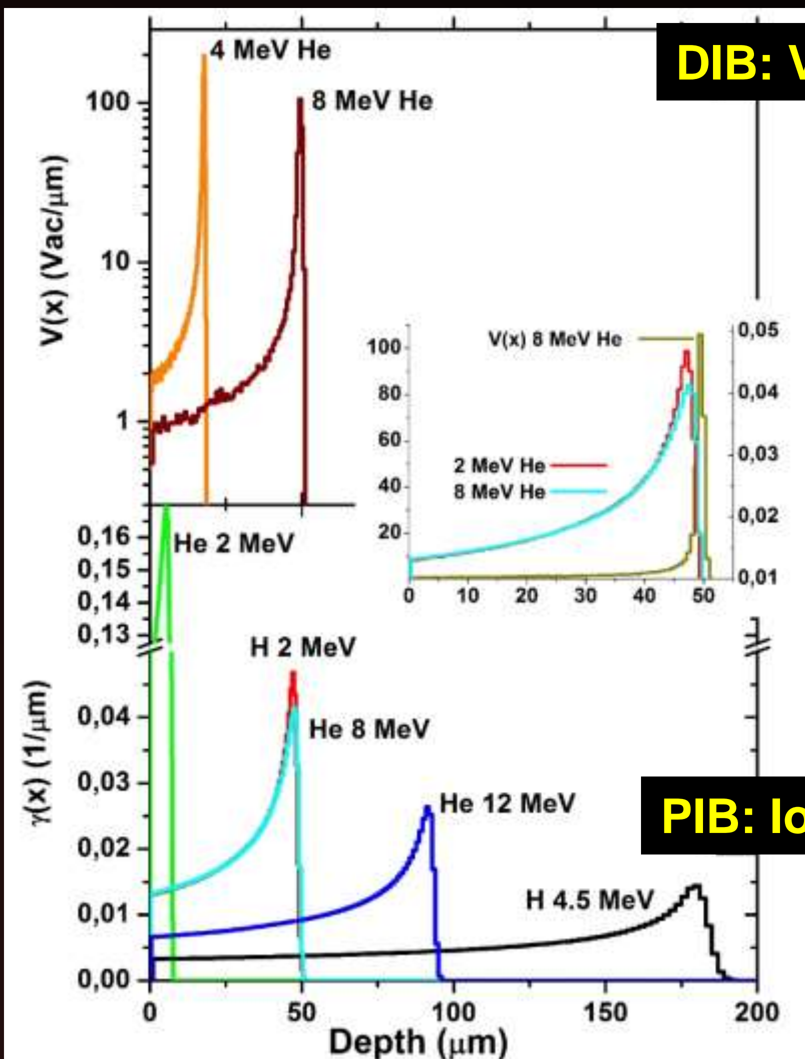

DIB: Vacancy profiles

PIB = Probing ion beam
DIB = Damaging ion beam

PIB: Ionization profiles

CCE degradation depends from

- Damaging ion energy and mass
- Probing ion energy and mass
- Polarization

DIB = Damaging ion beam

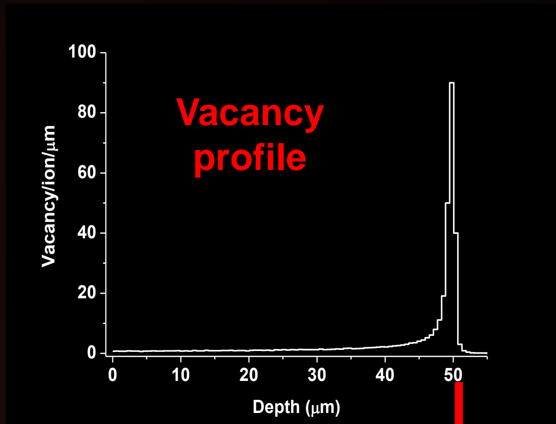

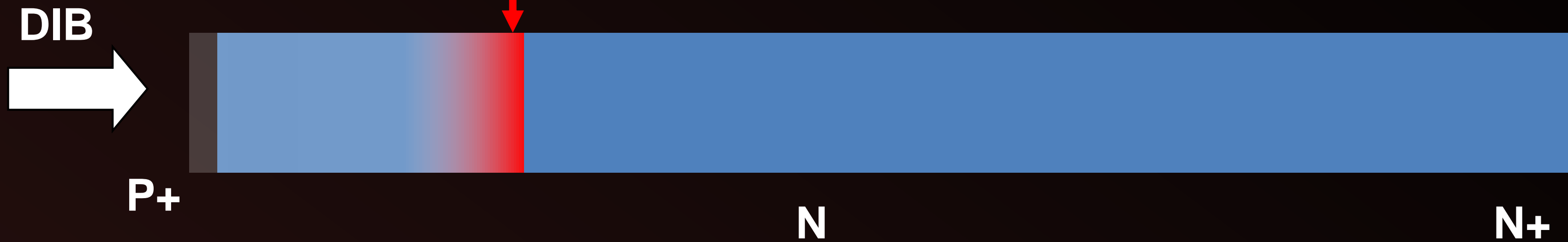

DIB = Damaging ion beam

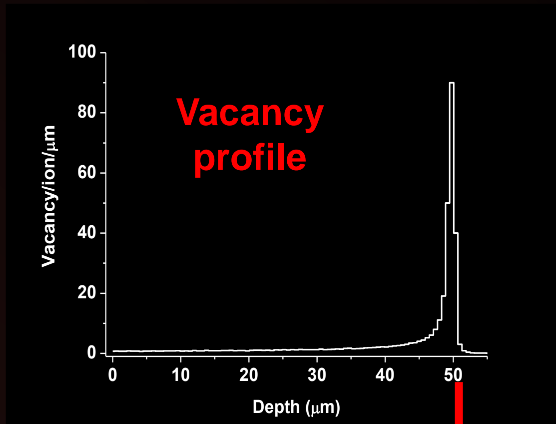

PIB

P+

N

N+

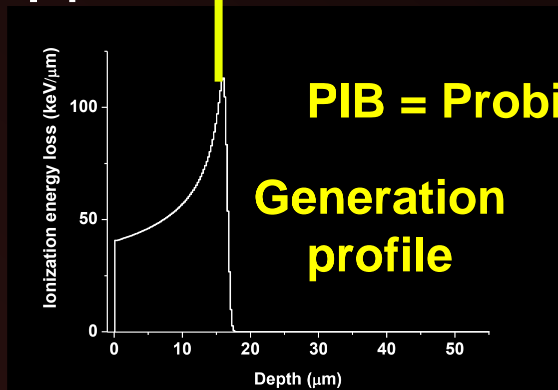

PIB = Probing ion beam

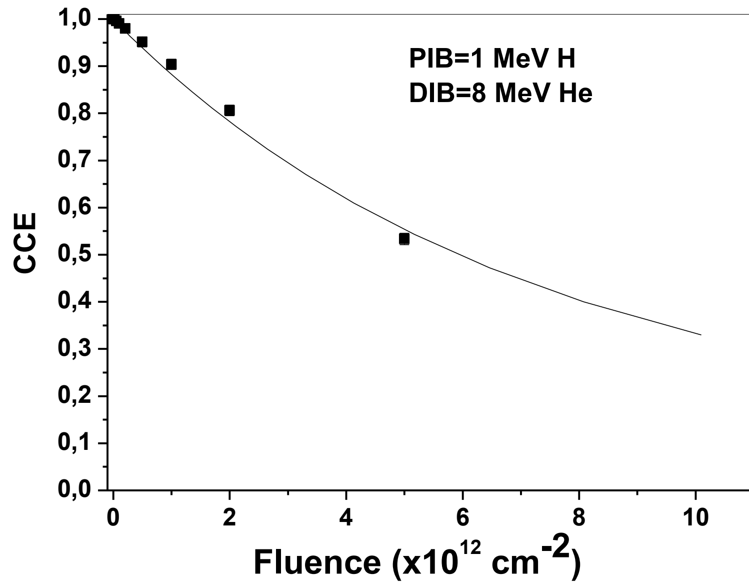

CCE
Fluence (x10^12 cm^-2)
PIB=1 MeV H
DIB=8 MeV He

Hole motion
Electron motion
PIB
P+
N
N+
Electric field
Generation profile
Ionization energy loss (keV/μm)
Depth (μm)

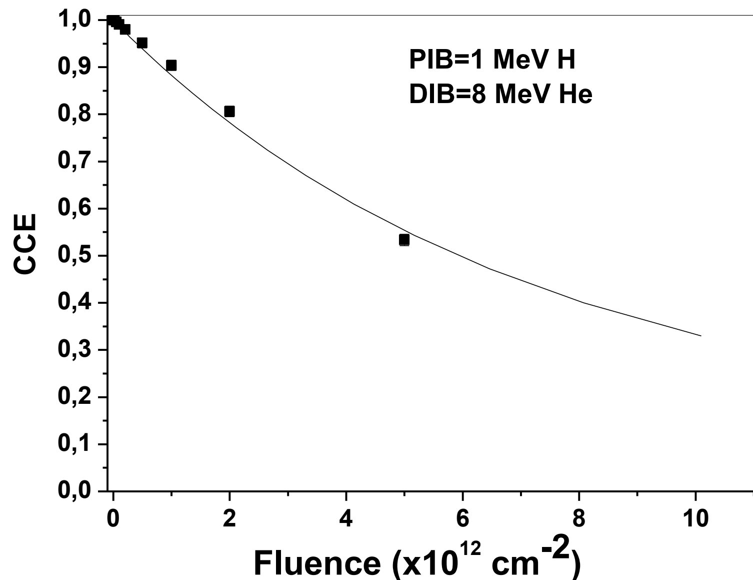

$$\eta_e(x,\Phi) = \frac{1}{w} \cdot \int_x^w dy \cdot \exp\left[-\int_x^y \frac{dz}{v_e(z) \cdot \tau_e(z,\Phi)} \right]$$

$$\frac{1}{\tau_e} = \frac{1}{\tau_0} + \left(k_e \cdot \sigma_e{}' \cdot v_{th}\right) \cdot Vac(x) \cdot \Phi$$

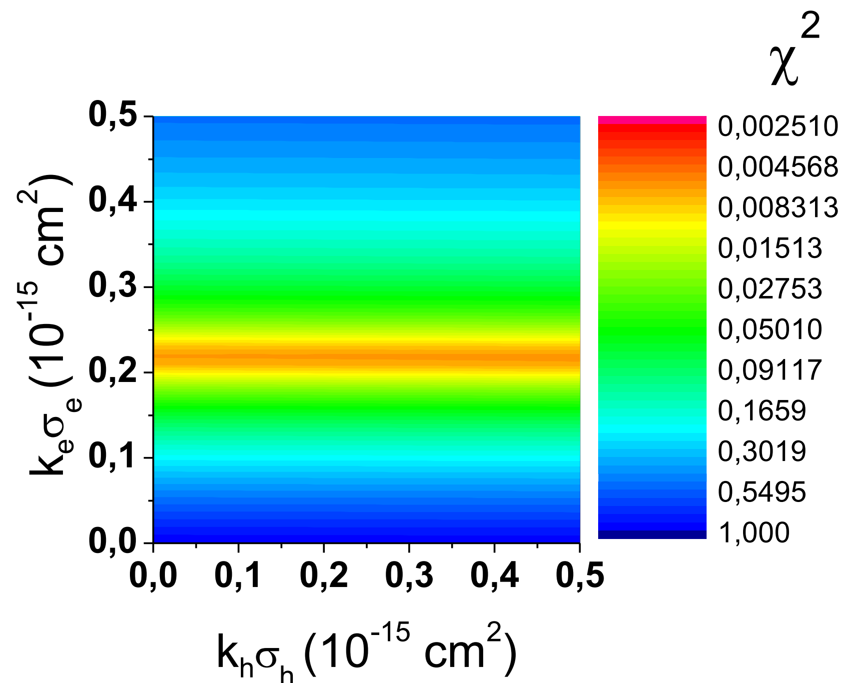

Residual map

DIB = Damaging ion beam

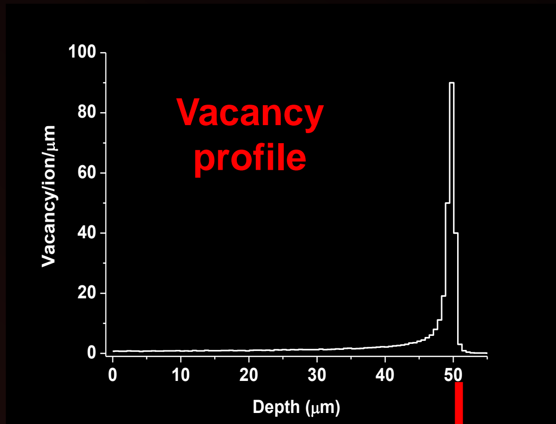

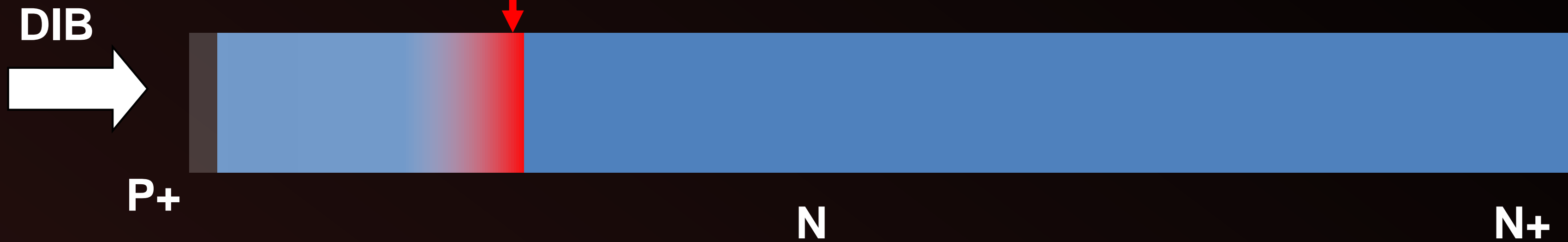

DIB = Damaging ion beam

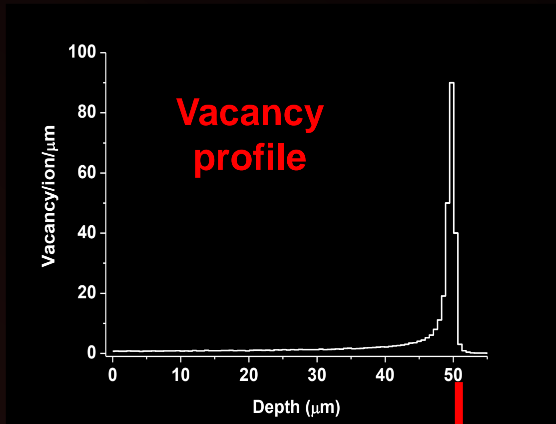

PIB

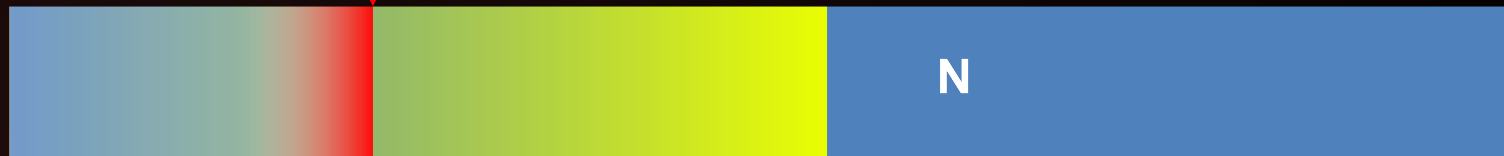

P+

N+

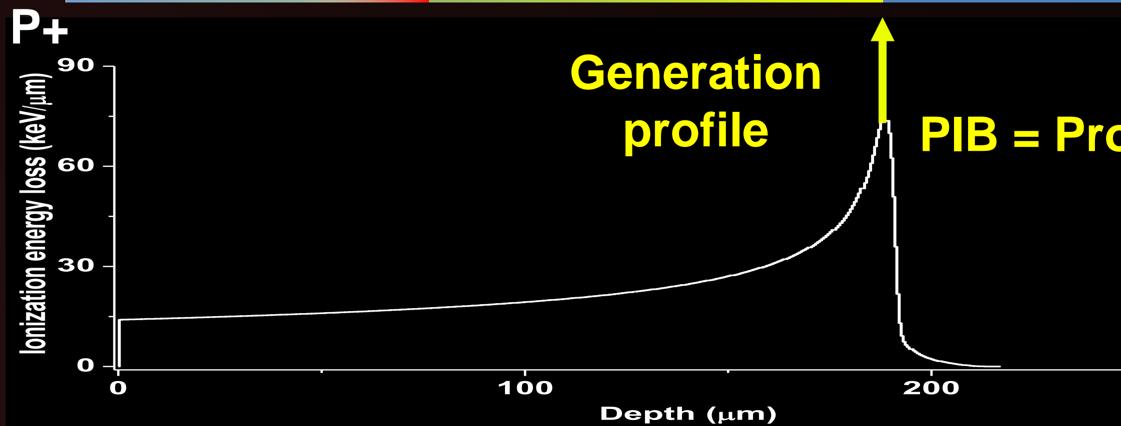

PIB = Probing ion beam

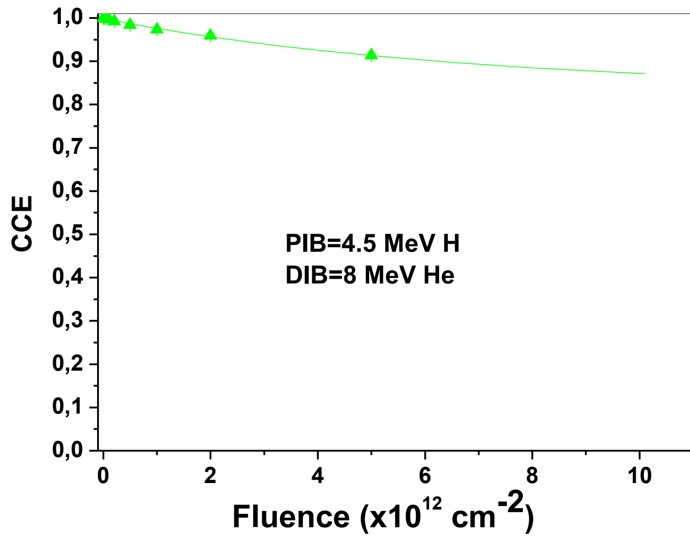

Hole motion

Electron motion

PIB

N

P+

N+

Generation profile

Ionization energy loss (keV/µm)

Depth (µm)

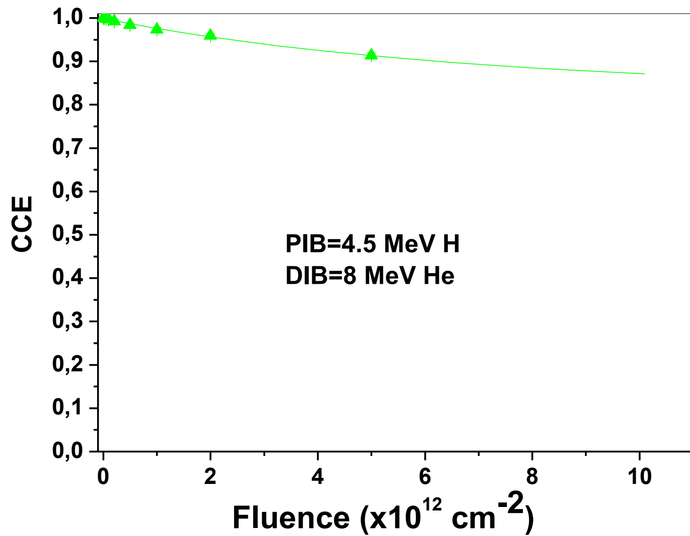

$$\eta_e(x,\Phi) = \frac{1}{w}\cdot\int_x^w dy \cdot \exp\left[-\int_x^y \frac{dz}{v_e(z)\cdot\tau_e(z,\Phi)}\right]$$

$$\eta_h(x,\Phi) = \frac{1}{w}\cdot\int_x^w dy \cdot \exp\left[-\int_y^x \frac{dz}{v_h(z)\cdot\tau_h(z,\Phi)}\right]$$

$$\frac{1}{\tau_e} = \frac{1}{\tau_0} + \left(k_e \cdot \sigma_e{}' \cdot v_{th}\right)\cdot Vac(x)\cdot\Phi$$

$$\frac{1}{\tau_h} = \frac{1}{\tau_0} + \left(k_h \cdot \sigma_h{}' \cdot v_{th}\right)\cdot Vac(x)\cdot\Phi$$

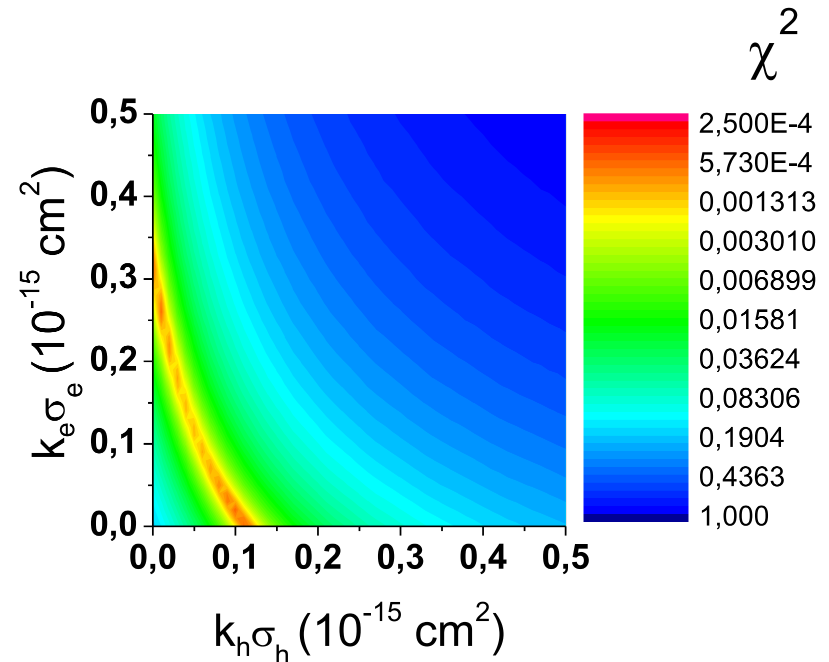

Residual map

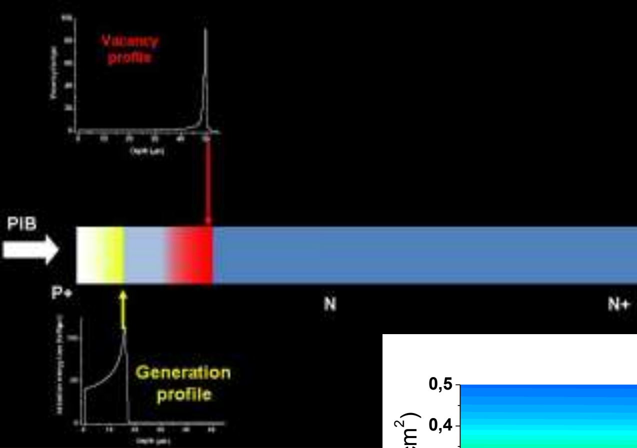

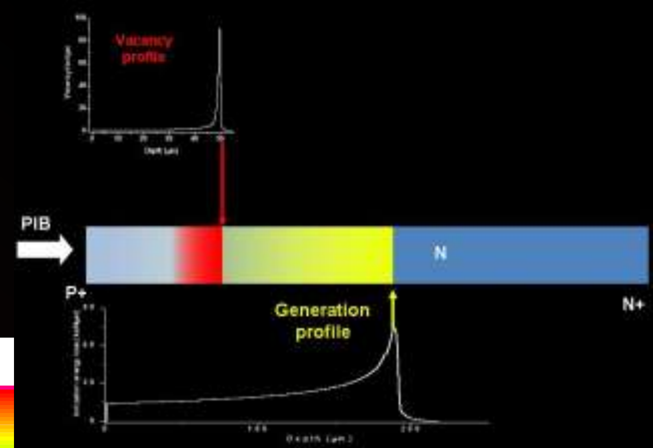

Short range PIB

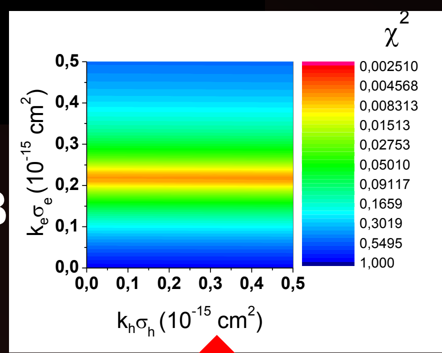

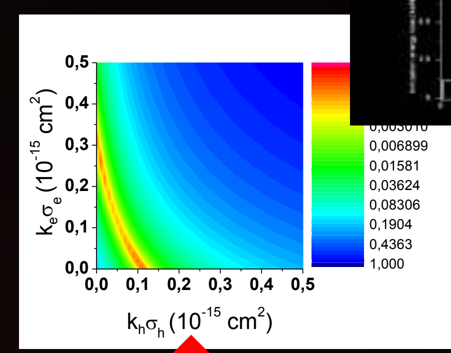

Long range PIB

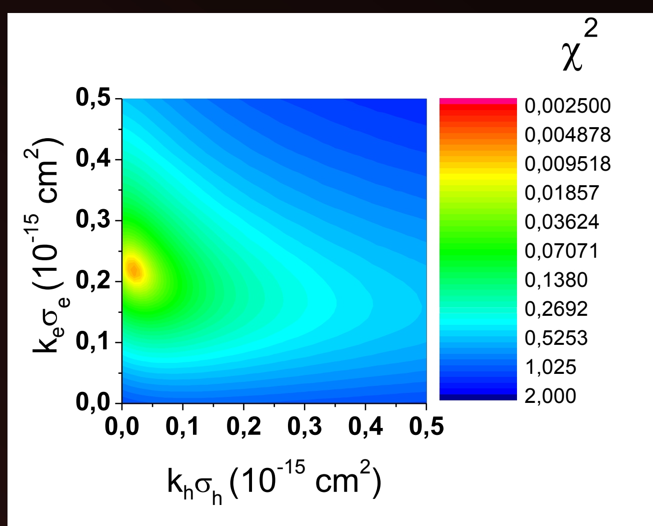

$k_e \cdot \sigma_e = 0.22 \cdot 10^{-15}\ cm^2$

$k_h \cdot \sigma_h = 0.02 \cdot 10^{-15}\ cm^2$

DIB: 8 MeV He

DIB: 4 MeV He

PIB= 2 MeV H a)
50 V
20 V
10 V
b)
50 V
20 V
10 V
PIB= 2 MeV H
PIB= 8 MeV He c)
50 V
20 V
10 V
50 V
10 V
PIB= 12 MeV He d)
50 V
20 V
PIB= 4.5 MeV H e)
50 V
20 V
10 V
PIB= 4.5 MeV H f)
CCE
Fluence (cm^{-2})

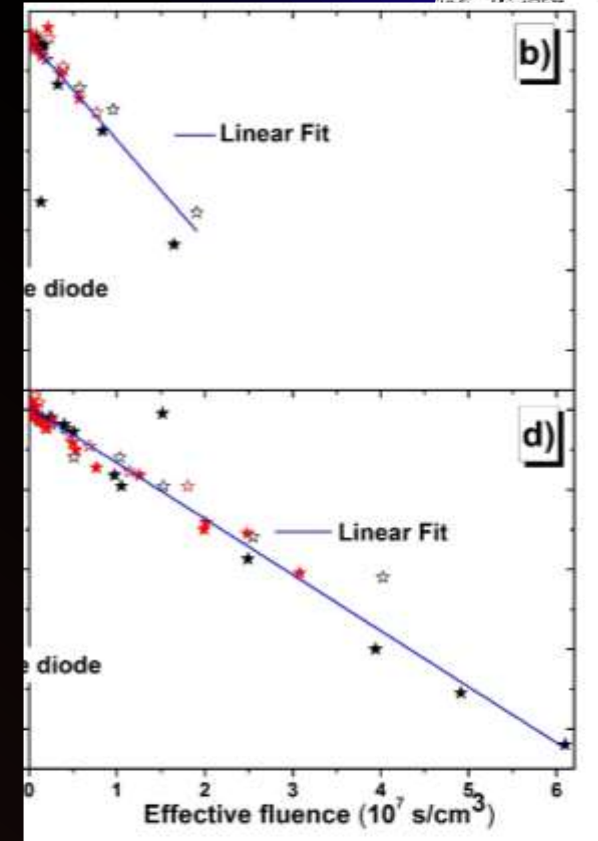

CCE degradation depends from

- ➢ **Damaging ion energy and mass**
- ➢ **Probing ion energy and mass**
- ➢ **Polarization**

The solid lines are the best fits obtained by means of our model considering
Different PIBs
Different DIBs (8 MeV, 4 MeV)
Different polarizations (10,20,50 V)

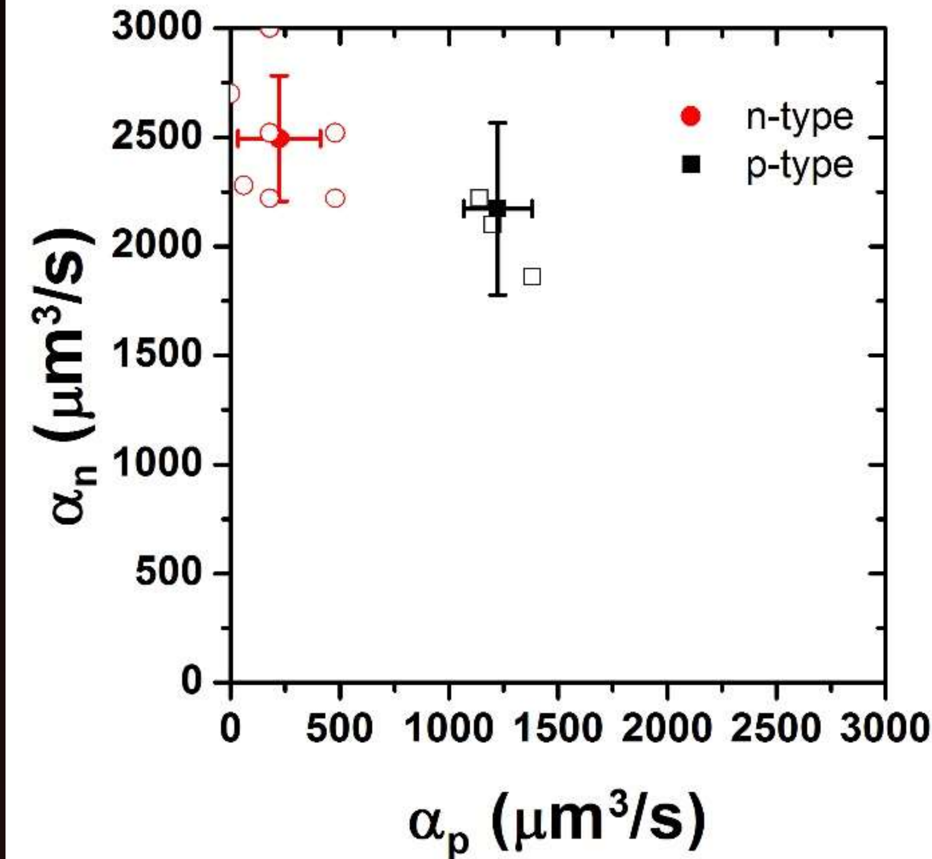

Recombination coefficient

$\alpha = k \cdot \sigma \cdot v_{th}$

Final measurement of the recombination coefficients;
n-type diode: $\alpha_p = (210 \pm 160) \mu m^3/s$; $\alpha_n = (2500 \pm 300) \mu m^3/s$;
p-type diode: $\alpha_n = (2200 \pm 300) \mu m^3/s$; $\alpha_p = (1310 \pm 90) \mu m^3/s$;
Open marks: dispersion of the combination of the fitting parameters.

Final measurement of the recombination coefficients;
n-type diode: $\alpha_p=(210 \pm 160)\mu m^3/s$;
$\alpha_n=(2500 \pm 300)\mu m^3/s$;
p-type diode: $\alpha_n=(2200 \pm 300)\mu m^3/s$;
$\alpha_p=(1310 \pm 90)\mu m^3/s$;

$\sigma_n=5 \cdot 10^{-15}$ cm^{-2} , $\sigma_p=5 \cdot 10^{-14}$ cm^{-2} (divancies in n-type diode)

kn=$2.4 \cdot 10^{-2}$, kp=$2.4 \cdot 10^{-4}$

40 and 4000 radiation induced defects are required to form 1 stable electron and hole recombination centre

MARLOWE

Low Level of damage

Electrostatics of the device

Vacancy profille (from SRIM; PAS)

Trap cross section (DLTS)

Shockley-Read-Hall Recombination/trapping model

Shockley-Ramo-Gunn Theorem
Adjoint equation formalism
Finite element method
Monte Carlo method
Semi-analytical approach in simple cases

Trap/vacancy ratio
A fingerprint of the semiconductor radiation hardness.

CONCLUSIONS

Under the assumption of **low damage level**,
the **CCE degradation** of a semiconductor device induced by ions of different mass and energy can be interpreted by means of a model based on
- The Shockley-Ramo-Gunn theorem for the charge pulse formation
- The Shockley-Read-Hall model for the trapping phenomena

If the generation occurs in the depletion region, an analytical solution of the adjoint equation can be calculated.

Adjusted NIEL scaling can be derived from the general theory in the case of constant vacancy profile.

The model leads to the evaluation of **k=(effective trap)/(vacancy),** which is independent
On the ion type and energy
On the applied bias voltage

The k factor is the fingerprint of the radiation hardness of the device

CONCLUSIONS

IBIC technique is ***a real-time*** Ion Beam Analysis technique for the functional characterization of electronic materials and devices

Strengths:

- Robust theoretical model to interpret charge or current pulse formation
- Fast signal generation (ps)
- Single ion sensitive (no invasive technique)
- Well known experimental technique (from nuclear physics)
- Use of focused ion beams ⇒ nano/micro-spectroscopy
- CCE mapping ⇒ failure analysis in microelectronics

Weaknesses:

- Mainly used to characterize detectors
- Decreasing interest of the scientific community in the last years

CONCLUSIONS

IBIC technique is a real-time Ion Beam Analysis technique for the functional characterization of electronic materials and devices

Potentiality

- Can be applied to any electronic device based on semiconductor or insulating materials.
- Can be coupled with other techniques requiring low current beams [e.g. IBIL or STIM (thin samples)].
- The analytical capability can be enriched if performed in different conditions [e.g. at different temperatures (see Ohshima), under illumination (priming effect)]
- Ions can be used both as damaging agents and as probes ⇒ **Double beams**
- Unprecedented sensitivity (much better than DLTS)
- Availability of a comprehensive model to evaluate the radiation hardness of a material at low damage level if coupled with other techniques for defect spectroscopy (e.g. Q-DLTS) and with refined computational models to evaluate vacancy production (MD simulations).

CONCLUSIONS

- **To improve key aspects of performances of IBIC**
- **To ensure transmission of competencies across generations**
- **To promote internationally the adoption of best practices**

- *Dissemination to inform the scientific community and industries about the potential of IBIC*
- An exhaustive methodology to evaluate vacancy profiles or, in general, ion interaction with matter is still not available – THEORY AND MODELS
- An user friendly software to simulate signals and maps from IBIC experiments and radiation damage

- Impact on social (may be scientific or technological) problems

Space applications (solar cells or SEU in IC)
Radiation hardness / Dosimetry
Modification/study of electronic properties to improve the performances of semiconductor devices

CONCLUSIONS

- To keep accelerator based IBT at the forefront of Scientific Endeavour
- To significantly increase human knowledge

NANO

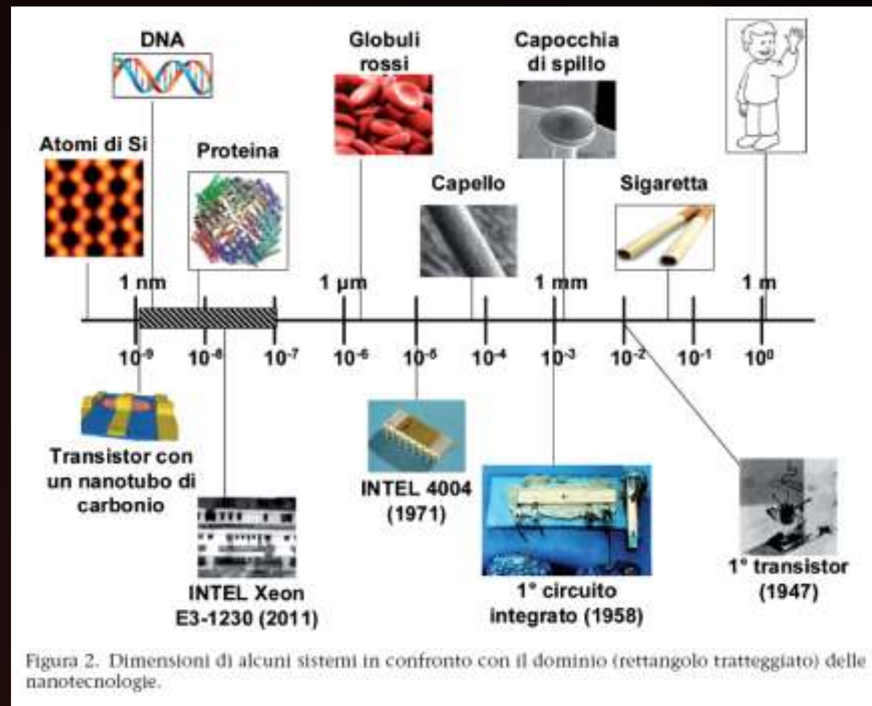

Figura 2. Dimensioni di alcuni sistemi in confronto con il dominio (rettangolo tratteggiato) delle nanotecnologie.

Nano beams?

Functional analysis of Nanostructured semiconductors?

Micro/nano machining

Why MeV ion beams?